

1-1-2014

# An Investigation Of Kinetic Effects Of Split Injection Timing On Low Temperature Combustion

Tejaswini A. Kamble  
*Wayne State University,*

Follow this and additional works at: [http://digitalcommons.wayne.edu/oa\\_theses](http://digitalcommons.wayne.edu/oa_theses)

 Part of the [Other Mechanical Engineering Commons](#)

---

## Recommended Citation

Kamble, Tejaswini A., "An Investigation Of Kinetic Effects Of Split Injection Timing On Low Temperature Combustion" (2014).  
*Wayne State University Theses*. Paper 305.

This Open Access Thesis is brought to you for free and open access by DigitalCommons@WayneState. It has been accepted for inclusion in Wayne State University Theses by an authorized administrator of DigitalCommons@WayneState.

**AN INVESTIGATION OF KINETIC EFFECTS OF SPLIT INJECTION TIMING ON LOW  
TEMPERATURE COMBUSTION**

by

**TEJASWINI A. KAMBLE**

**THESIS**

Submitted to the Graduate School

of Wayne State University,

Detroit, Michigan

in partial fulfillment of the requirements

for the degree of

**MASTER OF SCIENCE**

2014

MAJOR: MECHANICAL ENGINEERING

Approved by:

---

Advisor

Date

© COPYRIGHT BY  
TEJASWINI A. KAMBLE  
2014  
All Rights Reserved

## DEDICATION

I dedicate this work to my beloved parents, *Snehalata A. Kamble* and *A. S. Kamble*.

## ACKNOWLEDGEMENTS

I would like to express my special appreciation and thanks to my advisor Professor Dr. Marcis Jansons for giving me the opportunity to work in his Low Temperature Combustion Laboratory and also as Graduate Teaching Assistant for the course Fluid Mechanics. His constant support, patience and encouragement have always motivated me throughout my master thesis and graduate studies at Wayne State University. I greatly appreciate the time and effort he spent with me to analyze the data and sharing his profound knowledge during my thesis.

I am grateful to Dr. Naeim Henein and Dr. Dinu Taraza for letting me to be the part of their Center for Automotive Research during my graduate studies. I am obliged to Dr. Henein for sharing his wealth of knowledge related to internal combustion engines. I am also thankful to Mechanical Engineering Department Chair Dr. Walter Bryzik and Graduate Advisor Dr. Trilochan Singh for giving me an opportunity to be the part of this friendly and exciting academic environment.

I thank my lab mates- Kan Zha, Xin Yu, Jinqiao Wang, Alex Davidson and Xi Luo. It was a great learning experience for me to work with them in the LTC lab. I am also grateful to my friends for their support and motivation throughout my master's degree.

Finally, I want to thank my family for their relentless support and encouragement on every step towards completion of my studies and helping me to be where I am today.

## TABLE OF CONTENTS

Dedication .....	ii
Acknowledgements .....	iii
List of tables.....	vi
List of figures .....	vii
List of symbols & abbreviations .....	x
<b>Chapter 1 INTRODUCTION .....</b>	<b>1</b>
1.1 Overview.....	1
1.2 Advanced Combustion Strategies .....	2
1.3 Objective of present research .....	4
<b>Chapter 2 Literature Review .....</b>	<b>5</b>
2.1 Low Temperature Combustion .....	5
2.2 Conceptual LTC combustion model .....	7
2.3 LTC in $\Phi$ -T space .....	8
2.4 Fuel Considerations .....	10
2.5 Autoignition in LTC .....	11
2.6 Effect of Initial Temperature & Pressure .....	14
2.7 Effect of Injection Timing and Multiple Injections .....	15
2.8 Effect of Chemical Species .....	17

<b>Chapter 3 Model Description</b> .....	20
3.1 Chemkin Simulation Model .....	20
3.1.1 Calculation of Air-Fuel Ratio for Split Injection .....	22
3.1.2 Split Injection Model Setup .....	23
3.1.3 Single Injection Conditions .....	29
<b>Chapter 4 Results and Data Analysis</b> .....	32
4.1 Pressure & Temperature Profiles .....	32
4.2 Rate of Heat Release Profiles .....	35
4.3 Species Profile for the Different Pilot Injection Timings .....	46
4.3.1 Part A: Pilot injection timings from 165 CAD BTDC to 90 CAD BTDC .....	53
4.3.1 Part A: Pilot injection timings between 90 CAD BTDC to 12 CAD BTDC ...	58
4.3.1 Part A: Pilot injection timings between 12 CAD BTDC to 7 CAD BTDC .....	67
<b>Chapter 5 Conclusions and Recommendations</b> .....	72
5.1 Conclusions .....	72
5.2 Recommendations .....	74
References .....	75
Abstract .....	80
Autobiographical statement .....	82

## LIST OF TABLES

Table 3.1: Air- Fuel Mass Flow Rate for split injection .....	22
Table 3.2: Split Injection Simulation: Reactor 1: IC Engine 1 (C1).....	24
Table 3.3: Split Injection Simulation: Reactor 2: Gas Mixer 1 (C2) .....	25
Table 3.4: Split Injection Simulation: Reactor 2: Inlet sources (C2_Inlet1) .....	25
Table 3.5: Split Injection Simulation: Reactor 2: Inlet sources (C2_Inlet2) .....	25
Table 3.6: Split Injection Simulation: Reactor 3: IC Engine 2 (C3).....	26
Table 3.7: Split Injection Simulation: Reactor 4: Gas Mixer 2 (C4).....	27
Table 3.8: Split Injection Simulation: Reactor 4: Inlet sources (C4_Inlet1) .....	27
Table 3.9: Split Injection Simulation: Reactor 4: Inlet sources (C4_Inlet2) .....	27
Table 3.10: Split Injection Simulation: Reactor 5: IC Engine 3 (C5).....	28
Table 3.11: Single Injection Simulation: Reactor 2: Gas Mixer (C2) .....	30
Table 3.12: Single Injection Simulation: Reactor 2: Inlet sources (C2_Inlet1).....	30
Table 3.13: Single Injection Simulation: Reactor 2: Inlet sources (C2_Inlet2).....	30
Table 3.14: Single Injection Simulation: Reactor 3: IC Engine 2 (C3).....	31
Table 4.1: Reactions for rate of production of CH <sub>2</sub> O .....	57
Table 4.2: Reactions for rate of production of H <sub>2</sub> O <sub>2</sub> .....	65
Table 4.3: Reactions for rate of production of C <sub>2</sub> H <sub>2</sub> .....	66
Table 4.4: Reactions for rate of production of C <sub>4</sub> H <sub>6</sub> .....	66
Table 4.5: Reactions for rate of production of OH .....	71



## LIST OF FIGURES

Figure 1: Conceptual model for LTC combustion .....	7
Figure 2: Modern Diesel Engine Combustion Strategies plotted in $\Phi$ -T Space .....	8
Figure 3: Ignition Delay Profiles of different i-octane / n- heptane blends .....	12
Figure 4: Chemkin Simulation Model for Split Fuel Injection in HCCI Reactor .....	23
Figure 5: Chemkin Simulation Model for Single Fuel Injection Only in HCCI Reactor .....	29
Figure 6a: Pressure Traces for the split injection simulation for all the reactors combined .....	33
Figure 6b: Zoomed-in pressure traces showing increase in pressure due to pilot ignition .....	33
Figure 7a: Temperature traces for the split injection simulation for all the reactors combined .....	34
Figure 7b: Zoomed-in temperature traces showing increase in temperature due to pilot ignition ...	34
Figure 8a: Change in RHR traces with temperature for the split injection simulation for all the reactors combined .....	36
Figure 8b: Zoomed-in heat release traces showing LTHR of pilot fuel ignition and LTHR of main fuel ignition .....	36
Figure 9: Heat Release traces for the split injection simulation for all the reactors combined showing different stages of heat release events .....	37
Figure 10a: Heat Release traces for the split injection simulation for all the reactors combined .....	38
Figure 10b: Zoomed-in heat release traces showing LTHR of pilot fuel ignition and LTHR of main fuel ignition .....	38
Figure 11a: Zoomed-in heat release traces showing initial heat release for pilot timings from -165 CAD to -90 CAD .....	40
Figure 11b: Zoomed-in heat release traces showing initial heat release for pilot timings from -70 CAD to -12 CAD .....	40
Figure 11c: Zoomed-in heat release traces showing initial heat release for pilot timings from -11 CAD to -7 CAD and single fuel injection case .....	42

Figure 12: Relation between net heat release rate per CAD and HO <sub>2</sub> mole fraction for pilot injection timing of -25 CAD .....	43
Figure 13: Temperature, Pressure and accumulated heat release at 5 deg BTDC; Max RHR due to main fuel ignition and its crank angle location for different pilot injection timings from -165 CAD to -7 CAD and for the single injection (-5 CAD) only case.....	45
Figure 14: Normalized Mole Fraction of different species, Temperature & Pressure at 5 deg BTDC; Max RHR due to main injection and its crank angle location for different pilot injection timings from -165 CAD to -7 CAD and for the single injection (-5 CAD) only case .....	47
Figure 14a: Change in Normalized Mole Fraction of N <sub>2</sub> , O <sub>2</sub> , H <sub>2</sub> O, NC <sub>7</sub> H <sub>16</sub> and CO <sub>2</sub> for different pilot injection timings and single fuel injection case .....	48
Figure 14b: Change in Normalized Mole Fraction of CO, CH <sub>2</sub> O, H <sub>2</sub> O <sub>2</sub> , C <sub>2</sub> H <sub>4</sub> , CH <sub>3</sub> CHO and C <sub>2</sub> H <sub>5</sub> CHO for different pilot injection timings and single fuel injection case .....	48
Figure 14c: Change in Normalized Mole Fraction of CH <sub>2</sub> CO, NC <sub>3</sub> H <sub>7</sub> CHO, CH <sub>3</sub> OH, C <sub>2</sub> H <sub>3</sub> CHO and HOCHO for different pilot injection timings and single fuel injection case .....	49
Figure 14d: Change in Normalized Mole Fraction of C <sub>7</sub> H <sub>14</sub> O <sub>2</sub> -5, CO <sub>2</sub> , C <sub>7</sub> H <sub>14</sub> -2, C <sub>4</sub> H <sub>8</sub> -1, C <sub>7</sub> H <sub>14</sub> -3 and NC <sub>3</sub> H <sub>7</sub> COCH <sub>3</sub> for different pilot injection timings and single fuel injection case .....	49
Figure 14e: Change in Normalized Mole Fraction of SC <sub>3</sub> H <sub>5</sub> CHO, C <sub>7</sub> H <sub>14</sub> O <sub>1</sub> -4, C <sub>7</sub> H <sub>14</sub> -1, HO <sub>2</sub> , H <sub>2</sub> , C <sub>5</sub> H <sub>10</sub> -1 and C <sub>7</sub> H <sub>14</sub> O <sub>1</sub> -3 for different pilot injection timings and single fuel injection case.....	50
Figure 14f: Change in Normalized Mole Fraction of C <sub>4</sub> H <sub>7</sub> CHO <sub>1</sub> -1, C <sub>7</sub> H <sub>14</sub> O <sub>2</sub> -4, CH <sub>4</sub> , C <sub>2</sub> H <sub>2</sub> , C <sub>4</sub> H <sub>6</sub> , OH and O; Temperature and Pressure at 5 deg BTDC for different pilot injection timings and single fuel injection case.....	50
Figure 15: Division of species profile into three parts .....	52
Figure 16: Part A- Effect of Pilot injection timings from -165 CAD to -90 CAD on Main Ignition	53
Figure 17: Chemkin Model to Study the Effect of formaldehyde (CH <sub>2</sub> O) on Ignition Delay of Main Fuel Ignition .....	55
Figure 18: Effect of formaldehyde (CH <sub>2</sub> O) on ignition delay of main ignition .....	55
Figure 19a: Rate of Production of CH <sub>2</sub> O in Reactor 3 [IC Engine2].....	56
Figure 19b: Rate of Production of CH <sub>2</sub> O in Reactor 5 [IC Engine3] .....	56

Figure 20: Part B- Effect of Pilot injection timings between -90 CAD to -12 CAD on Main Ignition .....	59
Figure 20a: Effect of H <sub>2</sub> O <sub>2</sub> on ignition delay of main ignition .....	60
Figure 20b: Effect of C <sub>2</sub> H <sub>2</sub> on ignition delay of main ignition .....	61
Figure 20c: Effect of C <sub>4</sub> H <sub>6</sub> (1,3-butadiene) on ignition delay of main ignition .....	61
Figure 21a: Rate of Production of H <sub>2</sub> O <sub>2</sub> in Reactor 3 [IC Engine2] .....	62
Figure 21b: Rate of Production of H <sub>2</sub> O <sub>2</sub> in Reactor 5 [IC Engine3] .....	62
Figure 21c: Rate of Production of C <sub>2</sub> H <sub>2</sub> in Reactor 3 [IC Engine2] .....	63
Figure 21d: Rate of Production of C <sub>2</sub> H <sub>2</sub> in Reactor 5 [IC Engine3] .....	63
Figure 21e: Rate of Production of C <sub>4</sub> H <sub>6</sub> in Reactor 3 [IC Engine2] .....	64
Figure 21f: Rate of Production of C <sub>4</sub> H <sub>6</sub> in Reactor 5 [IC Engine3] .....	64
Figure 22: Part C- Effect of Pilot injection timings from -12 CAD to -5 CAD on Main Ignition ...	68
Figure 23: Temperature parameter study in CVC .....	69
Figure 24a: Rate of Production of OH in Reactor 3 [IC Engine2] .....	70
Figure 24b: Rate of Production of OH in Reactor 5 [IC Engine3] .....	70

## LIST OF SYMBOLS AND ABBREVIATIONS

ATDC	After top dead center
BTDC	Before top dead center
CAD	Crank angle degree, degrees
EGR	Exhaust gas recirculation
IMEP	Indicated mean effective pressure, bar
LTC	Low temperature combustion
NTC	Negative Temperature Coefficient Regime
RHR	Rate of Heat Release
LTHR	Low Temperature Heat Release
ITHR	Intermediate Temperature Heat Release
HTHR	High Temperature Heat Release
RPM	Revolutions per minute
TDC	Top dead center
HCCI	Homogeneous Charge Compression Ignition
RCCI	Reactivity-Controlled Compression Ignition
PCCI	Premixed Charge Compression Ignition
$NC_7H_{16}$	N-Heptane
$O_2$	Oxygen
$N_2$	Nitrogen
$CO_2$	Carbon Dioxide
$H_2O$	Water
OH	Hydroxy Radical

$\text{HO}_2$	Hydroperoxy Radical
$\text{H}_2\text{O}_2$	Hydrogen Peroxide
$\text{CH}_2\text{O}$	Formaldehyde
$\text{C}_4\text{H}_6$	1, 3-Butadiene
$\text{C}_2\text{H}_2$	Acetylene
$\text{NO}_x$	Oxides of Nitrogen
$\text{CO}$	Carbon Monoxide
UHC	Unburnt Hydrocarbons
PM	Particulate Matter
A/F	Air to Fuel ratio
ID, $\tau$	Ignition Delay
$\Phi$	Equivalence ratio

## CHAPTER 1

### INTRODUCTION

#### 1.1 Overview:

The diesel engine, invented in the late 19th century by Dr. Rudolf Diesel, is one of the most widely used engines among other types of internal combustion engines in use today. This energy efficient engine delivers good fuel economy and low greenhouse gas emissions. It is also well known for its reliability and durability characteristics. Since its beginning, the diesel engine has been used in a wide variety of sectors from transportation to energy generation. It is the most popular propulsion source for trucks, buses, ships, off road vehicles and other heavy duty applications. They are also used in electric generating plants for power generation. Recently, it has started gaining popularity among light duty applications too due to its various benefits.

Despite the advantages offered by a diesel engine, they have certain shortcomings like high nitric oxides (NO<sub>x</sub>) and particulate matter (PM) emissions followed by increased noise and finally high cost. The current focus is to achieve the stringent emission levels set by the government and to minimize the disadvantages of the diesel engine.

As a result of the introduction of the stringent diesel emission standards, a lot of different technologies are being used to control the harmful pollutants emitted by a diesel engine. This has led to the use of after treatment systems such as catalytic converter and diesel particulate filter. Although it has helped to cut emissions to a certain extent, it has also increased the total cost of the diesel engine. Since the combustion of the fuel plays a major role in the engine performance, fuel consumption as well as emission of pollutants, a lot of effort is being made to understand the diesel combustion process.

## 1.2 Advanced Combustion Strategies:

In an effort to improve the diesel engine performance and emissions, advanced combustion strategies are being researched which could help us to meet the tough emission regulations, minimize the need of the after treatment systems and decrease their cost and complexity. The advanced combustion strategies being explored are pre-, post- and in-cylinder combustion approaches [1] as follows:

The pre-combustion approach includes the use of alternative fuels. The primary concern of this approach is the modification of the molecular composition of the fuel, its aromatic content, the cetane number or the oxygen content in order to reduce the  $\text{NO}_x$  and PM emissions.

On the other hand, post-combustion strategies include the improvement of after treatment technologies for emission reduction. The after treatment systems in use today are Three Way Catalyst (TWC) for  $\text{NO}_x$ , CO and unburned hydrocarbons (UHC) reduction; Selective Catalytic Reduction (SCR) for the  $\text{NO}_x$  reduction; and the Diesel Particulate Filter for the PM emission reductions of the engine exhaust. However, these systems depend on various parameters like exhaust gas temperature, total pollutant concentration, exhaust flow rate and the volume of the filters etc., which can affect their performance.

The in-cylinder approach deals with the improvement of the combustion process in the engine itself by using different methods such as Exhaust Gas Recirculation (EGR), split-injection, varying swirl ratio, charge air cooling, controlling injection timings and combustion chamber design. Since there are no additional systems being added to the engine assembly, this strategy makes the overall system less complex and cost effective compared to other strategies. The main goal here is to modify the in-cylinder combustion process in order to make the engine user and environment friendly. This in-cylinder approach, though very promising demands meaningful understanding of the combustion mechanism. The in depth study of the underlying

chemical kinetics and its interaction with the fluid flow might contribute towards the development of this strategy.

The in-cylinder advanced combustion strategy that has been the subject of considerable research recently is the Low Temperature Combustion concept [2]. This is a general term used to address a number of advanced combustion strategies like Homogeneous Charge Compression Ignition (HCCI), Premixed Charge Compression Ignition and reactivity controlled compression ignition (RCCI). This concept has great potential of achieving high thermal efficiencies along with reducing  $\text{NO}_x$  and PM emissions simultaneously, but it often results in increased carbon monoxide (CO) and hydrocarbon (HC) emissions. Since these emissions as well as the performance of engines utilizing the LTC approach greatly depend on the combustion of fuel, it is very important to study the combustion mechanism of the LTC concept in order to meet the challenges posed by the Low Temperature Combustion strategy.

The biggest challenge faced by the Low Temperature Combustion concept is the control of kinetically driven autoignition of the fuel air mixture in the engine over appreciable load ranges. The high temperature heat release stage of autoignition process is preceded by comparatively slow chemical reactions of low temperature heat release stage of autoignition. These chemical changes taking place before high temperature heat release is the main area of interest as this could help in controlling the autoignition in LTC.



### 1.3 Objective of present research:

This work focused on the LTC concept, examines the chemical kinetics of split-injection timing and the effect of this parameter on combustion phasing and pressure rise rate. Detailed reaction mechanisms are applied in CHEMKIN-based kinetic simulations to model the production and composition of combustion intermediates produced by a pilot injection through different pressure-temperature histories. The influence of these intermediates on the following main injection is studied. The results will provide insight to the role of pilot injection timing on LTC control.

## CHAPTER 2

### LITERATURE REVIEW

#### 2.1 Low Temperature Combustion

Recent development in the field of diesel technology has been significant. The various technologies being developed in the pre-, post- and in-cylinder combustion areas have great potential to improve the diesel performance and emissions. The Low Temperature Combustion (LTC) concept is one such advanced in-cylinder combustion strategy which is undergoing considerable research. LTC is being considered as the future technology for diesel engines. This high efficiency combustion approach has the ability to lower the  $\text{NO}_x$  and PM emissions simultaneously.

The aim of Low Temperature Combustion is to attain high levels of fuel efficiency with almost no regulated harmful emissions. As the name implies, this approach works at low combustion temperature with the intention of favorably altering the  $\text{NO}_x$  and soot formation chemistry. They burn cool enough and lean enough to stay out of the  $\text{NO}_x$  and soot formation zones without compromising the thermal efficiency. This concept has many variants such as Homogeneous Charge Compression Ignition (HCCI), Premixed Charge Compression Ignition (PCCI), and Reactivity-Controlled Compression Ignition (RCCI) [3].

Homogeneous Charge Compression Ignition (HCCI) is a fusion of traditional diesel (stratified charge compression ignition) and gasoline (homogeneous charge spark ignition) engines. In HCCI, the goal is to attain a homogeneous mixture of fuel and air well before the combustion process, as in SI engines. This can be made possible by early injection of the fuel in the intake port or directly into the combustion chamber and allowing sufficient time between the injection and ignition event to allow complete mixing of air and fuel. This mixture undergoes

compression and thus auto ignites as in CI engines. Thus it burns instantaneously throughout, without the hot flame front of SI combustion or the locally rich flame front of CI combustion. There is no explicit control over the combustion event in an HCCI engine; therefore various conditions like temperature, compression ratio, residual exhaust gas, and air/fuel ratio that induce combustion can be adjusted throughout the engine cycle to attain desired combustion behavior. However, the difficulty in controlling combustion phasing still remains.

Premixed Charge Compression Ignition (PCCI), also called as partially premixed charge compression ignition (PPCI), is a variant of HCCI that focuses on controlling the combustion event by injecting a late fuel pulse in the compression stroke that commands the start of ignition. The intake air is partially premixed with early fuel pulse to create HCCI like conditions in which then the late fuel pulse is injected at or near TDC in an attempt to control the combustion phasing by letting the combustion occur over an extended period of time compared to the instantaneous HCCI combustion.

Reactivity-Controlled Compression Ignition (RCCI) aims to gain more control over combustion phasing by using multiple injections of various fuels at scheduled intervals. This provides control over the reactivity of the charge in the cylinder for optimal combustion duration and magnitude. A relatively low reactivity fuel is injected early in the engine cycle and mixes homogeneously with the air, which is followed by injection of a higher reactivity fuel later into the cylinder. This leads to pockets of differing A/F ratios and reactivity causing the combustion to occur at different points at varying rates.

## 2.2 Conceptual LTC combustion model:

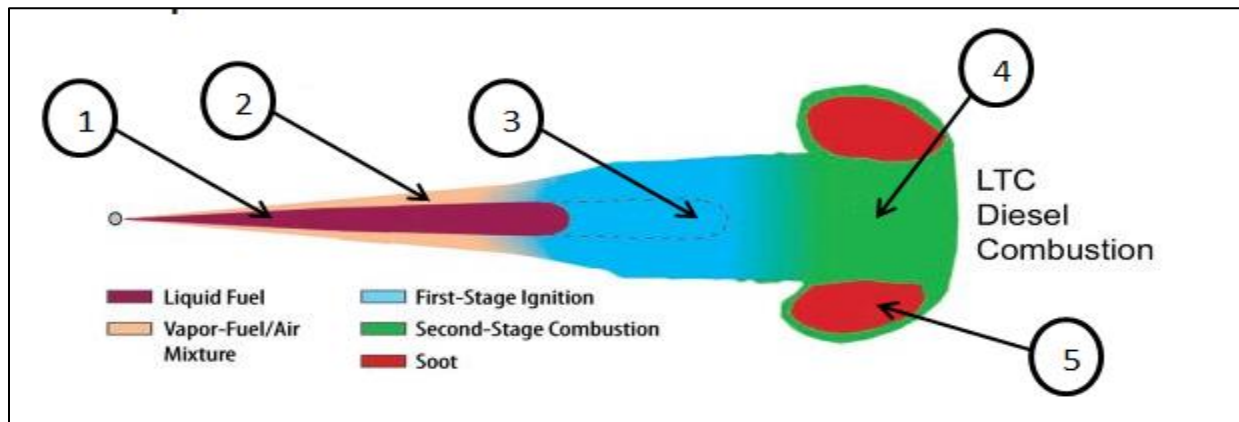


**Figure 1: Conceptual model for LTC combustion [4]**

Figure 1 shows the conceptual model for LTC combustion adapted from the conventional diesel combustion model [2, 4, 5]. In case of the low temperature early injection condition, the liquid fuel injection penetrates much farther (region 1) due to lower ambient gas temperature and density compared to the near-TDC injection in conventional diesel combustion system [5]. Fuel vaporization then forms an envelope around the fuel jet as shown by region 2. This region shows chemiluminescence from the energy released due to ignition reactions contributing to the vaporization of the fuel shown as region 3. This is followed by premix combustion reactions dominated by OH radicals, in region 4. It is inferred from this that a considerable amount of the jet cross section is nearly stoichiometric which is in contrast to the conventional diesel combustion where the stoichiometric region and OH fluorescence is seen at the perimeter of the diesel jet in the diffusion flame. The soot is formed in the region lacking OH, in the roll-up vortices at the head of the jet indicated by region 5. The experiment was performed on a heavy duty diesel engine operated with a single early fuel injection event and with 12.7% of O<sub>2</sub> to depict EGR conditions. It resulted in low NO<sub>x</sub> and elimination of in-cylinder soot completely.

### 2.3 LTC in $\Phi$ -T space:

The  $\Phi$ -T representation (local equivalence ratio versus local temperature) is a convenient way of depicting the different diesel combustion concepts. In the  $\Phi$ -T plot shown in the figure 2 compares the advanced diesel combustion concepts with conventional diesel combustion process.

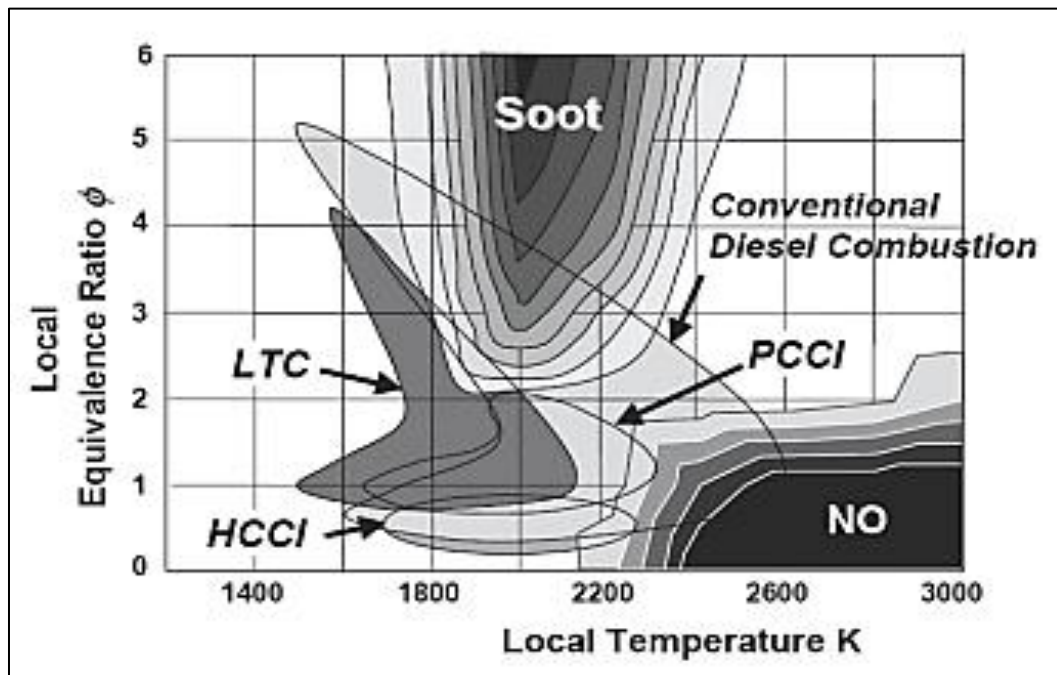


**Figure 2: Modern Diesel Engine Combustion Strategies plotted in  $\Phi$ -T Space**

It can be inferred from the plot how the reduction of NO<sub>x</sub> and soot can be achieved with specific combination of lower equivalence ratios and low temperatures. The conventional diesel combustion zone passes through the NO<sub>x</sub> and Soot formation islands. In contrast, the advanced combustion strategies like HCCI, PCCI and LTC modes narrowly avoid the high formation regions of NO<sub>x</sub> and soot emissions [2, 6, 7].

The multiple injection/split injection strategy is the most researched topic in order to realize low temperature combustion and to control the harmful emissions. The experiment conducted by Koci and Ra [6] on multiple fuel injections in the highly dilute diesel LTC regime

showed that optimal split injections are beneficial in reducing the UHC, CO and PM emissions, and achieved by altering the fuel distribution in the cylinder. In a study at IFP [8], it was found that a close spaced double injection strategy affects the ignition delay either directly or indirectly by increasing it which results in improved air-fuel mixture. This helps in optimizing HC and CO emissions and thus the EGR rate could be reduced at low load points which otherwise require high EGR ratios.

The study performed by Mendez and Thirouard at IFP [7] on multiple injection strategies in diesel combustion presented the advantages of using multiple injections (double injection) to achieve stringent emissions by increasing the ignition delay. They indicated that the increase in ignition delay leads to longer mixing period thereby resulting in more homogeneous fuel-air mixture. This results in decrease in equivalence ratio and subsequent soot formation.

In another investigation [9], it was shown that the ignition delay increases with delayed or retarded second injection timing in the case of double injection leading to low gas temperature in the chamber. When the fuel is injected into this low temperature region, the high temperature thermal cracking of diesel fuel is inhibited resulting in low soot. It was also presented in this study that injection pressure greatly affects emissions in multiple injection strategies. High injection pressure helps in soot oxidation which is good for its reduction in the late cycle whereas low injection pressure gives rise to more heterogeneity in the mixture and thus decreases the in-cylinder bulk temperature thereby reducing the  $\text{NO}_x$  production. The split injection also resulted in reduction in noise due to distribution of the heat releases of combustion [6-8].

## 2.4 Fuel Considerations:

The LTC concept (premixed approach) has been studied using different types of fuels which include diesel, gasoline, natural gas and other alternative fuels. Although the ideal fuel depends on various factors like engine design, engine operating conditions and the way LTC is being implemented [2], the fuel properties such as fuel ignitability or fuel volatility [2, 10] can have a large impact on the performance and emissions of the LTC engine. In the largely premixed mode, the combustion takes place only if air and fuel are sufficiently well mixed to cause the ignition. Thus, how well the fuel and air mix and how easily it ignites are two important deciding parameters for good & clean engine performance. The thorough mixing of air and fuel depends on the temperature and fluid flow inside the engine. The ignitability of the fuel is also important as it uncovers the underlying chemical kinetic characteristics of that fuel when mixed with air. The fuel structure has important role to play in the control of ignition delay [11]. The presence of the  $-\text{CH}_2-\text{CH}_2-\text{CH}_2-$  chain allows the formation of 6-member low strain C-C-C-O-O-H rings, which exhibits two-stage ignition with reduced ignition delay, which is in agreement with previous findings. It was seen that these two stage ignition is associated with isomerization reactions in peroxy radicals. Different fuels were tested in this study which exhibited two stage ignition with ignition delay increasing in the order: n-heptane < 1-heptene < methylcyclohexane = 2-heptene < 1,3-cyclohexadiene < 3-heptene < cyclohexane < cyclohexene < iso-octane < toluene (not ignited).

The fuel ignition characteristics can be modified to control the ignition delay. For example- the control of ignition timing of n-heptane using port injection of additives acting as reaction inhibitors was studied in a single cylinder engine under HCCI conditions [12]. The additives used for suppression of ignition were methanol, ethanol, isopropanol and methyl tert-

butyl ether (MTBE). The experiment showed that the suppression effectiveness increased in the order of MTBE < isopropanol < ethanol < methanol. However, ethanol was known to be the best additive for retarding the ignition timing considering thermal efficiency and emissions at applied operating ranges.

## 2.5 Autoignition in LTC:

Autoignition of the fuel plays a major role in the process of combustion in diesel engine [2, 13]. The LTC concept is one where fuel is premixed with air, and the autoignition occurs when the fuel-air has formed an optimal homogeneous mixture for the combustion to happen. This takes relatively long time when compared to conventional diesel combustion. The period between the start of fuel injection and the start of combustion determined from the rapid pressure rise in the combustion chamber is known as ignition delay [14, 15]. Once this ignition delay period is over and the ideal temperature is reached, the mixture autoignites and the subsequent chemical reactions become very fast and are accompanied by rapid heat release due to the conversion of reactants to products. Therefore, the ignition delay period is used not only to attain the homogeneous mixture of air and fuel but also to control the combustion phasing. In general, the ignition delay time is given by the following Arrhenius expression [2]:

$$\tau = AP^{-n} \exp\left[\frac{B}{T}\right] \quad (1)$$

The above expression shows the dependence of ignition delay ( $\tau$ ) on temperature (T). The values of constants A, n and B depends on the fuel used. This equation can be used to express the ignition delay at some temperature points but in the intermediate temperature zone, the ignition delay varies very little with temperature. Figure 3 shows the plot of ignition delay versus Temperature for various blends of i-octane and n-heptane [2, 16]:



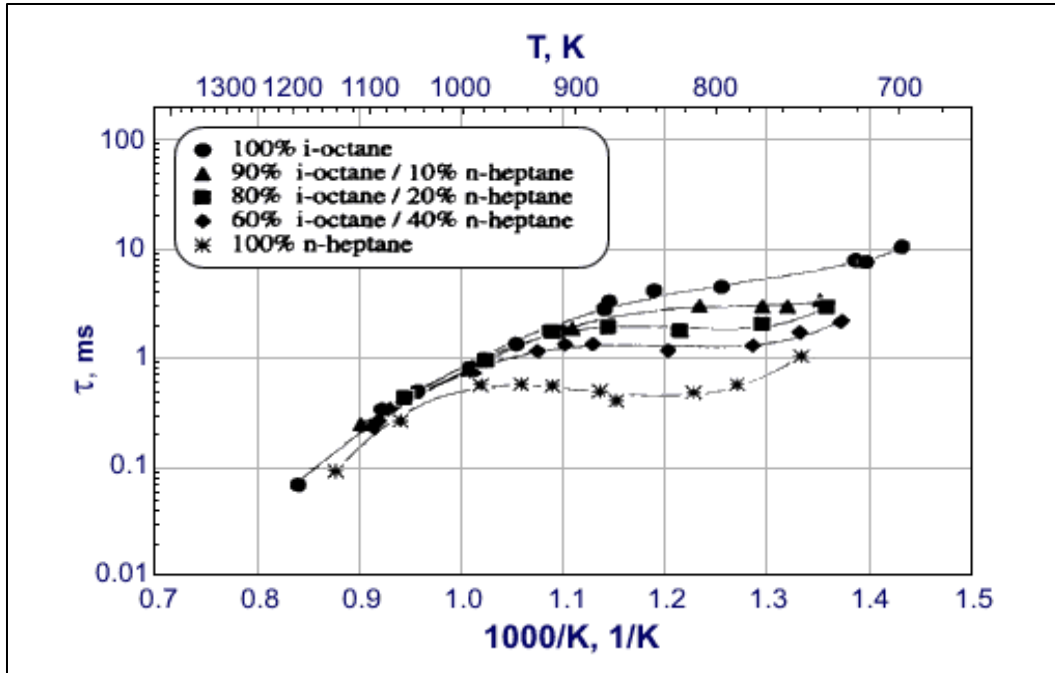


**Figure 3: Ignition Delay Profiles of different i-octane / n-heptane blends for  $\Phi=1$  and 1 atm pressure [16]**

As we can see,  $\tau$  varies only a little in the intermediate temperature range. However, for certain fuels like n-heptane,  $\tau$  actually increases with rise in temperature in the intermediate temperature range [2, 16]. This region where ignition delay  $\tau$  increases with increase in temperature is described as Negative Temperature Coefficient (NTC) regime. A study [17] on this reverse behavior of ignition delay (that is increase in ignition delay with temperature rise for some of the fuels) reported that the ignition delay starts to decrease again with further increase in temperature (around 50 K-100 K higher than the start of NTC).

The autoignition of the fuel exhibits two stages of heat release. The heat release observed in the NTC region is the first stage of autoignition and is known as low temperature heat release (LTHR) because it occurs at low temperatures ranging from 600 K to 800 K [15, 37], which is associated with low rate of heat release. However, in a research conducted by Kuwahara [38], the low temperature oxidation and the NTC regime is noted in the temperature range of 800 K to

1000 K. It is followed by the main heat release or high temperature heat release (HTHR) which is the second and final stage of autoignition of the fuel. In some preceding studies [36, 37], an intermediate temperature heat release (ITHR) was also observed between the LTHR and HTHR of main fuel ignition. It appears as a small peak on the main HTHR trace unlike LTHR which appears as a separate peak before HTHR. It was also mentioned that ITHR shows to happen only at higher in-cylinder temperatures [850 K – 1050 K] and appears as a “shoulder” on the main heat release event. The chemistry associated with the NTC regime is most commonly described as “low temperature chemistry” as it is known to be different than the chemistry related to high temperature heat release. The LTHR can have a significant effect on HTHR. An optimum combustion phasing could be realized due to the low initial mixture temperature of LTHR which could also lower the HTHR rate and thus help to control the combustion noise and the maximum load achieved by the engine [2].

## **2.6 Effect of Initial Temperature & Pressure:**

CFD simulations [18] have been carried out to understand the effects of intake gas temperature on auto-ignition of n-heptane, and indicated that the oxidation reactions got slowed down with drop in gas temperature at the beginning of LTC regime, and resulted in increased RHR in LTC regime. The low gas temperature also led to delay in the occurrence of NTC regime and displayed drop in RHR.

Furthermore, the decrease in intake temperature has shown to shift the start of combustion close to TDC [19]. It was also established [20- 23] that the ignition delay decreases with increase in initial temperature, which also results in a decrease in maximum heat released during combustion and that it can be used as a means to control the combustion phasing. In one investigation [23], it was found that inlet temperature could be varied to influence the

autoignition process without altering the overall energy content of the mixture since the heat release did not seem to change with inlet temperature.

Multi-timescale modelling of ignition and flame regimes of an n-heptane/ air mixture in a 1D spark assisted HCCI reactor [24] revealed that the initial mixture temperature and pressure plays an important role in flame dynamics. It was indicated that based on initial temperature, there exists at least six different combustion regimes- initial single flame front propagation regime, a coupled low temperature double flame regime, a coupled high temperature double flame regime, a decoupled low and high temperature double flame regime followed by low temperature ignition regime, a single high temperature flame regime and finally a hot ignition regime. The low and high temperature flames have distinct kinetic properties and are highly influenced by the low temperature chemistry. It was also proved that the ID reduces with increase in temperature and pressure of the charge. Also, the NTC regime shifts to higher temperatures with increase in pressure. The low temperature flame front showed rapid decomposition of n-heptane and associated increase in  $\text{HO}_2$ ,  $\text{H}_2\text{O}_2$ , aldehydes ( $\text{CH}_2\text{O}$ ,  $\text{CH}_3\text{CHO}$ , and  $\text{C}_2\text{H}_5\text{CHO}$ ). It was seen in flux analysis that small olefins like  $\text{C}_2\text{H}_4$ ,  $\text{C}_3\text{H}_6$  are formed from the decomposition of alkyl radicals,  $\text{C}_7\text{H}_{14}\text{O}_{2.5}$  and  $\text{nC}_7\text{ket}_{24}$  after isomerization and breakdown of  $\text{C}_7\text{H}_{14}\text{OOH}$  and  $\text{O}_2\text{C}_7\text{H}_{14}\text{OOH}$ . The onset of HTF front was defined by the reduction of  $\text{H}_2\text{O}_2$ ,  $\text{HO}_2$ ,  $\text{CO}$  resulting in formation of  $\text{H}_2\text{O}$  and  $\text{CO}_2$ .

A constant volume vessel was used to study the ignition of n-heptane sprays [25]. It was found that the ignition delay was sensitive to initial temperature and pressure. The ignition delay was longer for temperature less than 850 K at pressure range from 2 MPa to 4 MPa. However, it showed little sensitivity to temperature greater than 850 K at pressure equal to 4 MPa. This was explained using mixture homogeneity at ignition as follows- at temperature less than 850 K, the chemical reactions do not accelerate until the homogeneous mixture is formed but when the

temperature is high, chemical reactions are very fast and heterogeneous combustion occurs over a wide range of equivalence ratio. Also, each spray would exhibit two stage ignition with a NTC regime characterized by two stage pressure rises at low ambient pressures. Moreover, a further study revealed that ignition delay depends on the pressure rise of the first stage [11]. The ignition delay decreases with increase in pressure [11, 21, 26] and becomes approximately zero as pressure increase beyond 1 MPa, the point at which main combustion starts.

## **2.7 Effect of Injection Timing and Multiple Injections:**

Combustion phasing can have a significant effect on performance and emissions of an engine. It was proposed by Koci and Ra [6] that appropriate injection timing can be used to attain optimal ignition delay and phasing. A study on the effects of charge dilution and injection timing in an LTC diesel engine [21] concluded that advancing the injection timing will lead to increase in peak in-cylinder pressure. However, when the injection timing was fixed, the charge dilution decreased the peak in-cylinder pressure due to high heat capacity of diluent gases and slow premixed combustion reactions.

Early injection PCCI regime tests were carried out using a single cylinder DI diesel engine [27], in which it was shown that the ignition delay and ignition dwell are prolonged with injection timing advance due to lower ambient temperature, pressure and density of the mixture. The ignition dwell is also increased with injection pressure. This enhances the fuel-air mixing leading to low emissions of CO, HC and soot.

One of the promising strategies to control the ignition timing and combustion phasing of the main heat release in HCCI is NVO strategy [10, 26]. NVO strategy incorporates early EVC and late IVO in which the first fuel injection is made during the NVO period, followed by main injection at the end of NVO. Research has shown that NVO injection advances combustion by both chemical and thermal effects [10]. It was reported [26] that retarding the NVO fuel injection

advances the main combustion phasing (Main CA50) and also the ARHR. However, the occurrence of NVO CA50 (CAD at which 50% of NVO apparent heat release occurs) showed a clear retard with delayed NVO injection timing. Even the increase in the injected fuel mass had a retarding effect on NVO CA50 event but an advancing effect on main combustion event. As the NVO injection is delayed, the temperature at IVO increases but it was seen to decrease after 45 CAD BTDC. This was attributed to the decrease in NVO heat release. The temperature at IVO decreased with advanced injection timings because of the high heat loss from the cylinder.

A study conducted at Sandia National Laboratories [28] regarding pilot injection ignition under LTC conditions put forth some important observations. It stated that pilot ignition gets impeded in a dilute low temperature mixture characterized by extended ignition delay due to the formation of overly lean mixture. Also, the ignition delay may increase further even if a small quantity of pilot fuel is injected into this overly formed lean mixture or if the injection pressure is increased under these conditions. Furthermore, if a highly rich mixture is formed in a relatively short period of time, it will prolong the ignition delay as well.

Mueller [29] examined the dual-injection case where he analyzed the mixing and combustion of the early and main injected fuel. It was pointed out using the heat release data that the early injected fuel burns in HCCI like mode with cool flame followed by premixed, high temperature combustion whereas the main fuel burns in a conventional manner in which a short premixed burn phase is followed by a longer mixing controlled combustion.

## 2.8 Effect of chemical species:

The role played by certain chemical species is very significant in combustion. In an investigation of effects of ethanol on ignition delay of n-heptane [30], it was found that increase in ethanol addition to n-heptane/air mixtures increases the ignition delay, and increases the initial temperature corresponding to the low temperature heat release. Also, the peak of low temperature heat release decreases with increase in ethanol volume, and results in an increase in engine IMEP. The most well-known chemical species for inhibition of ignition delay is formaldehyde (HCHO) [15, 18, 30]. It increases the ignition delay, retards the LTHR and also decreases the peak magnitude of the apparent heat release rate (ARHR) in a diesel engine. It was also clarified that the NTC regime is characterized by high concentration of formaldehyde and that the oxidation reactions take place once it starts to drop [18].

A kinetic examination of autoignition of alkanes revealed that  $\text{HO}_2\text{-H}_2\text{O}_2$  chemistry can have a significant effect on ignition delay in the temperature range of 600 K to 1100 K, particularly at pressures higher than 1 atm [32]. Outside this temperature range, the  $\text{HO}_2$  reactions are unlikely to be having significant impact on auto ignition. One research [33] suggested that the thermal decomposition of  $\text{H}_2\text{O}_2$  and consumption of HCHO which results in hot ignition flame can be used as an important perspective for controlling HCCI ignition timing.

Kinetic analysis conducted by Wong and Karim [34] to study the effects of recirculated exhaust gases on auto ignition of homogeneous n-heptane/ air mixture in engines showed that the peroxy radical, the hydroperoxy-alkyloxy radical, and hydroperoxides, as well as  $\text{H}_2\text{O}_2$ , promoted auto ignition whereas ethylene, epoxy cycloheptane and formaldehyde were responsible for inhibiting auto ignition. They found that the auto ignition promoters did not show gradual accumulation during cool flame reactions due to their consumption as soon as it was produced in the pre-combustion reactions. It was also proved that there exist two sets of cool

flame reactions- the first set is defined by the production of auto ignition promoters with little heat release and the second set of reactions show consumption of these species occurring at high temperature with high heat release and formation of complete combustion products like  $H_2O$ . They reported that the autoignition tendency of an n-heptane/air mixture will increase if the mixture has undergone the first set of reactions only, and that the autoignition will be dominated by kinetic effects and not the thermal effects. But if it has attained second set of reactions, then, the auto ignition tendency will be less. As the oxidation proceeds further, the kinetic effects will lessen whereas thermal effects will intensify with negligible change in auto ignition tendency.

Some researchers [28] presented the effect of exhaust gas CO and  $H_2O$  on the ignition delay at near TDC temperatures. They reported that CO addition (5000 ppm) extended the ignition delay by 0.5-1.0 CAD at 880 K near TDC temperature. This effect was counter balanced by  $H_2O$  which showed to decrease the ignition delay by 1 CAD. It was also shown that even NO (in small quantities as few ppm) has significant effect on ignition delay where it results in shortening of ignition delay.

The effect of acetylene on iso-octane was studied in HCCI combustion [35] employing a negative valve overlap (NVO) strategy. It was found that acetylene at part-per-thousand levels advances combustion phasing. If combustion phasing is held constant, then it increases peak heat release rate. It was also discovered that if acetylene is produced and not consumed during NVO then it will be carried over to the main combustion event where it will advance the ignition and enhance combustion.

All these advances in the low temperature combustion area attest that it is going to be a promising technology for future diesel engines as well as other engines. LTC concept uses a low equivalence ratio and low temperature which helps in avoiding the  $NO_x$  and soot formation zones in  $\Phi$ -T space. Various parameters were varied and analyzed in the literature to understand

its effects on LTC in order to control the autoignition in LTC. The fuel structure, its volatility and ignitability along with other design factors play important role in realizing the formation of perfectly homogeneous mixture for LTC. It was seen that the ignition delay decreases with increase in temperature and pressure. However, for n-heptane, the ignition delay increased in the intermediate temperature range and decreased when the temperature was further increased. The multiple injections and varying injection timings have shown to have a substantial effect on the in-cylinder conditions and the ignition delay. It was found that the ignition delay of pilot fuel combustion gets impeded in low temperature mixture and also when extra small quantity of fuel is added to this mixture. The ignition delay might prolong even if a highly rich mixture is formed in relatively short period of time. The chemical species such as ethanol, formaldehyde posed inhibiting effect on ignition delay whereas other species such as acetylene, peroxy radical, the hydroperoxy-alkyloxy radical, and hydroperoxides, as well as  $H_2O_2$ , had advancing effect on ignition delay.

The work done in this research examines the effect of the intermediate species formed due to combustion of pilot fuel at varying pilot injection timings on combustion phasing of the main fuel ignition. This would help in understanding the role played by chemical kinetics of charge towards controlling the autoignition/combustion phasing of mixture through different pressure, temperature and heat release profiles.



## CHAPTER 3

### MODEL DESCRIPTION

Split injection of fuel is one of the in-cylinder strategies being studied in HCCI engines with LTC conditions due to its numerous benefits. As we have seen in the literature, a common challenge in the implementation of HCCI is the control of ignition timing. The auto ignition of fuel is preceded by relatively small chemical changes in fuel/air mixtures. In HCCI, a greater control of autoignition will be achieved through a better understanding of these chemical reactions of this process. This work examines the chemical kinetics of split-injection timing and the effect of this parameter on combustion phasing and pressure rise rate. Detailed reaction mechanisms are applied in CHEMKIN-based kinetic simulations to model the production and composition of combustion intermediates produced by a pilot injection through different pressure-temperature histories.

#### 3.1 Chemkin Simulation Model

A zero-dimensional closed internal combustion engine simulator model was employed in Chemkin-Pro to simulate the HCCI system. The assumptions that were considered in this simulation were: the engine model is adiabatic, homogeneous and single zone to depict only the kinetics of LTC and not the entire actual engine conditions. The combustion was modelled using n-heptane fuel and detailed mechanism of n-heptane, version 3.1 from Lawrence Livermore National Laboratory. N-Heptane was chosen in this study for the following reasons [34]:

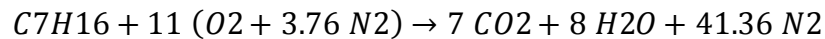
- N-heptane displays the characteristics of more complex hydrocarbon fuels specially the cool flame and the different stages of ignition.
- It is used as a reference fuel to determine the knock rating of different fuels.

- The cetane number of n-heptane is around 60 which is close to a good quality diesel fuel; therefore it can be used successfully to represent the diesel ignition phenomena.

### 3.1.1 Calculation of Air-Fuel Ratio for Split Injection:

The ideal HCCI combustion is illustrated by a lean, perfectly homogeneous mixture where the equivalence ratio at any point in the mixture is approximately equal to the average equivalence ratio. In this work, the fuel mass is distributed equally (1:1 ratio) between the pilot and main fuel addition; and the equivalence ratio is set at 0.5 depicting ideal HCCI process. In order to maintain the total equivalence ratio equal to 0.5 in the system, the appropriate mass flow rate of air was calculated for 1 g/s of fuel flow rate in each of the split injection as follows:

Stoichiometric Combustion Reaction:



Using this reaction, we get the stoichiometric  $A/F = 15.18$

Since, equivalence ratio  $\Phi = (Stoichiometric\ A/F)/(Actual\ A/F)$

Therefore, for  $\Phi = 0.5$ , we get the Actual  $A/F = 30.4$

The fuel is being split equally in the pilot and main injections.

Air	Pilot Injection	Main Injection
$x$	$y$	$y$

Thus, for 1:1 split injection of fuel, we have

$$\text{Pilot } A/F = x/2y = \text{Actual } A/F = 30.4$$

Therefore, Pilot  $A/F = 60.8$

For main injection,

$$\text{Main } A/F = (x + y) / y = 60.8 + 1 = 61.8$$

Thus, during main combustion, the equivalence ratio was maintained approximately as 0.5.

Therefore, the air and fuel mass flow rate employed in the simulation is:

	<b>Pilot Injection</b>	<b>Main Injection</b>
	g/sec	g/sec
<i>Air</i>	60.8	61.8
<i>Fuel</i>	1	1

**Table 3.1: Air and Fuel mass flow rate for split injection**

### 3.1.2 Split Injection Model Setup:

The split injection model was built using a network of reactor models as a cluster shown in figure 4. The simulation model is run for pilot injection timing sweep from 165 deg BTDC to 7 deg BTDC followed by the main injection at 5 deg BTDC. The steps involved in this simulation are as follows:

- **Reactor 1: IC Engine 1 (C1):** The simulation starts with first reactor that is IC Engine 1 (C1) in which only air is compressed from the starting crank angle 180 deg BTDC for the required crank angle duration. The simulation conditions for reactor 1 are shown in table 3.2. During this step, the compression of air leads to increase in temperature and pressure. The output of IC Engine1 is used to initialize the inlet source 1 (C2\_Inlet1) which connects to the Gas Mixer 1 (C2).

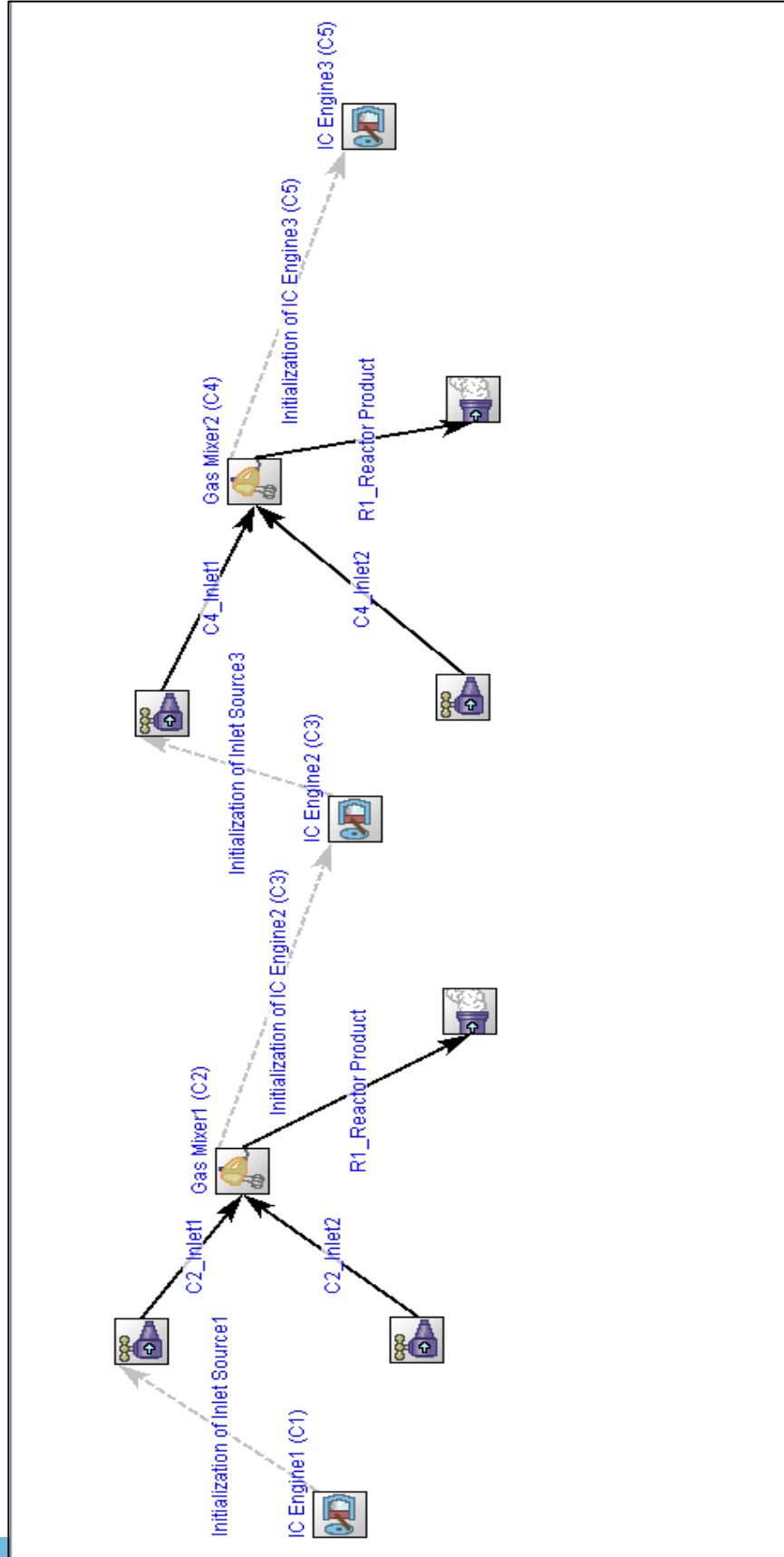


Figure 4: Chemkin Simulation Model for Split Fuel Injection in HCCI Reactor

<b>Reactor Properties</b>	
<b>IC Engine 1 (C1)</b>	0-D, Closed, Homogeneous
Compression Ratio	14
Engine Cylinder Displacement volume	500 cm <sup>3</sup>
Engine Connecting Rod to Crank Radius Ratio	3.28
Engine Speed	1200 RPM
Temperature	300 K
Pressure	1 Atm
Heat loss	0.0 Cal/sec
Starting Crank Angle (ATDC)	-180 degrees
Engine Crank Angle	-(Starting Crank Angle – Pilot Injection timing) degrees
Reactant Species Mole Fraction	N <sub>2</sub> : 0.79 O <sub>2</sub> : 0.21

**Table 3.2: Simulation conditions of Reactor 1: IC Engine 1**

- **Reactor 2: Gas Mixer 1 (C2), Inlet sources (C2\_Inlet1 & C2\_Inlet2):** The pilot fuel is added to this Gas Mixer 1 through C2\_Inlet2. Note that the Gas Mixer is a non-reactive reactor model. The temperature and pressure conditions of Gas Mixer 1, C2\_Inlet1, C2\_Inlet2 are initialized with temperature and pressure attained at the end of IC Engine1 as shown in table 3.3, 3.4 and 3.5 respectively. The Gas Mixer 1 is connected to the IC Engine 2 (C3) where the combustion of homogeneous mixture of pilot fuel and air takes place.

<b>Gas Mixer 1 (C2)</b>	Non-Reactive Gas Mixer
Temperature	Temperature at the end of IC Engine 1 (C1)
Pressure	Pressure at the end of IC Engine 1 (C1)

**Table 3.3: Simulation conditions of Reactor 2: Gas Mixer 1**

<b>C2_Inlet1</b>	Inlet Source 1 to Gas Mixer 1 (C2)
Temperature	Temperature at the end of IC Engine 1 (C1)
Mass Flow Rate	60.8 g/sec
Species	Species at the end of IC Engine 1 (C1)

**Table 3.4: Simulation conditions of Reactor 2: Inlet sources (C2\_Inlet1)**

<b>C2_Inlet2</b>	Inlet Source 2 to Gas Mixer 1 (C2)
Temperature	Temperature at end of IC Engine 1 (C1)
Mass Flow Rate	1.0 g/sec
Species	$nC_7H_{16}$ [n-Heptane]
Species [nC7H16] Mole Fraction	1

**Table 3.5: Simulation conditions of Reactor 2: Inlet sources (C2\_Inlet2)**

- **Reactor 3: IC Engine 2 (C3):** The IC Engine 2 starts at the crank angle at which the IC Engine 1 was stopped and is run until 5 deg BTDC. The temperature and pressure of the charge rises further during this stage. The conditions used for simulating this reactor are given in table 3.6. The IC Engine 2 is connected to the non-reactive Gas Mixer 2 (C4) via C4\_Inlet1 which is initialized with IC Engine 2 output.

Reactor Properties	
IC Engine 2 (C3)	0-D, Closed, Homogeneous
Compression Ratio	14
Engine Cylinder Displacement volume	500 cm <sup>3</sup>
Engine Connecting Rod to Crank Radius Ratio	3.28
Engine Speed	1200 RPM
Temperature	Initialized by Gas Mixer 1 (C2)
Pressure	Initialized by Gas Mixer 1 (C2)
Heat loss	0.0 Cal/sec
Starting Crank Angle (ATDC)	Pilot Injection timing
Engine Crank Angle	-[Pilot Injection timing-Main Injection Timing] degrees
Reactant Species Mole Fraction	Initialized by Gas Mixer 1 (C2)

**Table 3.6: Simulation conditions of Reactor 2: IC Engine 2**

- **Reactor 4: Gas Mixer 2 (C4), Inlet sources (C4\_Inlet1 & C4\_Inlet2):** The main fuel is added to the Gas Mixer 2 using C4\_Inlet2. Here the Gas Mixer 2, C4\_Inlet1, C4\_Inlet2 are initialized with temperature and pressure attained at the end of IC Engine 2 as shown below in table 3.7, 3.8 and 3.9 respectively.

<b>Gas Mixer 2 (C4)</b>	Non-Reactive Gas Mixer
Temperature	Temperature at the end of IC Engine 2 (C3)
Pressure	Pressure at the end of IC Engine 2 (C3)

**Table 3.7: Simulation conditions of Reactor 4: Gas Mixer 2**

<b>C4_Inlet1</b>	Inlet Source 1 to Gas Mixer 2 (C4)
Temperature	Temperature at the end of IC Engine 2 (C3)
Mass Flow Rate	61.8 g/sec
Species	Species at the end of IC Engine 2 (C3)

**Table 3.8: Simulation conditions of Reactor 4: Inlet sources (C4\_Inlet1)**

<b>C4_Inlet2</b>	Inlet Source 2 to Gas Mixer 2 (C4)
Temperature	Temperature at the end of IC Engine 2 (C3)
Mass Flow Rate	1.0 g/sec
Species	$nC_7H_{16}$ [n-Heptane]
Species [nC7H16] Mole Fraction	1

**Table 3.9: Simulation conditions of Reactor 4: Inlet sources (C4\_Inlet2)**



- **Reactor 5: IC Engine 3 (C5):** Finally, the main combustion takes place in the last reactor that is IC Engine 3 (C5) which is fed by Gas Mixer 2. The simulation conditions are shown in table 3.10. The combustion of main fuel results in rapid increase of temperature and pressure of the mixture, thus leading to high temperature heat release. The IC Engine 3 starts at 5 deg BTDC and was run for 20 CAD. The temperature and pressure at the start of IC Engine 2 and IC Engine 3 is the temperature and pressure attained at the end of IC Engine 1 and IC Engine 2 respectively.

<b>Reactor Properties</b>	
<b>IC Engine 3 (C5)</b>	0-D, Closed, Homogeneous
Compression Ratio	14
Engine Cylinder Displacement volume	500 cm <sup>3</sup>
Engine Connecting Rod to Crank Radius Ratio	3.28
Engine Speed	1200 RPM
Temperature	Initialized by Gas Mixer 2 (C4)
Pressure	Initialized by Gas Mixer 2 (C4)
Heat loss	0.0 Cal/sec
Starting Crank Angle (ATDC)	-5 degrees
Engine Crank Angle	20 degrees
Reactant Species Mole Fraction	Initialized by Gas Mixer 2 (C4)

**Table 3.10: Simulation conditions of Reactor 4: IC Engine 3**

The output resolution on crank angle basis is set by selecting time interval used for printing and saving the data in the output control panel of IC Engine 1, IC Engine 2 and IC Engine 3.

It was calculated and set according to the following relation:

$$t = \frac{\theta/360}{\text{speed}/60}$$

Where  $\theta$  is in CA degrees and speed is in RPM.

Therefore, at 1200 RPM, for IC Engine 1,  $t = 140 \mu\text{sec}$  for  $\theta = 1 \text{ degree}$

For IC Engine 2,  $t = 69 \mu\text{sec}$  for  $\theta = 0.5 \text{ degrees}$

For IC Engine 3,  $t = 14 \mu\text{sec}$  for  $\theta = 0.1 \text{ degrees}$

### 3.1.3 Single Fuel Injection Conditions:

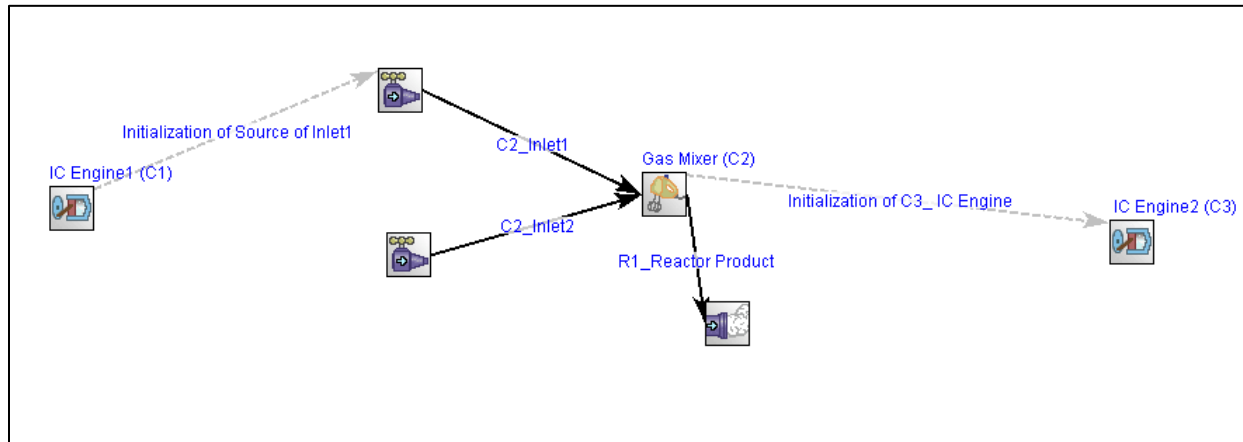


**Figure 5: Chemkin Simulation Model for Single Fuel Injection Case in HCCI Reactor**

The single injection case was simulated in order to use as a reference for split injection cases. The reactor model network was developed as shown in figure 5 to simulate the HCCI combustion for single fuel injection case. In this, we have IC Engine 1 (C1) in which only air is compressed for the required crank angle duration from 180 deg BTDC to 5 deg BTDC. This leads to increase in pressure and temperature of the charge. The reactor 1 is connected to the Gas Mixer through C2\_Inlet1. The fuel is added to the Gas Mixer by C2\_Inlet2. The non-reactive

Gas mixer is used to initialize the last reactor that is IC Engine 2 (C3) which has the starting crank angle of single fuel addition at 5 deg BTDC.

The conditions used in the first reactor (IC Engine 1) are the same as those used in the split injection model (table 3.2). The conditions for Gas Mixer and IC Engine 2 are as follows:

- **Reactor 2: Gas Mixer (C2), Inlet sources (C2\_Inlet1 & C2\_Inlet2):**

<b>Gas Mixer 1 (C2)</b>	Non-Reactive Gas Mixer
Temperature	Temperature at the end of IC Engine 1 (C1)
Pressure	Pressure at the end of IC Engine 1 (C1)

**Table 3.11: Simulation conditions of Reactor 2: Gas Mixer (C2)**

<b>C2_Inlet1</b>	Inlet Source 1 to Gas Mixer 1 (C2)
Temperature	Temperature at the end of IC Engine 1 (C1)
Mass Flow Rate	30.4 g/sec
Species	Species at the end of IC Engine 1 (C1)

**Table 3.12: Simulation conditions of Reactor 2: Inlet sources (C2\_Inlet1)**

<b>C2_Inlet2</b>	Inlet Source 2 to Gas Mixer 1 (C2)
Temperature	Temperature at the end of IC Engine 1 (C1)
Mass Flow Rate	1.0 g/sec
Species	$nC_7H_{16}$ [n-Heptane]
Species [nC7H16] Mole Fraction	1

**Table 3.13: Simulation conditions of Reactor 2: Inlet sources (C2\_Inlet2)**

The mass flow rate of air is 30.4 g/sec with fuel 1 g/sec in this case in order to maintain the equivalence ratio of the mixture at 0.5.

- **Reactor 3: IC Engine 2 (C3):**

<b>Reactor Properties</b>	
<b>IC Engine 2 (C3)</b>	0-D, Closed, Homogeneous
Compression Ratio	14
Engine Cylinder Displacement volume	500 cm <sup>3</sup>
Engine Connecting Rod to Crank Radius Ratio	3.28
Engine Speed	1200 RPM
Temperature	Initialized by Gas Mixer (C2)
Pressure	Initialized by Gas Mixer (C2)
Heat loss	0.0 Cal/sec
Starting Crank Angle (ATDC)	Main Injection timing =-5 degrees
Engine Crank Angle	20 degrees
Reactant Species Mole Fraction	Initialized by Gas Mixer (C2)

**Table 3.14: Simulation conditions of Reactor 3: IC Engine 2**

## CHAPTER 4

### RESULTS AND DATA ANALYSIS

This section shows the results obtained for different pilot injection sweep from 165 deg BTDC to 7 deg BTDC followed by a main injection at 5 deg BTDC in Chemkin based simulation of split injection in HCCI Engine. The effect of split injection on important parameters of the engine such as pressure, temperature, and rate of heat release during the entire cycle is analyzed. Moreover, the chemical kinetic changes taking place during pilot combustion and its impact on the main combustion is also examined.

#### 4.1 Pressure and Temperature Profiles:

The pressure and temperature traces were plotted using the results obtained from the Chemkin simulation of split injections as shown in figure 6a and figure 7a, respectively. They show the pressure and temperature profiles obtained from the HCCI engine simulation for the pilot injection timing sweep from 165 deg BTDC to 7 deg BTDC. The pressure and temperature trace of a single fuel injection (5 deg BTDC) case is also shown in the figure. The change in pressure and temperature is clearly visible in the shown figure which is the result of ignition of the pilot fuel followed by ignition of main fuel.

For the different pilot injection timings from -165 CAD to -7 CAD, the pressure is rising gradually but the ignition takes place only later in the cycle that is from -10 CAD onwards as seen in figure 6a and figure 6b. Once the ignition of pilot fuel occurs, there is further rise in pressure and temperature of the mixture due to the associated heat release.

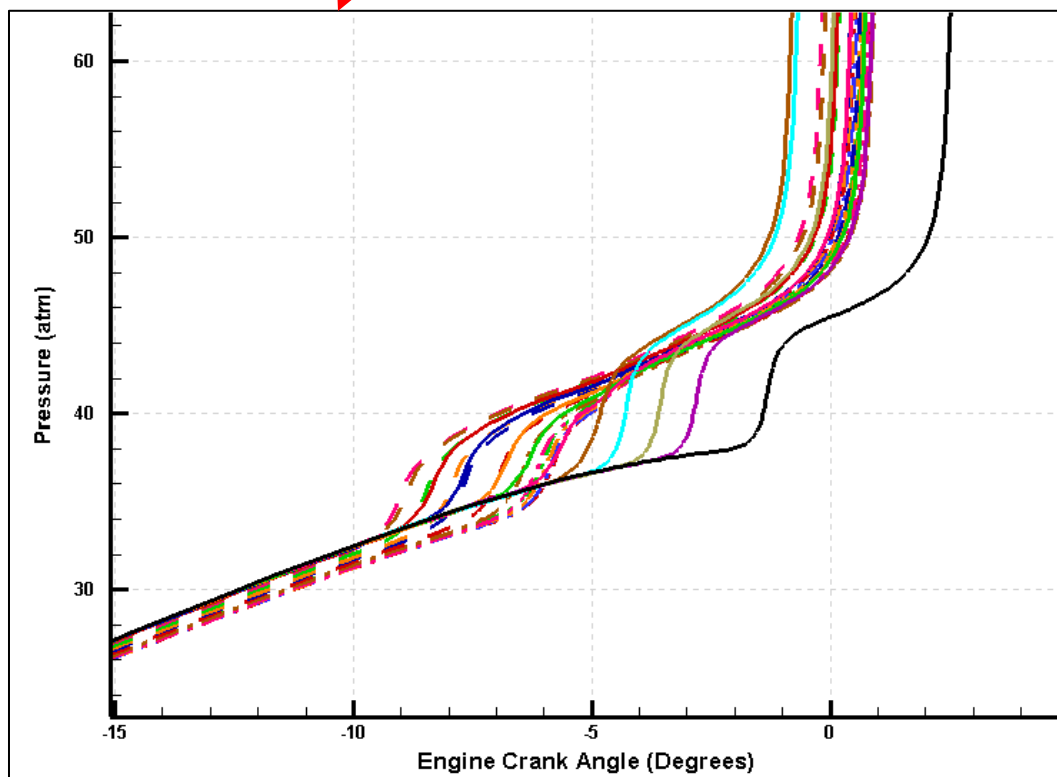
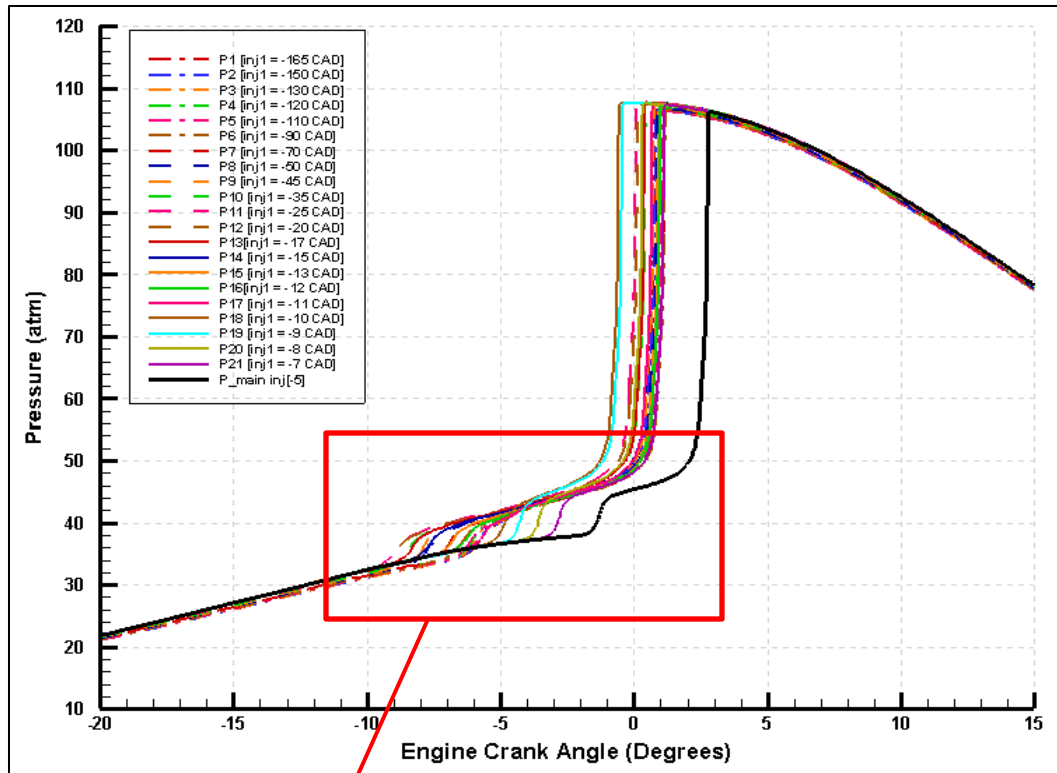


Figure 6a: Pressure Traces for the split injection simulation for all the reactors combined; Figure 6b: Zoomed-in pressure traces showing increase in pressure due to pilot ignition

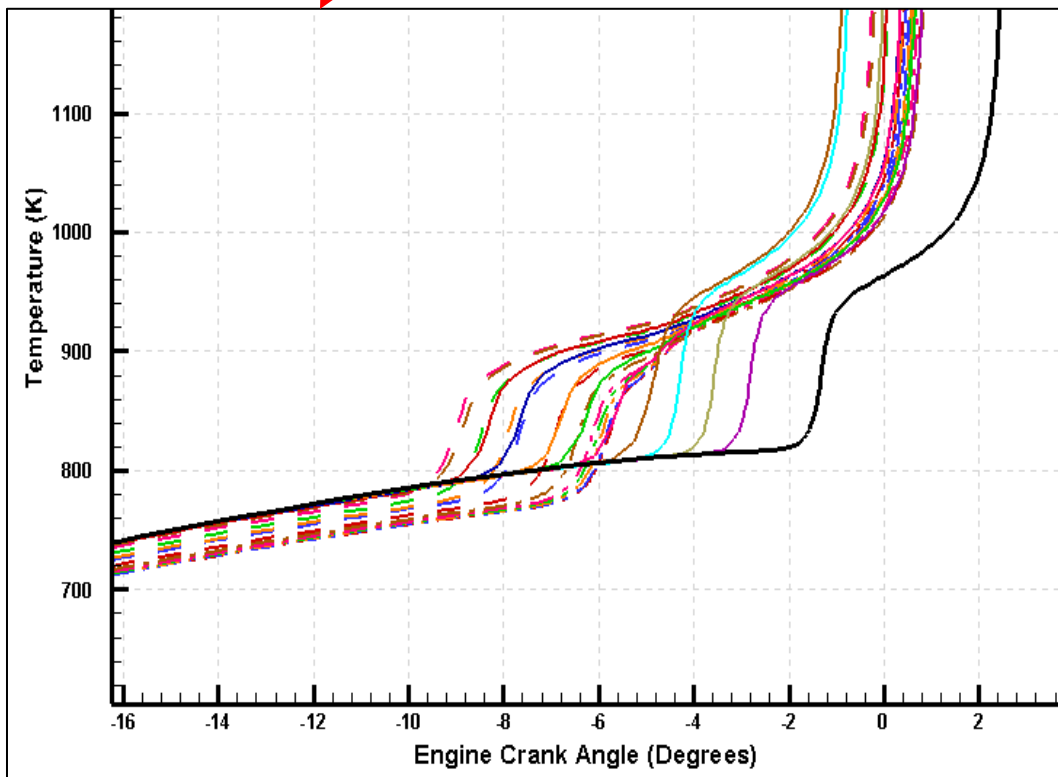
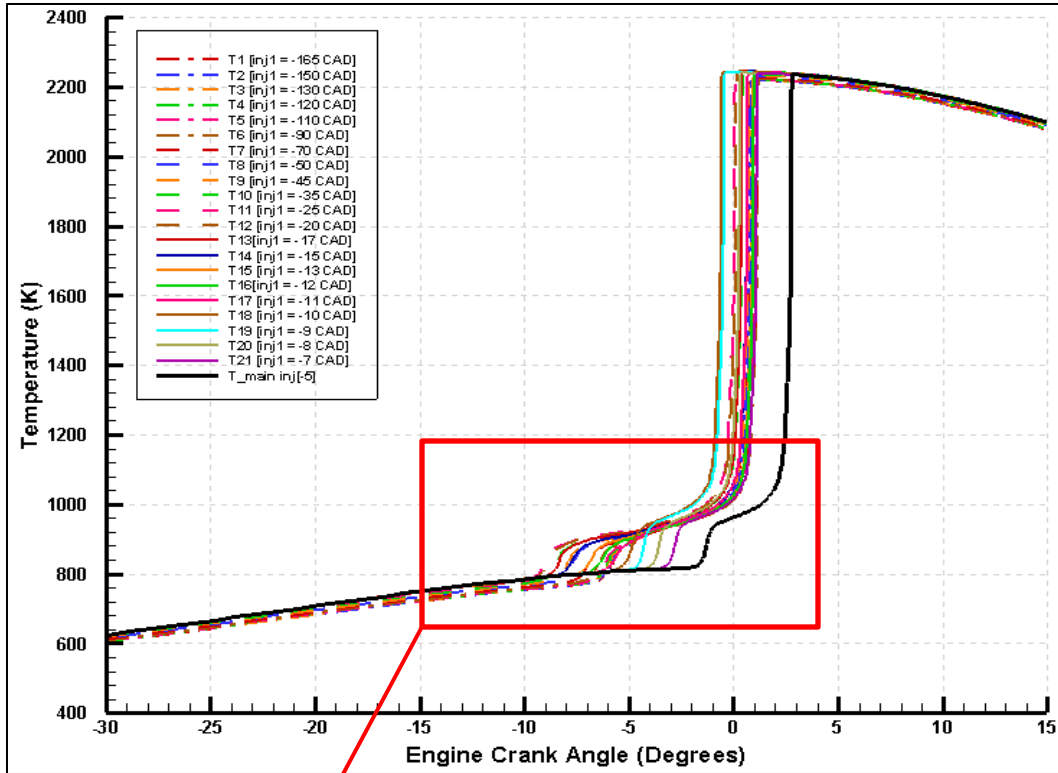


Figure 7a: Temperature traces for the split injection simulation for all the reactors combined; Figure 7b: Zoomed-in temperature traces showing increase in temperature due to pilot ignition

The pilot fuel ignition followed by ignition of main fuel at -5 CAD results in rapid increase in pressure and temperature. The pressure and temperature reach their peak values near TDC. It can be inferred from the plots that the ignition of the pilot fuel takes place only when a certain temperature ( $>750$  K) is reached as shown in figure 7b which also shows that the start of combustion of pilot fuel does not depend on the pilot injection timing.

#### 4.2 Rate of Heat Release Profiles:

The heat released per crank angle degree (RHR) was plotted with respect to temperature using the simulation results as illustrated in figure 8a. The maximum RHR reached in the entire cycle (after main fuel addition) is approximately equal to 2600 Cal/deg for the entire pilot injection timing sweep. The heat release plots show the different stages of heat released during the entire cycle. Four stages of heat release was observed in the entire cycle (figure 8a and figure 9) -

i. LTHR of the pilot fuel ignition

which is followed by three stage ignition of main fuel-

ii. LTHR of the main fuel ignition,

iii. ITHR of the main fuel ignition,

iv. HTHR of the main fuel ignition.

The change in RHR with temperature as shown in figure 8a displays the temperature of the mixture during LTHR of the pilot fuel ignition, LTHR and HTHR of main fuel ignition. The low temperature heat release of the pilot fuel ignition and LTHR of the main fuel ignition can be clearly seen in figure 8b. The main fuel ignition shows an intermediate temperature heat release (ITHR) between the LTHR and HTHR of main fuel ignition. It appeared as a small peak or shoulder on the main HTHR trace (as seen in figure 8a and 9) unlike



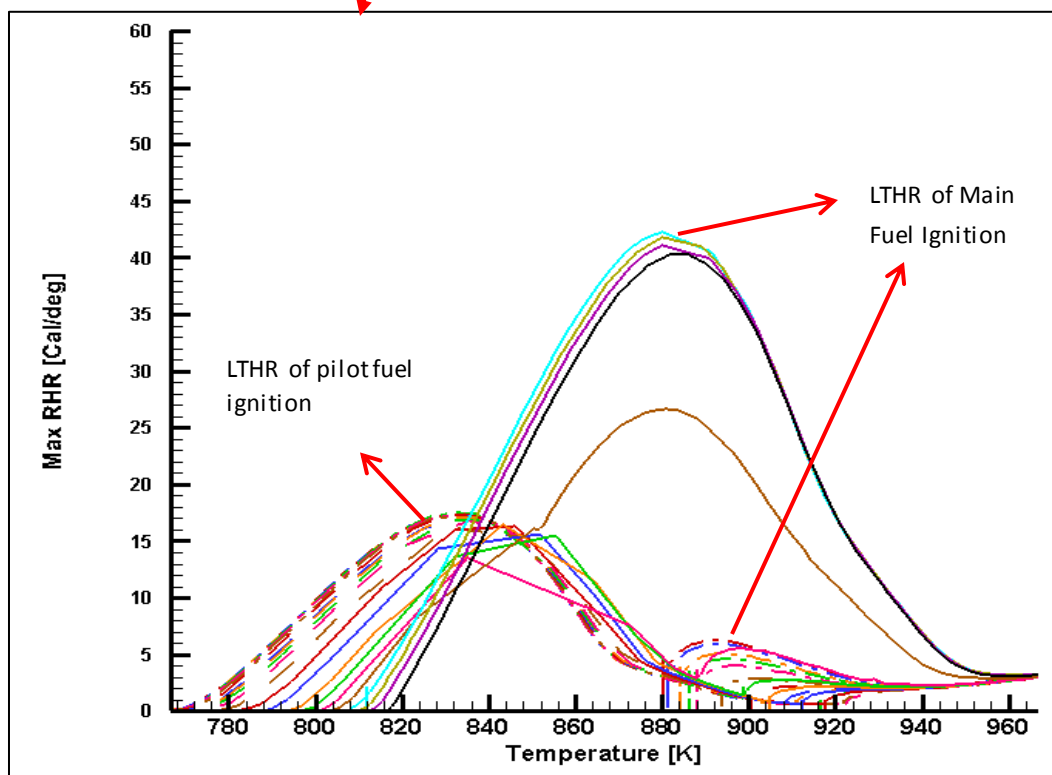
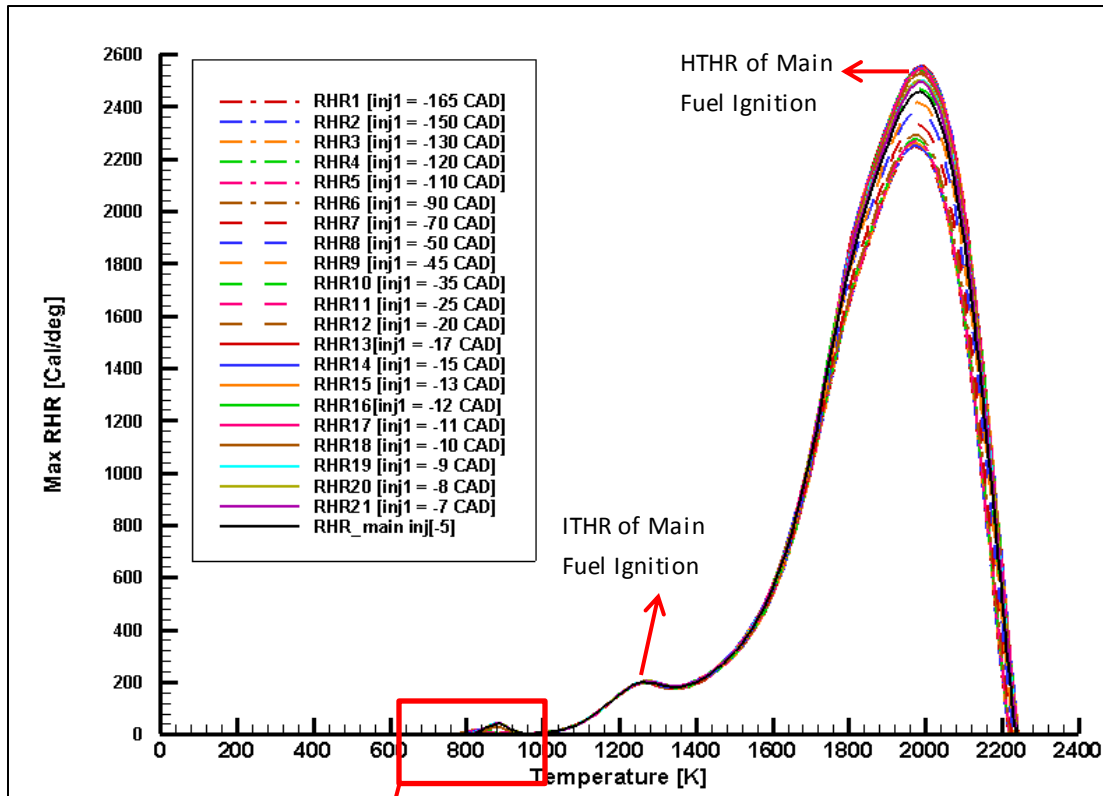


Figure 8a: Change in RHR traces with temperature for the split injection simulation for all the reactors combined; Figure 8b: Zoomed-in heat release traces showing LTHR of pilot fuel ignition and LTHR of Main fuel ignition

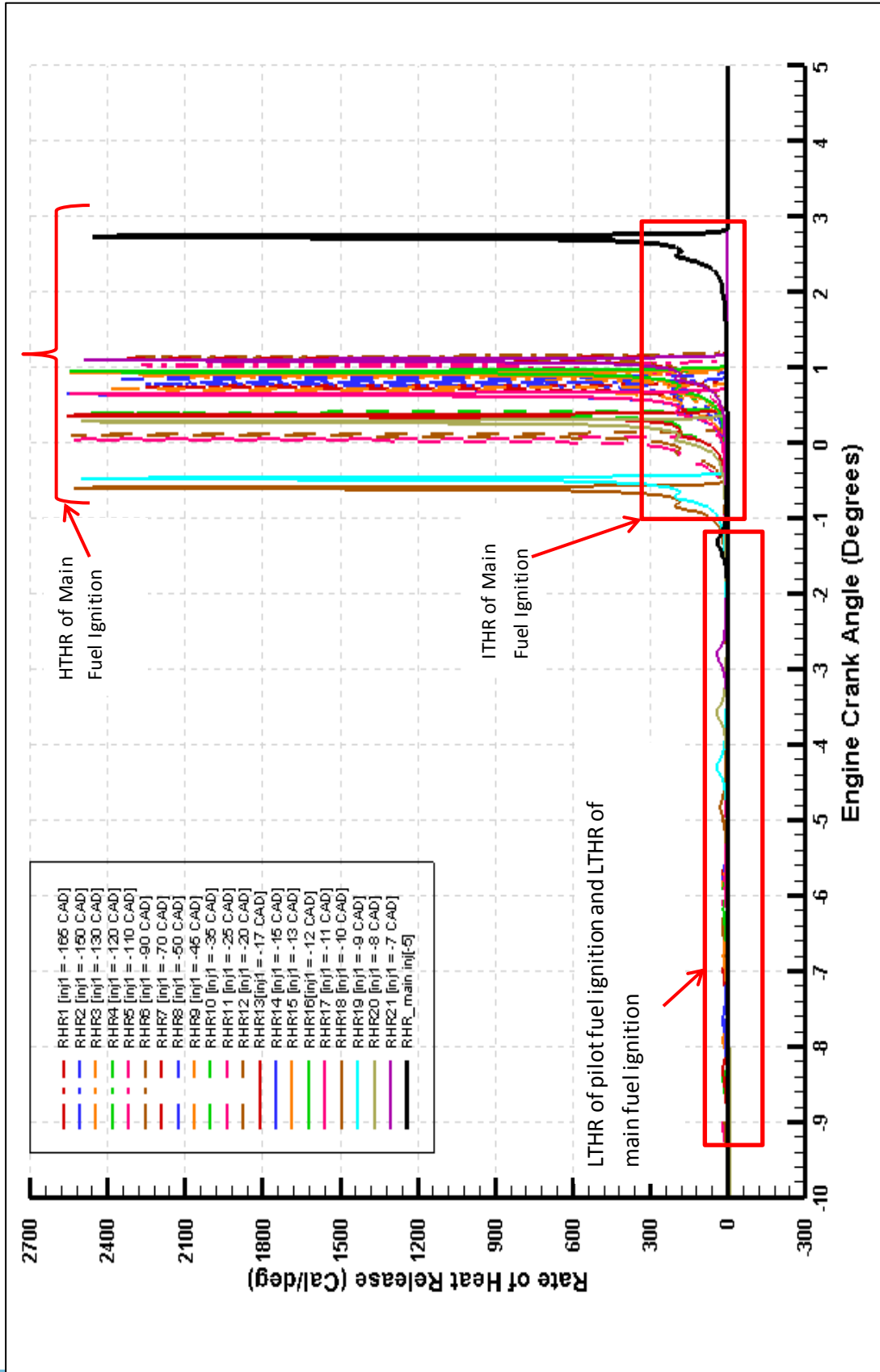


Figure 9: Heat Release traces for the split injection simulation for all the reactors combined showing different stages of heat release events

LTHR which appears as a separate peak before HTHR. The ignition of pilot fuel starts after 750 K. The peak magnitude of low temperature heat release due to pilot ignition takes place when the temperature reaches around 820 K to 860 K. The addition of main fuel to this mixture formed by pilot ignition at this temperature adds more chemical energy and is followed by LTHR peak of main fuel ignition occurring when temperature is in between 860 K to 920 K. The ITHR peak occurs at temperature approximately equal to 1250 K. The HTHR peak of main fuel ignition occurs when the temperature is very high (approximately between 1900K- 2000 K).

The heat released per crank angle degree (RHR) was plotted with respect to CAD using the simulation results as illustrated in figure 10a. Figure 10b shows the first stage heat release in split injection due to the combustion of pilot fuel as well as the LTHR of the main fuel ignition. The ignition of pilot fuel takes place after -10 CAD in the cycle. This can be due to the temperature required for the initiation of successful combustion of the pilot fuel. It was observed from temperature profile that the minimum temperature required for ignition of pilot fuel is approximately equal to 750 K as seen in figure 7b and figure 8b. Therefore, although the mixture is homogeneous, the ignition starts only when the required conditions are met. The chemistry of the pilot fuel combustion plays an important role in the combustion and combustion phasing of the main fuel.

For advanced pilot injection timings (-165 CAD to -90 CAD), the heat release of the pilot fuel ignition is followed by three stage ignition of the main fuel (figure 11a). When the main fuel is added at -5 CAD into the ignited mixture of pilot fuel and air, a low temperature regime characterized by LTHR of the main fuel can be clearly seen in the shown figure. This LTHR is

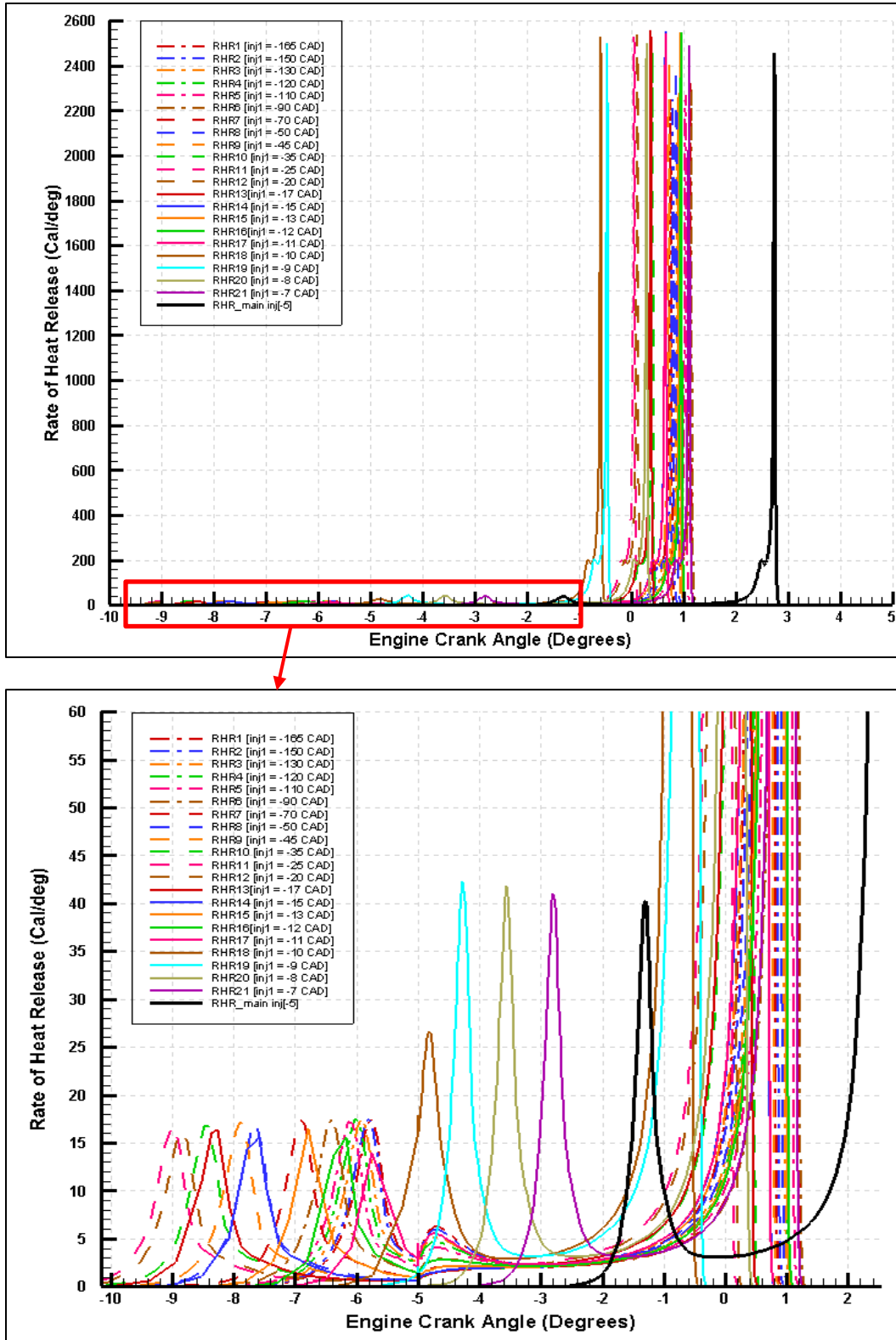


Figure 10a: Heat Release traces for the split injection simulation for all the reactors combined; Figure 10b: Zoomed-in heat release traces showing LTHR of pilot fuel ignition and LTHR of main fuel ignition

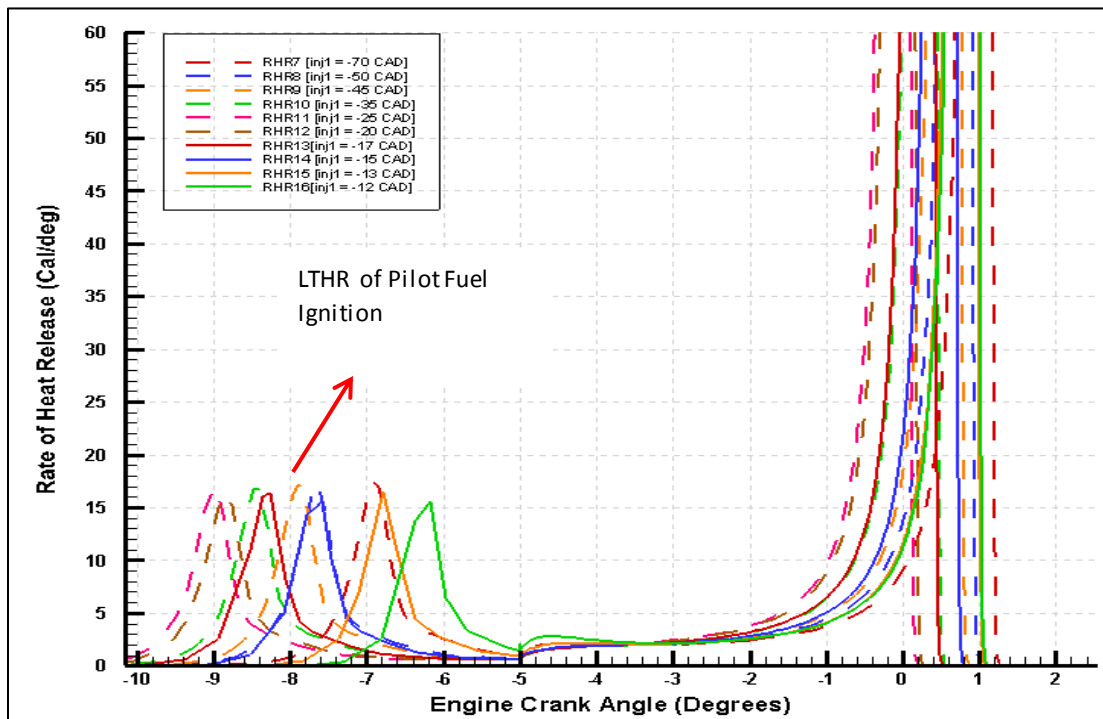
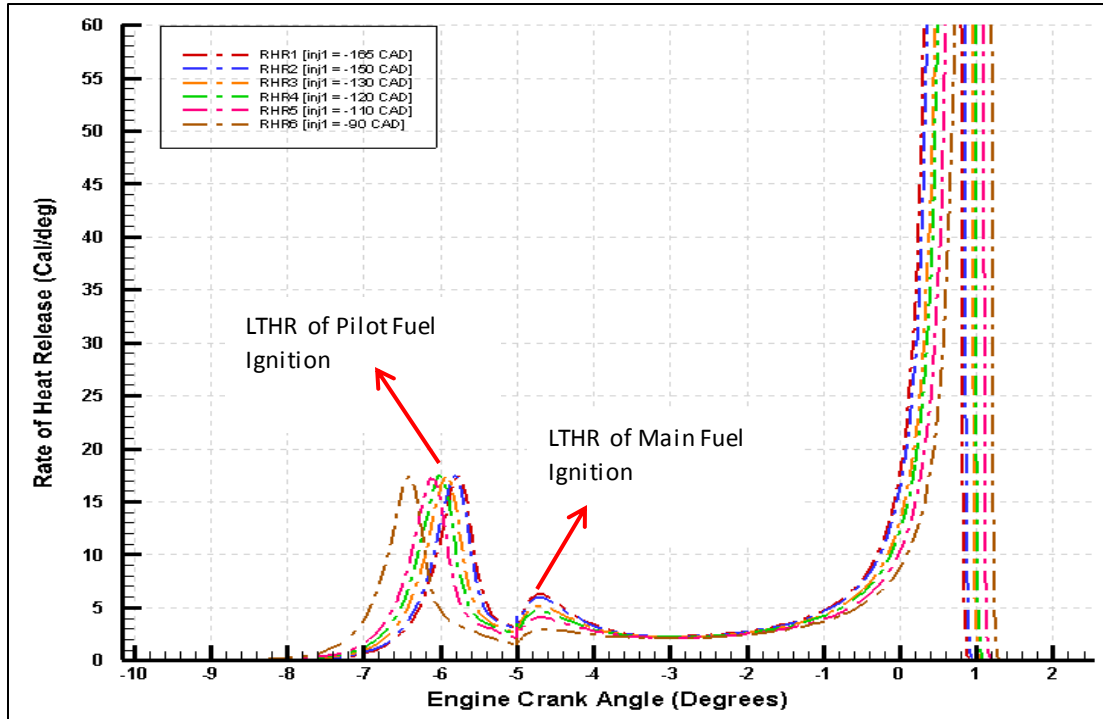


Figure 11a: Zoomed-in heat release traces showing initial heat release for pilot timings from -165 CAD to -90 CAD; Figure 11b: Zoomed-in heat release traces showing initial heat release for pilot timings from -70 CAD to -12 CAD

followed by NTC regime which is shown by the drop in heat release rate. The start of ITHR followed by HTHR of the main fuel takes place after a few crank angle degrees (~4 CAD) as seen in figure 9 or 10a. The pilot injection timings from -165 CAD to -90 CAD exhibit all the four stages of heat release- first stage of heat release due to the pilot fuel ignition, second stage is LTHR of the main fuel ignition, and third stage is ITHR of the main fuel ignition and fourth stage as HTHR of the main fuel ignition.

On the other hand, the pilot injections timings from -70 CAD to -12 CAD do not exhibit the all the stages of ignition of the main fuel as shown in figure 11b. In these cases, the LTHR together with NTC regime of the main ignition is very low that it can be considered negligible. Therefore, these pilot timings have the first stage of heat release due to pilot ignition which is directly followed by the main fuel ITHR and HTHR.

For the pilot injection at -11 CAD, all the four stages of heat release appear in the combustion cycle (figure 11c) - the first stage of heat release due to pilot fuel ignition seen at ~-6.5 CAD which is then followed by the second stage heat release due to the main fuel ignition i.e. LTHR at -5 CAD with the third and fourth stage of heat release of the main fuel ignition happening later in the cycle around TDC.

For pilot injection timing -10 CAD, it can be seen from figure 11c that the first stage heat release due to the ignition of the pilot fuel starts before the main fuel is added at -5 CAD but as soon as the main fuel is added to the pilot mixture, heat release rates increase starting at -5 CAD as seen in figure 11c. It seems that the heat released here is due to the oxidation of both, pilot as well as the main fuel; this could be the reason because the magnitude of the heat release here is relatively greater than that for the advanced pilot injection timings from -165 CAD to -11 CAD. Also, the ITHR and HTHR of the main fuel ignition for the pilot timing at -10 CAD is advanced than other pilot injection cases.

Furthermore, as the pilot injections are retarded from -9 CAD to -7 CAD, it appears that the ignition of pilot fuel does not occur (figure 11c). When the main fuel is injected at -5 CAD into these retarded pilot fuel and air mixtures, the LTHR of the main fuel ignition takes place with more intense LTHR peaks than for the other advanced pilot timings. These cases i.e. pilot injection timings from -9 CAD to -7 CAD behave more like the single fuel injection case. The LTHR is followed by NTC regime leading finally to ITHR and HTHR.

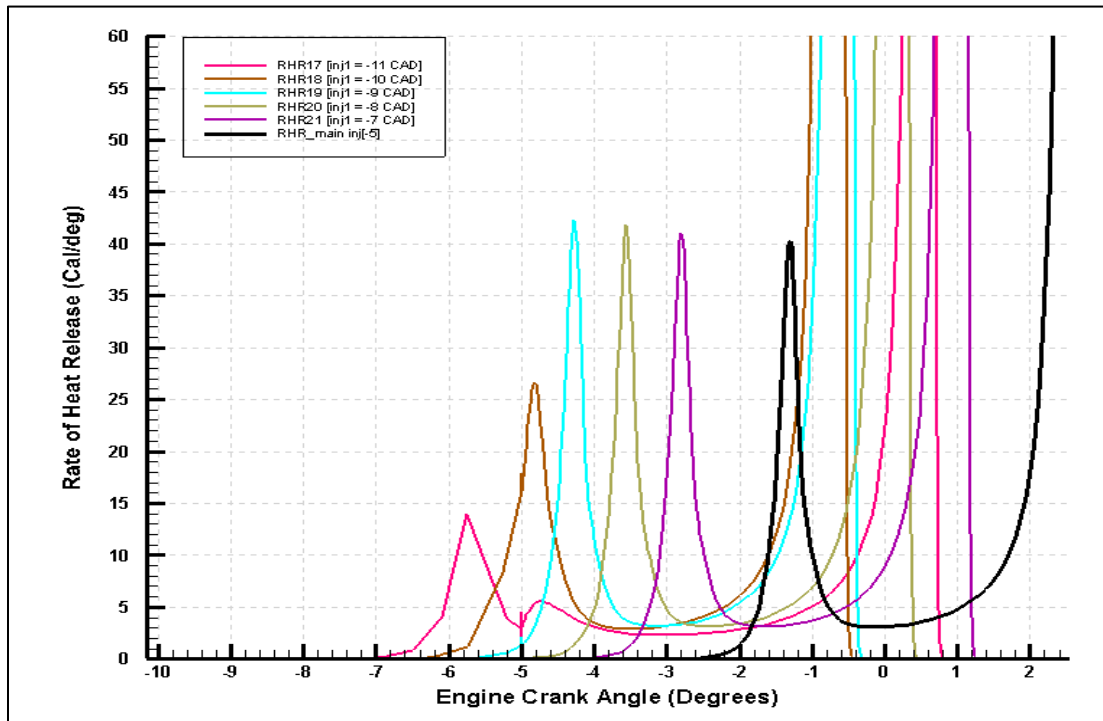


**Figure 11c: Zoomed-in heat release traces showing initial heat release for pilot timings from -11 CAD to -7 CAD and single injection case (-5 CAD)**

The third stage of heat release event, i.e. ITHR, occurred for all the pilot injection timings cases. The LTHR and ITHR showed correlation with  $\text{HO}_2$  species as shown in figure 12 for the pilot injection timing case of -25 CAD. Both of these heat release events start with increase in  $\text{HO}_2$  mole fraction and reach their peak value when  $\text{HO}_2$  is also at its peak level. Once the  $\text{HO}_2$  level starts to decrease, the LTHR and ITHR also decline. This shows that the  $\text{HO}_2$  plays an important role here.

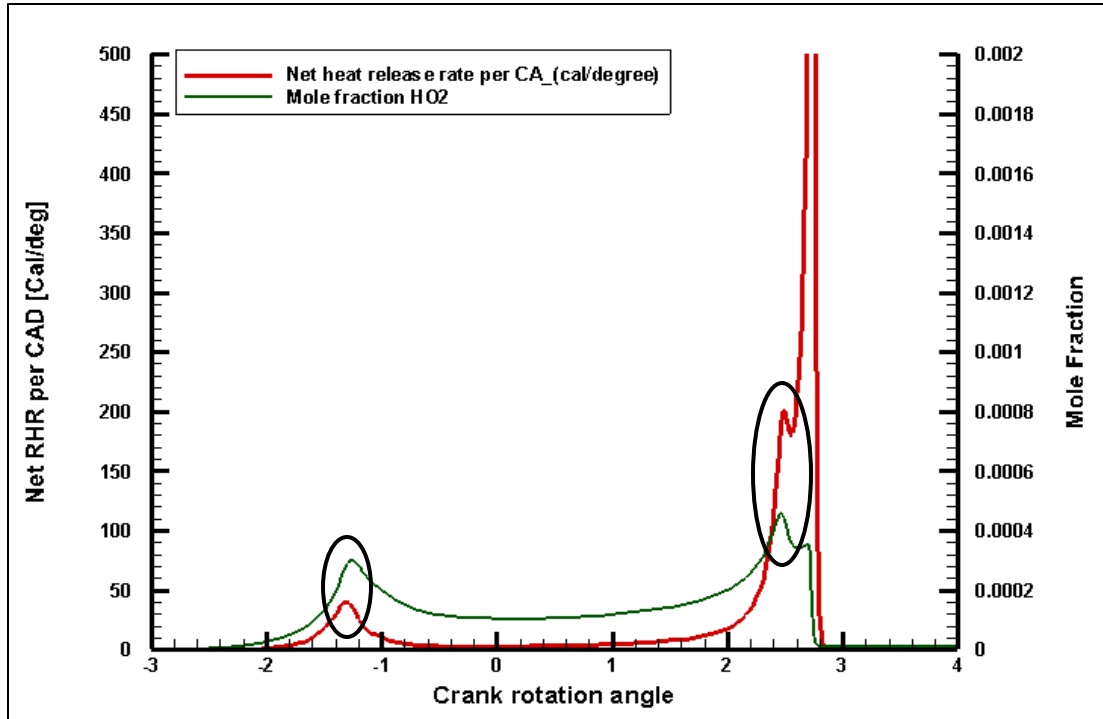


**Figure 12: Relation between net heat release rate per CAD and HO<sub>2</sub> mole fraction for pilot injection timing of -25 CAD**

The combustion phasing of the main fuel ignition for all the varied pilot injection timings occur in an unusual way during the combustion cycle as shown in figure 13. The plot also shows the temperature, pressure and accumulated heat release at the start of main fuel addition i.e. 5 deg BTDC. The accumulated heat release is highest for the pilot injection timing of -25 CAD compared to other pilot timings; which also results into high amount of heat release due to main fuel ignition for that particular pilot timing. The crank angle at which the maximum heat release takes place is observed to show varying trend. It gets retarded with pilot injection timings from -165 CAD to -90 CAD; then advances for pilot injection timings between -90 CAD to -25 CAD; again gets retarded for pilot injection timings from -20 CAD to -12 CAD; advances for pilot injection timings between -12 CAD to -10 CAD; finally again shows retarded behavior for pilot injection timings from -10 CAD onwards up to -7 CAD. The HTHR of -10 CAD pilot injection timing is advanced than other pilot injection timings. The single injection case has the retarded



combustion phasing compared to all the split injection cases. The single injection case has the LTHR at around 1.5 CAD BTDC with HTHR peak event at 2.8 CAD ATDC.

This combustion phasing due to different pilot injection timings could be the result of substantial chemical changes happening before the main fuel addition. This is explained in the next section.

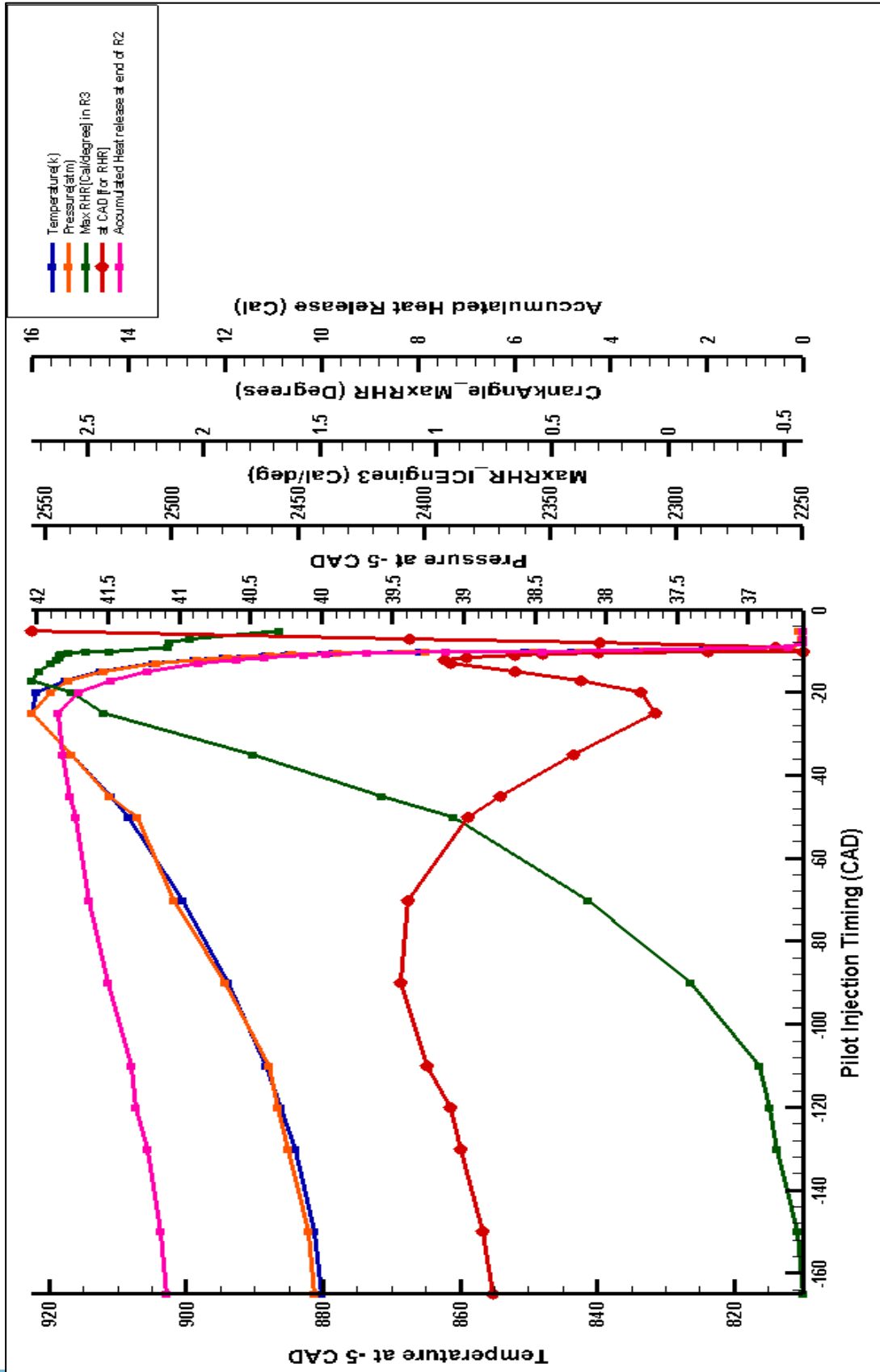


Figure 13: Temperature, Pressure and Accumulated heat release at 5 deg BTDC; Max RHR due to main fuel ignition and its crank angle location for different pilot injection timings from -165 CAD to -7 CAD and for the single injection (-5 CAD) only case

### 4.3 Species Profile for the different pilot injection timings:

The chemical species formed due to the reactions during the combustion of the pilot fuel/air mixture plays a significant role in the combustion of the main fuel/air mixture and its phasing during the combustion cycle. The mole fractions of species obtained in the cycle were normalized by their maximum value for their particular case. The normalized mole fraction of species present at the beginning of main fuel injection i.e. at -5 CAD is plotted with respect to the pilot injection sweep from -165 CAD to -5 CAD as shown in figure 14. The pressure and temperature of the mixture at the start of main injection is also shown. The maximum net heat release rate occurring in the last reactor due to the main injection is plotted along with the crank angle location of it for the different pilot injection timings. The time taken by the main fuel to achieve high temperature heat release or maximum net heat release rate after it is added at -5 CAD indicates the combustion phasing of the main fuel ignition. In order to analyze the kinetic effect of the different species formed in the second reactor (I C Engine 2) on the ignition of the main fuel in the last reactor (I C Engine 3), top 40 species according to their mole fractions were considered at -5 CAD. Although top 40 species were considered, the plot shows the traces of 36 species which were common to all the cases of pilot timings. The 4 species which were not common in all did not seem to be significant enough to have an impact on the combustion phasing and are not shown in this plot. The plot shown in figure 14 is simplified in figures 14a, 14b, 14c, 14d, 14e and 14f; by plotting only few species in each of the figure.

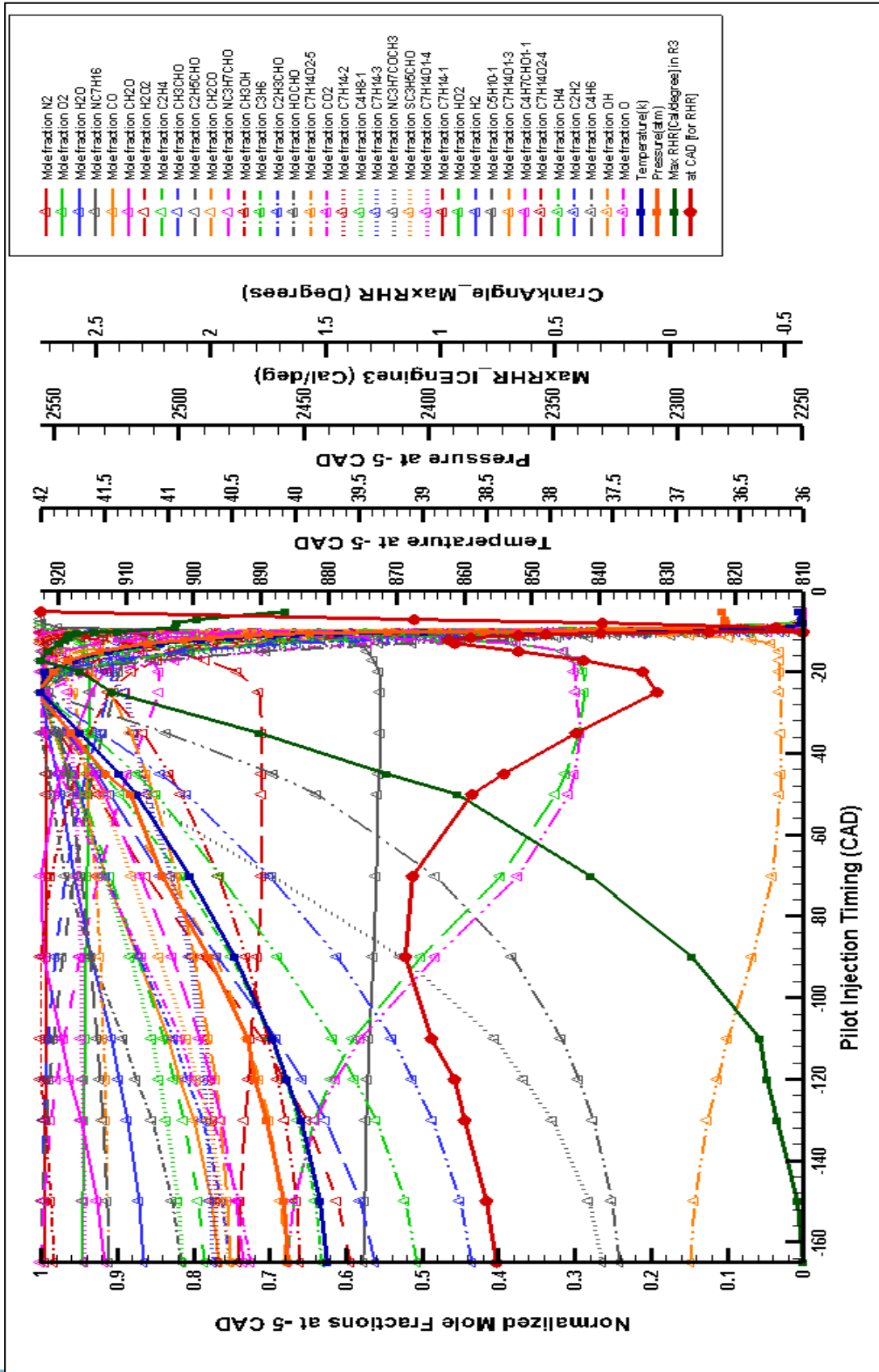


Figure 14: Normalized Mole Fraction of different species, Temperature & Pressure at 5 deg BTDC; Max RHR due to main injection and its crank angle location for different pilot injection timings from -165 CAD to -7 CAD and for the single injection (-5 CAD) only case

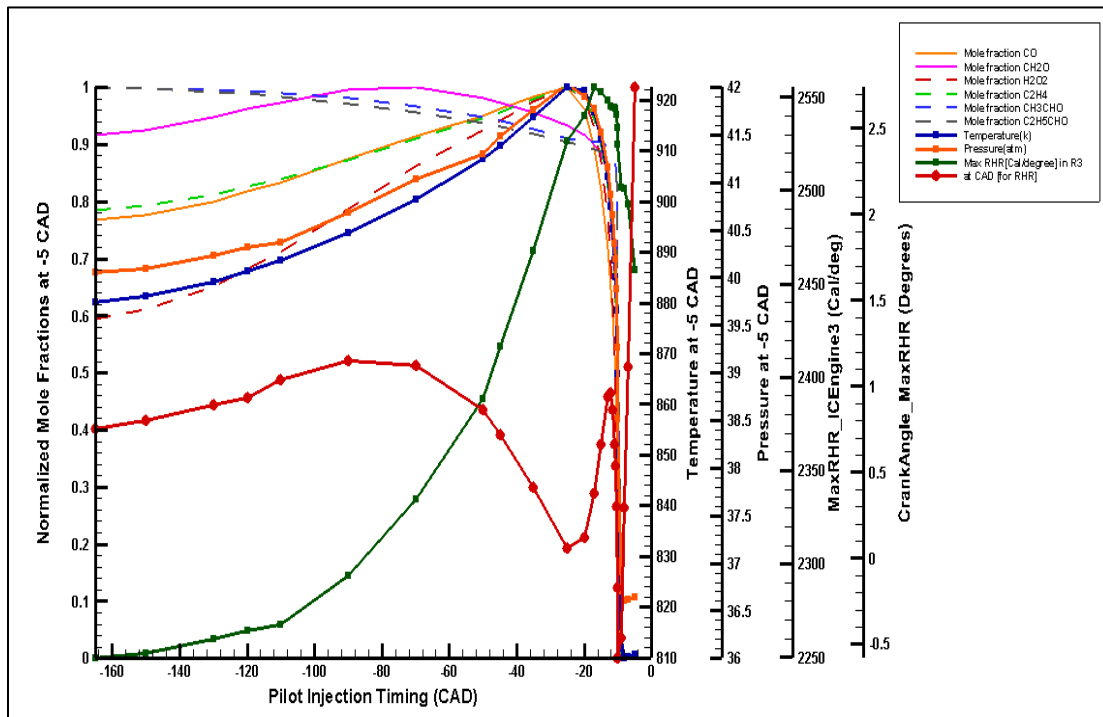
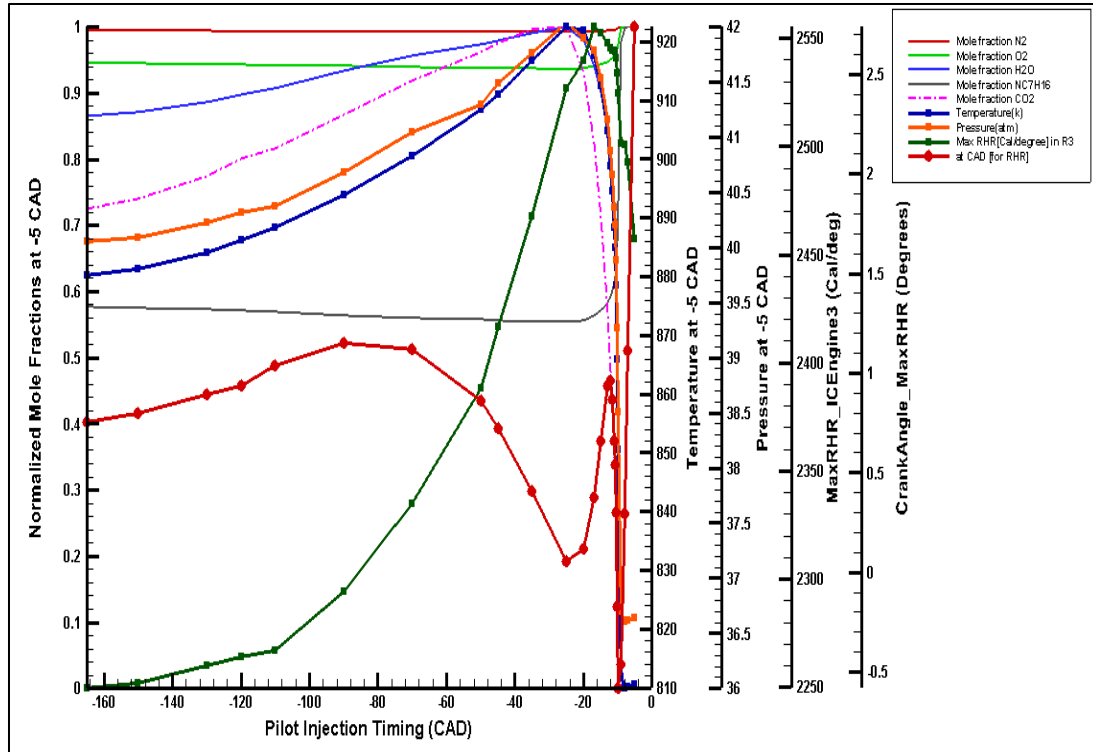
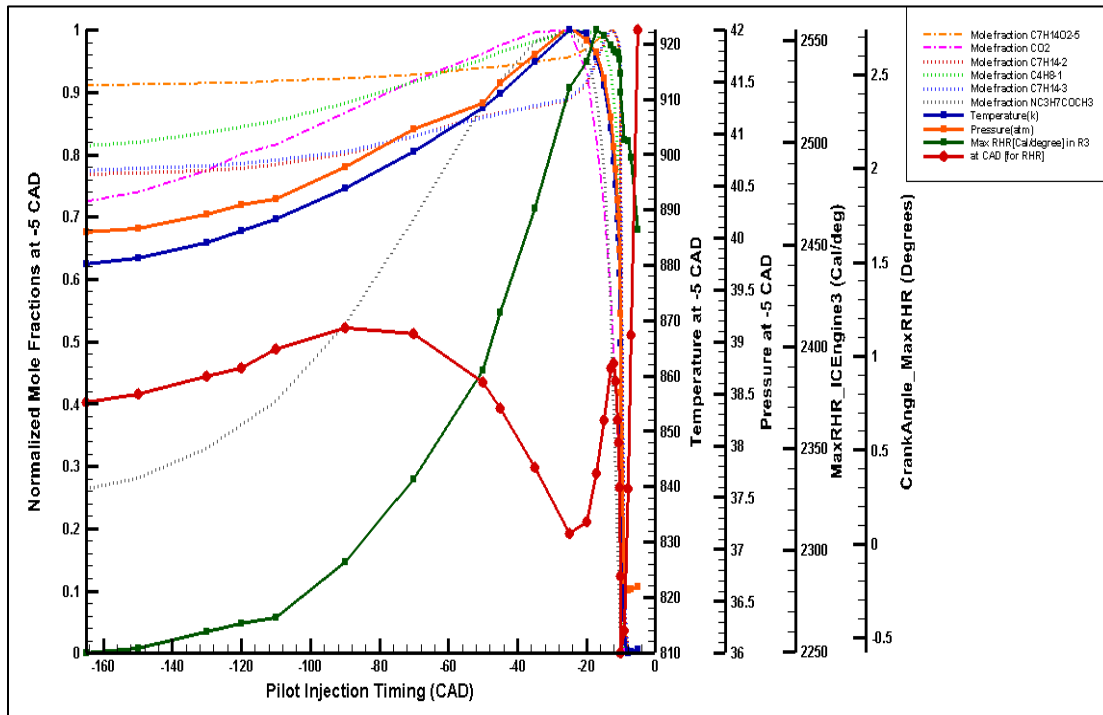
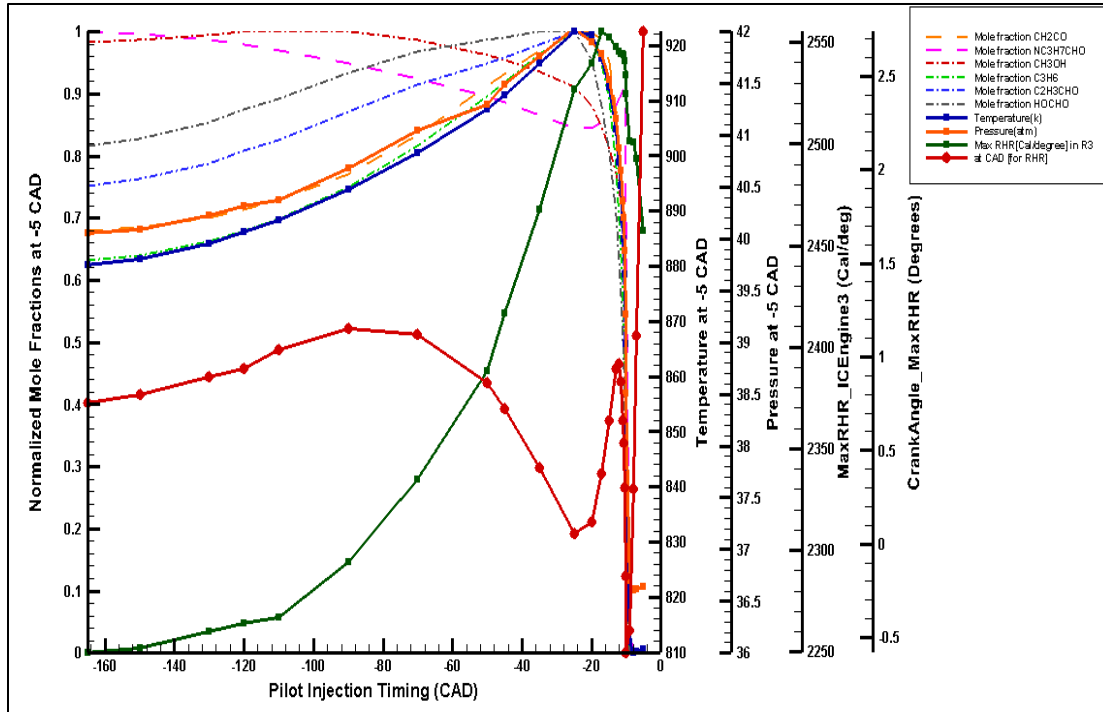
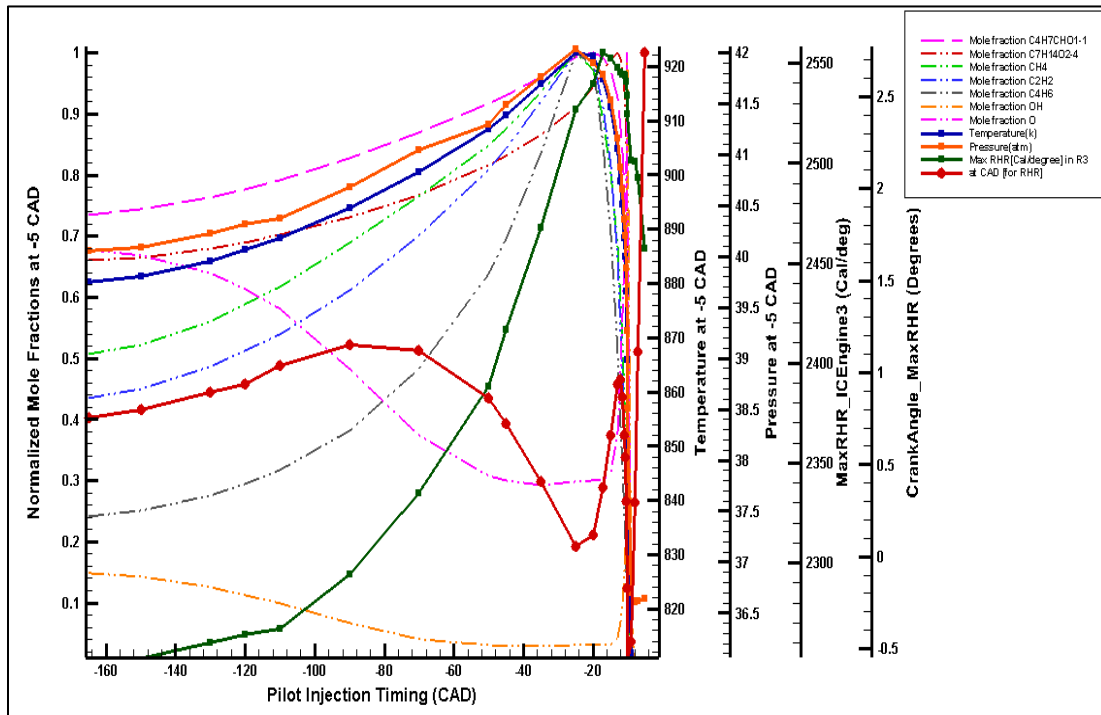
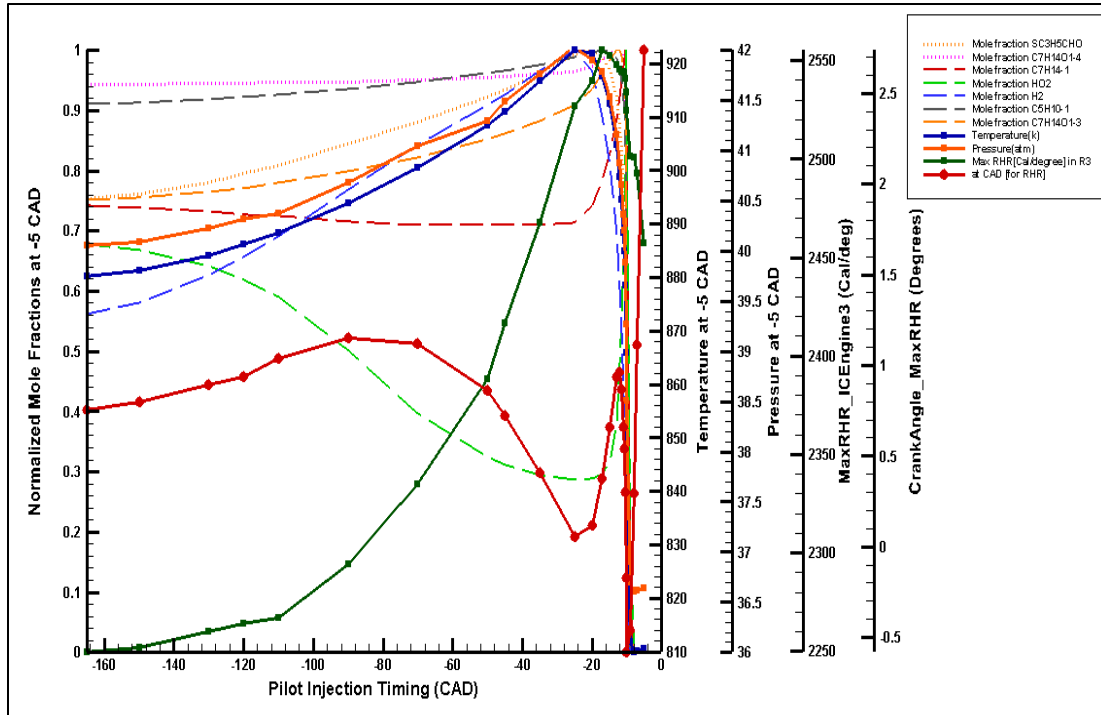


Figure 14a: Change in Normalized Mole Fraction of  $N_2$ ,  $O_2$ ,  $H_2O$ ,  $NC_7H_{16}$  and  $CO_2$  for different pilot injection timings and single fuel injection case; Figure 14b: Change in Normalized Mole Fraction of  $CO$ ,  $CH_2O$ ,  $H_2O_2$ ,  $C_2H_4$ ,  $CH_3CHO$  and  $C_2H_5CHO$  for different pilot injection timings and single fuel injection case



**Figure 14c: Change in Normalized Mole Fraction of  $\text{CH}_2\text{CO}$ ,  $\text{NC}_3\text{H}_7\text{CHO}$ ,  $\text{CH}_3\text{OH}$ ,  $\text{C}_2\text{H}_3\text{CHO}$  and  $\text{HOCHO}$  for different pilot injection timings and single fuel injection case; Figure 14d: Change in Normalized Mole Fraction of  $\text{C}_7\text{H}_{14}\text{O}_2-5$ ,  $\text{CO}_2$ ,  $\text{C}_7\text{H}_{14}-2$ ,  $\text{C}_4\text{H}_8-1$ ,  $\text{C}_7\text{H}_{14}-3$  and  $\text{NC}_3\text{H}_7\text{COCH}_3$  for different pilot injection timings and single fuel injection case**



**Figure 14e:** Change in Normalized Mole Fraction of  $\text{SC}_3\text{H}_5\text{CHO}$ ,  $\text{C}_7\text{H}_{14}\text{O}_{1-4}$ ,  $\text{C}_7\text{H}_{14}-1$ ,  $\text{HO}_2$ ,  $\text{H}_2$ ,  $\text{C}_5\text{H}_{10}-1$  and  $\text{C}_7\text{H}_{14}\text{O}_{1-3}$  for different pilot injection timings and single fuel injection case; **Figure 14f:** Change in Normalized Mole Fraction of  $\text{C}_4\text{H}_7\text{CHO}_{1-1}$ ,  $\text{C}_7\text{H}_{14}\text{O}_{2-4}$ ,  $\text{CH}_4$ ,  $\text{C}_2\text{H}_2$ ,  $\text{C}_4\text{H}_6$ ,  $\text{OH}$  and  $\text{O}$ ; Temperature and Pressure at 5 deg BTDC for different pilot injection timings and single fuel injection case

In order to explain the effect of species on ignition delay shown in figure 14, it is being divided into three parts- Part A, Part B and Part C as presented in figure 15. The following is the division of pilot injection timings by taking into consideration their effect on the ignition delay of the main fuel ignition:

1. Part A – Pilot injection timings from 165 CAD BTDC to 90 CAD BTDC
2. Part B – Pilot injection timings between 90 CAD BTDC to 12 CAD BTDC
3. Part C – Pilot injection timings between 12 CAD BTDC to 7 CAD BTDC; & Single injection case at 5 CAD BTDC

The pilot injection timings were divided into three parts because each part shows a specific behavior which is due to a particular reason playing an important role in that respective part. This is explained in the following sections as follows:



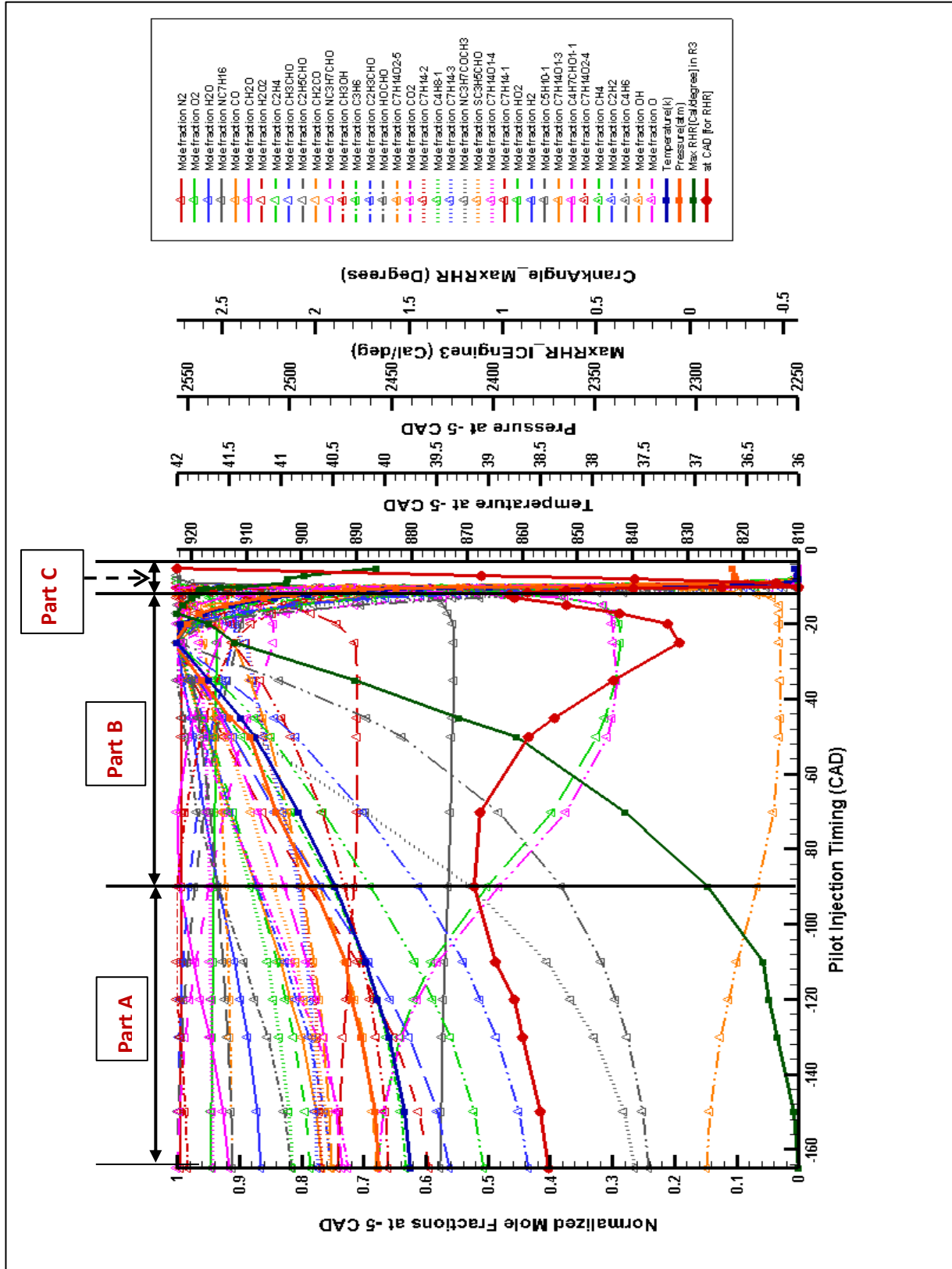
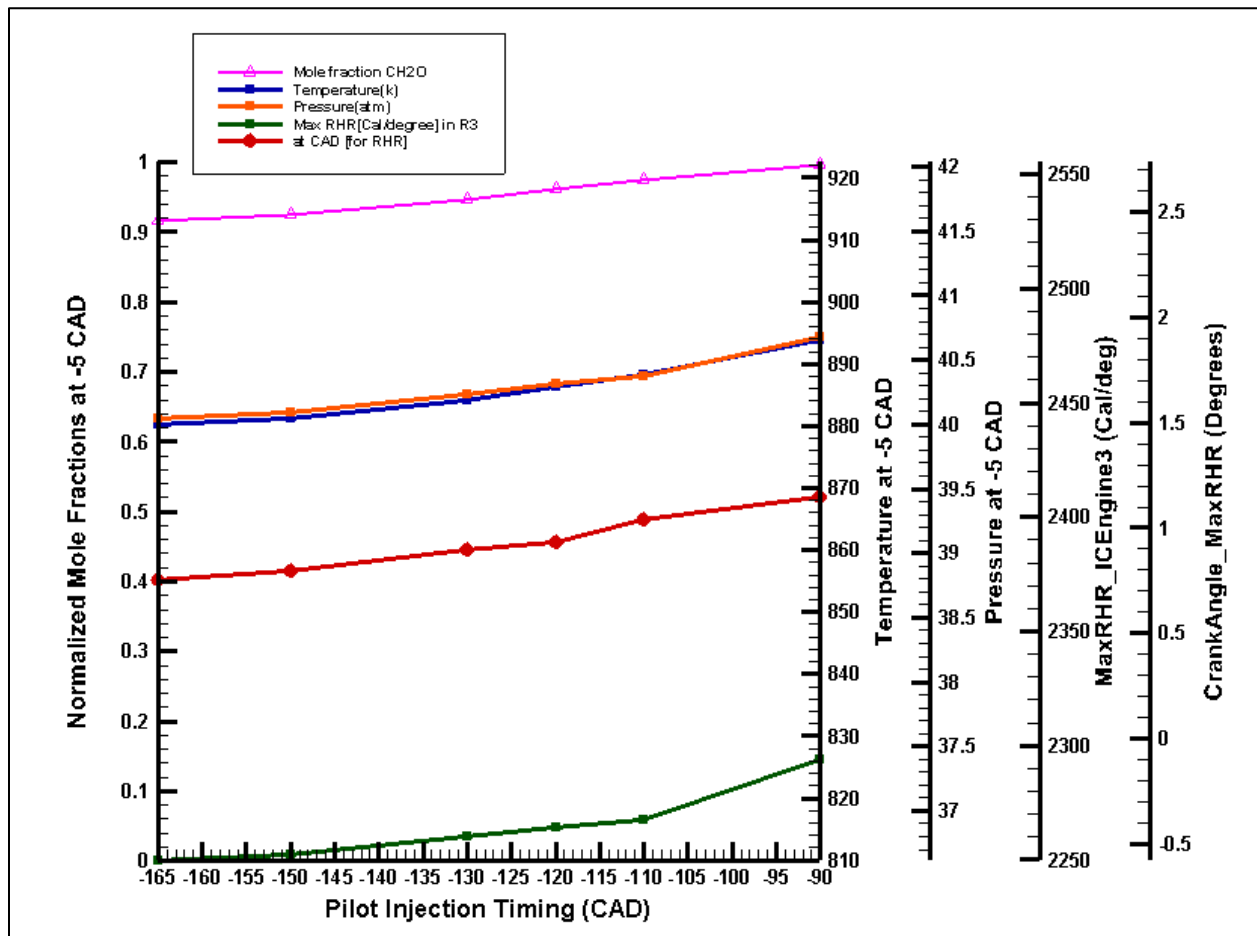


Figure 15: Division of species profile into three parts

#### 4.3.1 Part A: Pilot injection timings from 165 CAD BTDC to 90 CAD BTDC



**Figure 16: Part A- Effect of Pilot injection timings from -165 CAD to -90 CAD on Main Ignition**

This part deals with the effects of very advanced pilot injection timings (from -165 CAD to -90 CAD) on the ignition of the subsequent main injection. Figure 16 shows that as the pilot timing is retarded from -165 CAD to -90 CAD, the combustion phasing of the HTHR of the main ignition is delayed. In this part, the temperature and pressure at the start of main fuel addition is increasing with retarded pilot injection timings as the effect of compression of the charge in the reactor 1 and reactor 2; and so is the maximum heat released per CAD (HTHR) of main fuel ignition in the last reactor. The initial temperature and pressure have shown to advance the ignition delay of main injection in the literature. Although the temperature and pressure are

rising in this range of pilot injection timings (-165 CAD to -90 CAD), but the crank angle at which this HTHR occurs is getting delayed. As mentioned earlier, this range of pilot injection timings also exhibit all the stages of heat release due to ignition of main fuel- LTHR with NTC regime followed by ITHR and HTHR during main ignition as displayed in figure 9 and 11a. The specie that seem to have an effect on ignition delay of pilot injection timings in the part A is formaldehyde ( $\text{CH}_2\text{O}$ ). The normalized mole fraction of  $\text{CH}_2\text{O}$  taken at start of main fuel addition i.e. at -5 CAD is increasing as the timing is retarded from -165 CAD to -90 CAD. This shows that increase in  $\text{CH}_2\text{O}$  has a retarding effect on the combustion phasing of main fuel ignition even when the temperature and pressure are rising.

To examine further the effect of  $\text{CH}_2\text{O}$  on the ignition delay of the main fuel, it was added to the main fuel in varying amounts keeping the pilot injection timing constant (-90 CAD). For this purpose, an additional inlet source (C4\_Inlet3) was connected to Gas Mixer 2 (as shown in figure 17) and Chemkin's parameter study facility was used to run multiple runs of varying  $\text{CH}_2\text{O}$  flow rate. In the parameter study, the mass flow rate of  $\text{CH}_2\text{O}$  was varied from 0.02 g/sec to 0.1 g/sec. The temperature and pressure were initialized with the end temperature and pressure of IC Engine 2.

Figure 18 shows the ignition delay of the main ignition in IC Engine 3 calculated by max ( $dT/dt$ ) plotted against the added mole fraction of  $\text{CH}_2\text{O}$ . By running this parameter study of  $\text{CH}_2\text{O}$ , it was verified that  $\text{CH}_2\text{O}$  can increase the ignition delay of the main injection by approximately 0.15 degrees per 1000 ppm in the last reactor as shown in figure 18.

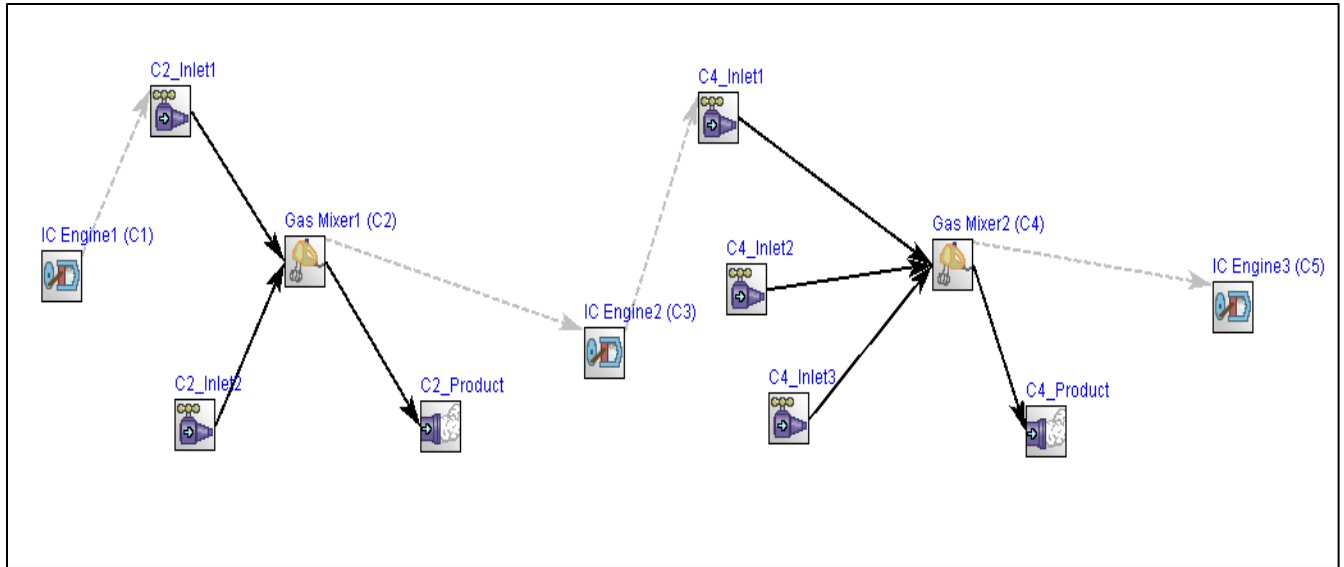


**Figure 17: Chemkin Model to Study the Effect of formaldehyde (CH<sub>2</sub>O) on Ignition Delay of Main ignition**

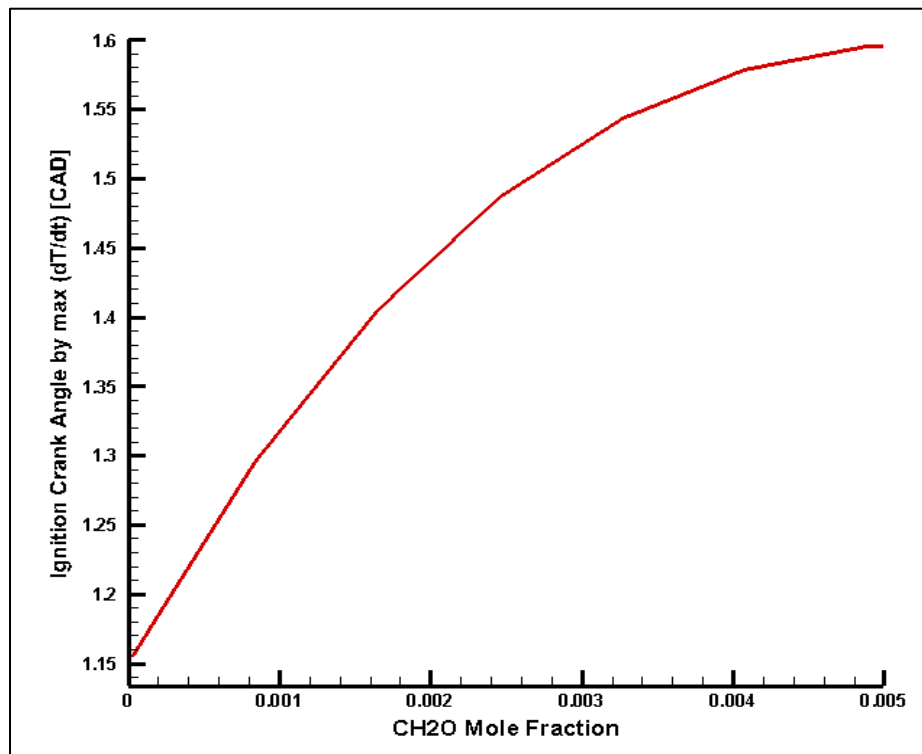


**Figure 18: Effect of formaldehyde (CH<sub>2</sub>O) on ignition delay of main ignition**

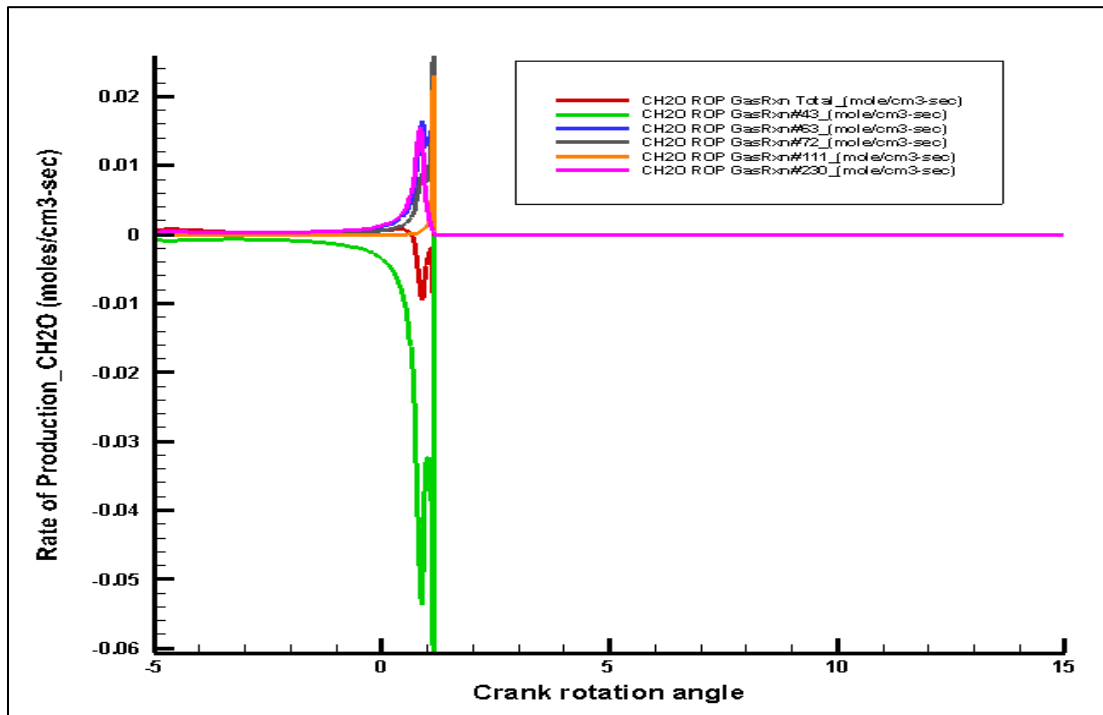
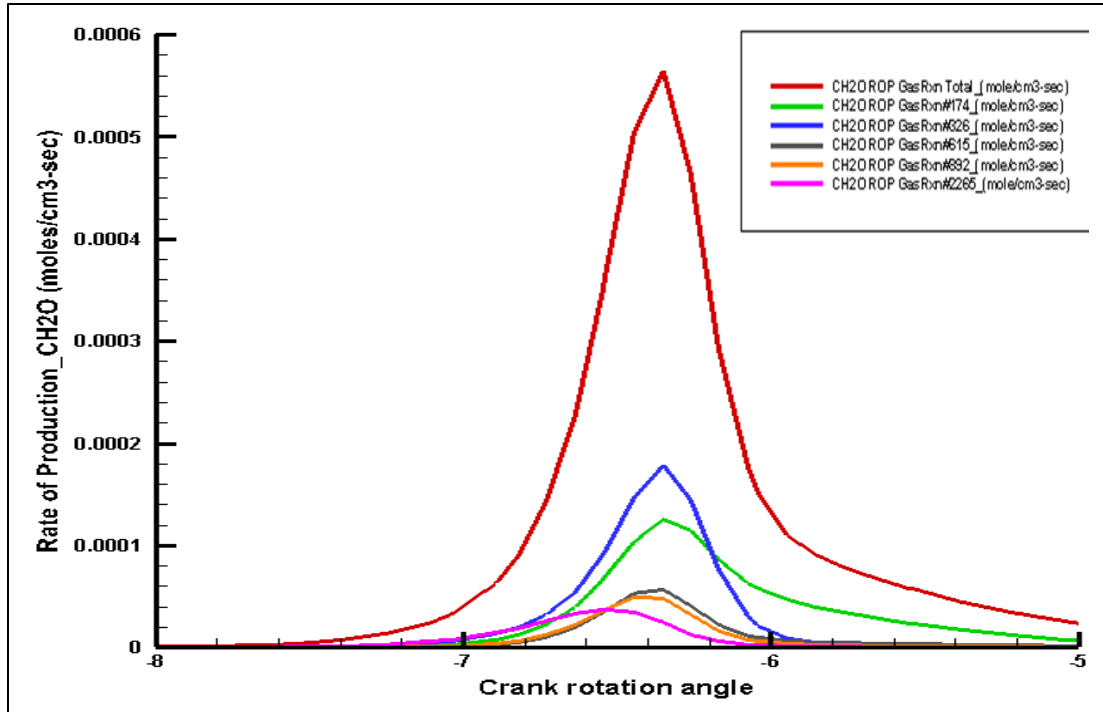


Figure 19a: Rate of Production of CH<sub>2</sub>O in Reactor 3 [IC Engine2]  
 Figure 19b: Rate of Production of CH<sub>2</sub>O in Reactor 5 [IC Engine3]

Figure 19a and 19b shows the top five reactions playing important roles in the rate of production of CH<sub>2</sub>O species in each of reactors 3 and 5 for pilot injection timing at -90 CAD. All the reactions, i.e. Rxn# 174, 326, 615, 892 and 2265 from reactor 3 lead to CH<sub>2</sub>O formation in reactor 3. In Rxn# 43, the reaction of CH<sub>2</sub>O with OH results in a rapid decrease in its level during main combustion in reactor 5. The reactions with their respective Arrhenius constants for forward and reverse reactions are given in Table 4.1.

Reaction #	Reactions	Arrhenius Coefficients					
		Forward Reaction			Reverse Reaction		
		A	n	Ea	A	n	Ea
Reactor 3 [IC Engine 2]							
174	C <sub>2</sub> H <sub>5</sub> O=CH <sub>3</sub> +CH <sub>2</sub> O	1.32E+20	-2.018	2.08E+04	3.00E+11	0.00E+00	6.34E+03
326	CH <sub>3</sub> COCH <sub>2</sub> O=CH <sub>3</sub> CO+CH <sub>2</sub> O	3.73E+20	-2.176	1.73E+04	1.00E+11	0.00E+00	1.19E+04
615	NC <sub>3</sub> H <sub>7</sub> O=C <sub>2</sub> H <sub>5</sub> +CH <sub>2</sub> O	2.72E+21	-2.45	1.57E+04	1.00E+11	0.00E+00	3.50E+03
892	PC <sub>4</sub> H <sub>9</sub> O=NC <sub>3</sub> H <sub>7</sub> +CH <sub>2</sub> O	1.56E+21	-2.44	1.52E+04	5.00E+10	0.00E+00	3.46E+03
2265	C <sub>7</sub> H <sub>15</sub> O-1=CH <sub>2</sub> O+C <sub>6</sub> H <sub>13</sub> -1	6.02E+20	-2.18	2.48E+04	1.00E+11	0.00E+00	1.19E+04
Reactor 5 [IC Engine 3]							
43	CH <sub>2</sub> O+OH=HCO+H <sub>2</sub> O	7.82E+07	1.63	-1055	4.89E+06	1.811	2.90E+04
63	CH <sub>3</sub> O (+M)=CH <sub>2</sub> O+H(+M)	6.80E+13	0	2.62E+04			
72	CH <sub>2</sub> OH+O <sub>2</sub> =CH <sub>2</sub> O+HO <sub>2</sub>	2.41E+14	0	5017	3.15E+13	0.42	2.51E+04
111	CH <sub>3</sub> +O=CH <sub>2</sub> O+H	5.54E+13	0.05	-136	3.83E+15	-0.147	6.84E+04
230	CH <sub>2</sub> CHO+O <sub>2</sub> =>CH <sub>2</sub> O+CO+OH	8.95E+13	-0.6	1.01E+04			

**Table 4.1: Reactions for rate of production of CH<sub>2</sub>O**

### 4.3.2 Part B: Pilot injection timings between 90 CAD BTDC to 12 CAD BTDC

The effect of pilot injection timings between -90 CAD to -12 CAD on main injection at -5 CAD is explained in this part. As the pilot injection timing is swept from -90 CAD to -25 CAD, the combustion phasing at first advances but after -25 CAD and up to -12 CAD, it is seen that the combustion phasing is delayed. This is elucidated using the chemistry of important intermediate species formed during pilot combustion (figure 19).

The species that play an important role here are formaldehyde ( $\text{CH}_2\text{O}$ ), hydrogen peroxide ( $\text{H}_2\text{O}_2$ ), acetylene ( $\text{C}_2\text{H}_2$ ) and 1,3-butadiene ( $\text{C}_4\text{H}_6$ ). It was seen that an increase in  $\text{H}_2\text{O}_2$  and  $\text{C}_2\text{H}_2$  mole fraction has an advancing effect on main injection combustion. It is also shown in other research [34, 35] that these species, even when present in small amounts, can promote the autoignition of the mixture. Also,  $\text{CH}_2\text{O}$  is known to be a autoignition inhibitor. In this part, the  $\text{CH}_2\text{O}$  mole fraction leaving Reactor 2 is decreasing as the pilot injection timings are retarded. Although the  $\text{CH}_2\text{O}$  is not decreasing by a substantial amount, it may be the reason for the advancing of ignition here; this holds true only for pilot timings until -25 CAD because after that the  $\text{CH}_2\text{O}$  shows no effect on combustion phasing as seen in figure 19. The  $\text{C}_4\text{H}_6$  (1,3-butadiene) is another specie whose mole fractions correlate with a reduction in ignition delay time. The mole fraction of these three species is at its peak for a pilot injection timing of -25 CAD for which the combustion phasing is advanced compared to others. When the mole fraction starts to drop, from -25 CAD onwards, the heat release event is retarded.

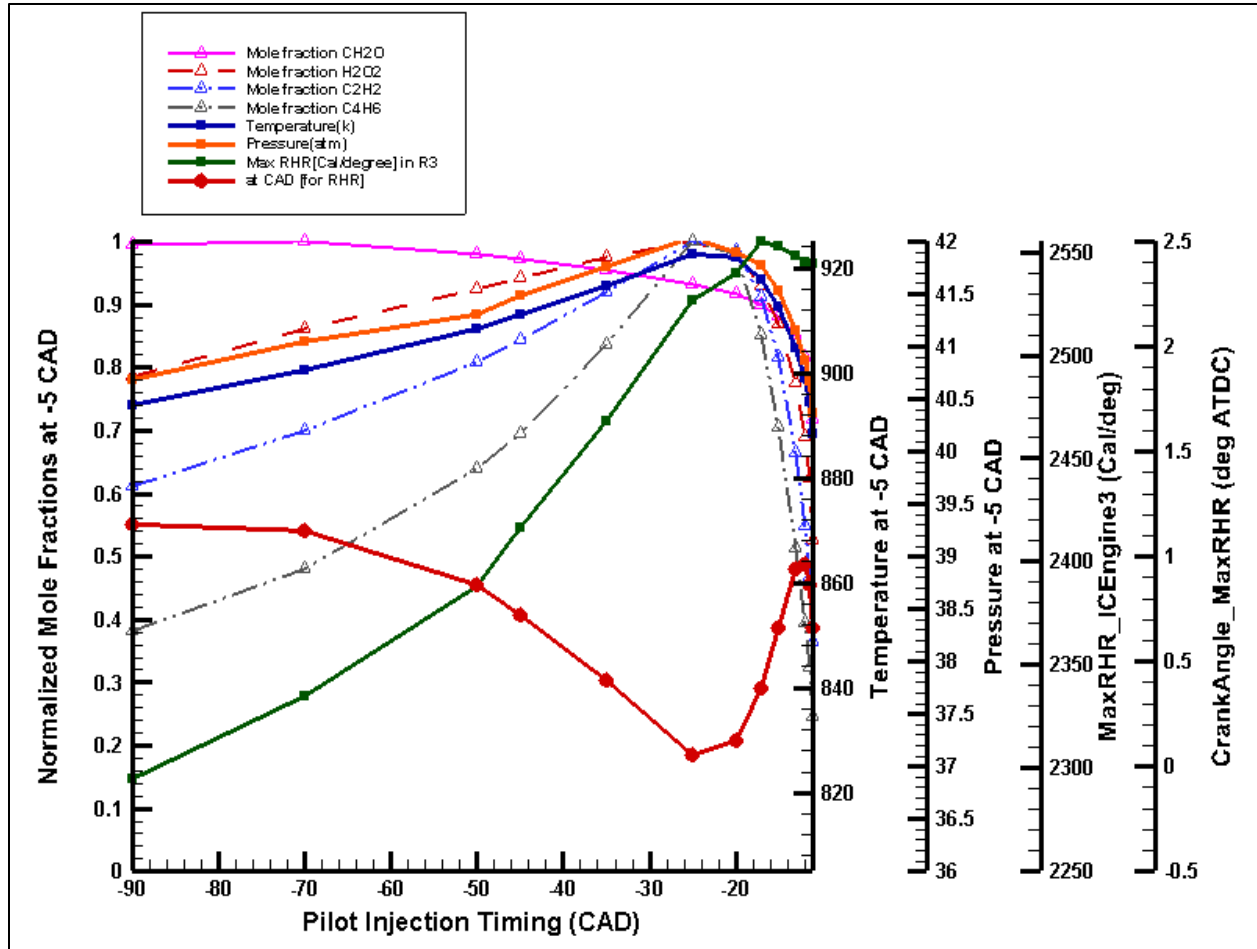


**Figure 19: Part B- Effect of Pilot injection timings between -90 CAD to -12 CAD on Main Ignition**

To prove the effect of  $\text{H}_2\text{O}_2$ ,  $\text{C}_2\text{H}_2$  and  $\text{C}_4\text{H}_6$  on the ignition delay of the main injection, the parameter study was set up in the same manner as shown in figure 17 for the  $\text{CH}_2\text{O}$  study. The species were added externally to the last reactor (one specie at a time) in varying amounts while keeping the pilot injection timing constant (-25 CAD). The temperature and pressure were initialized with the end temperature and pressure of IC Engine 2. Figure 20a, 20b and 20c show the ignition delay of the main ignition in IC Engine 3 calculated by  $\max(dT/dt)$  plotted against the mole fraction of  $\text{H}_2\text{O}_2$ ,  $\text{C}_2\text{H}_2$  and  $\text{C}_4\text{H}_6$  added to the main fuel. As seen from the figure,  $\text{H}_2\text{O}_2$  advances the ignition by 0.6 degrees;  $\text{C}_2\text{H}_2$  is advancing it by 0.2 degrees; and  $\text{C}_4\text{H}_6$  by 0.1



degrees per 1000 ppm mole fraction of respective specie. By running this parameter study, it was verified that these species have an advancing effect on the ignition delay of the main injection in the IC Engine 3, with  $H_2O_2$  having a greater effect than  $C_2H_2$ , followed by  $C_4H_6$ .

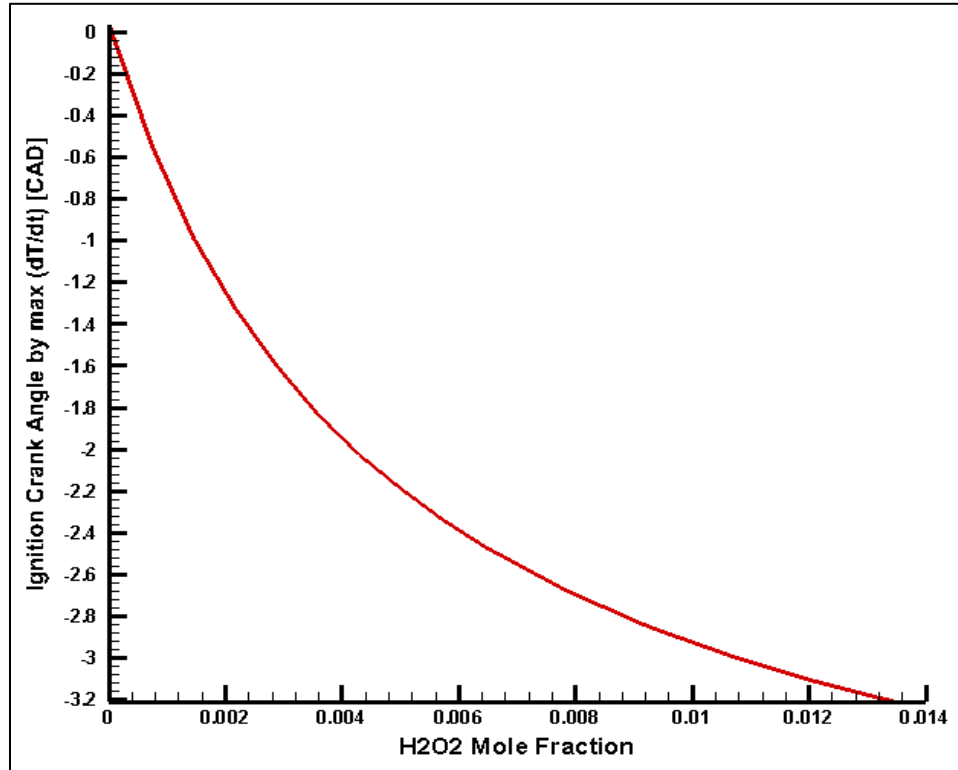


Figure 20a: Effect of  $H_2O_2$  on ignition delay of main ignition

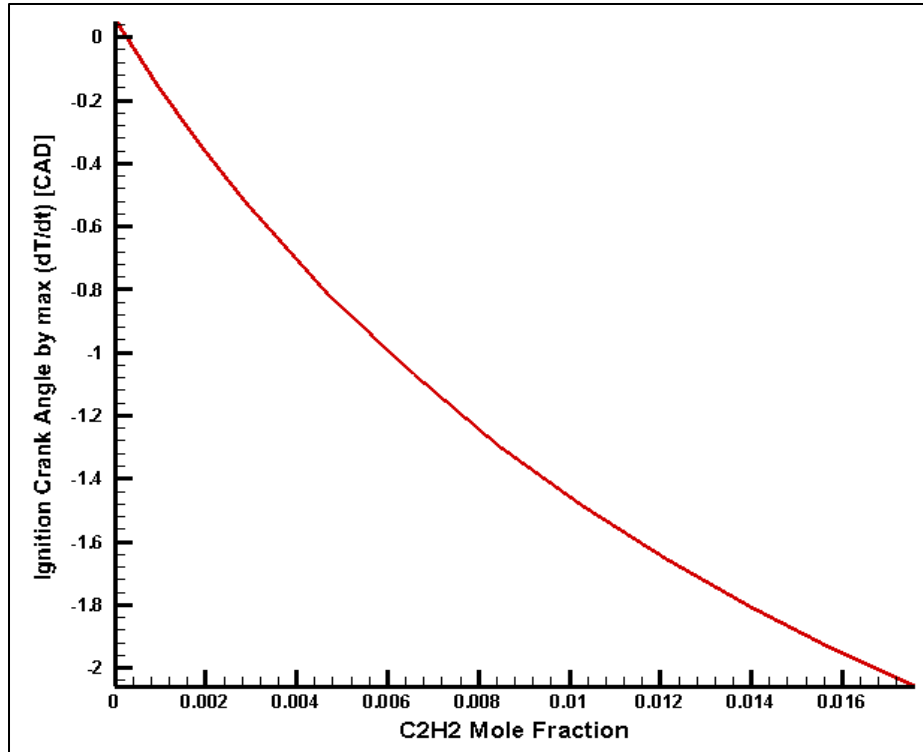


Figure 20b: Effect of  $C_2H_2$  on ignition delay of main ignition

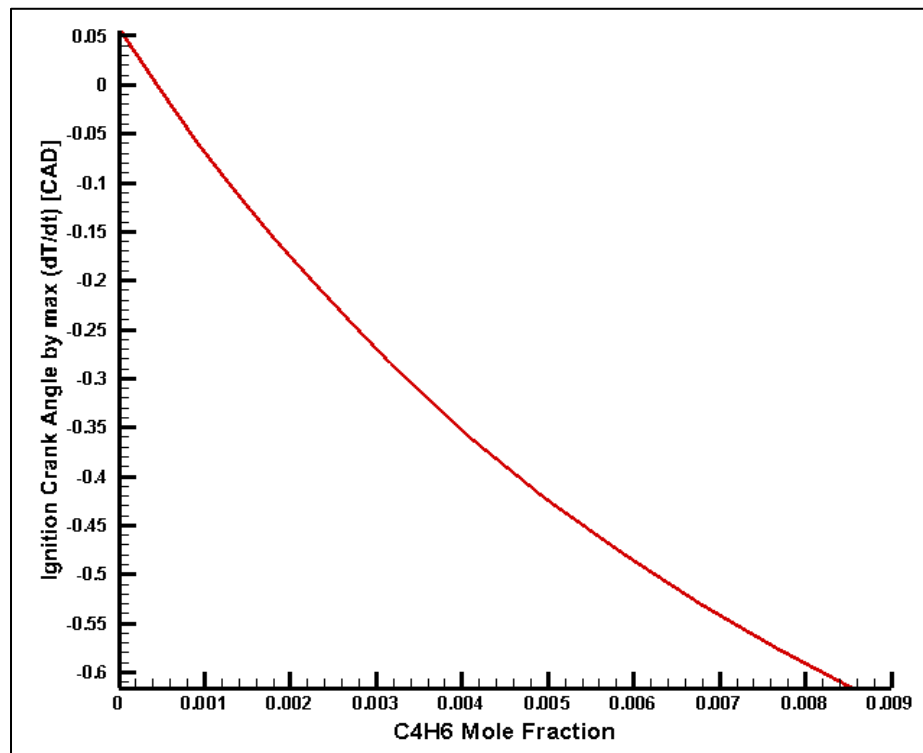


Figure 20c: Effect of  $C_4H_6$  (1,3-butadiene) on ignition delay of main ignition

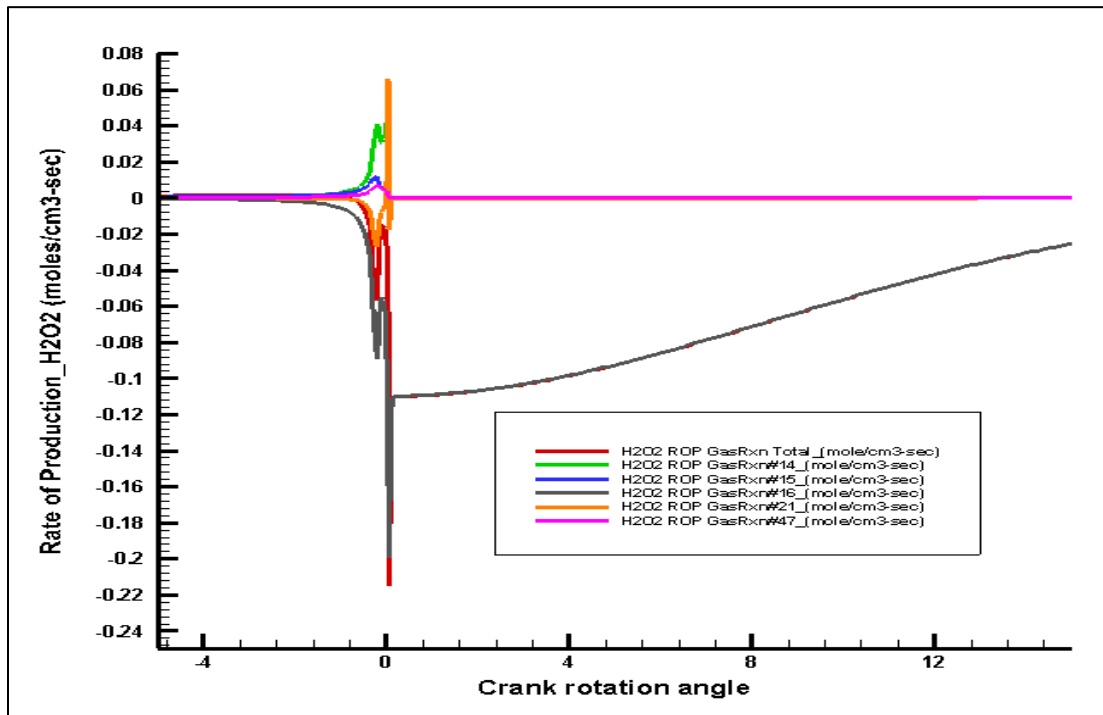
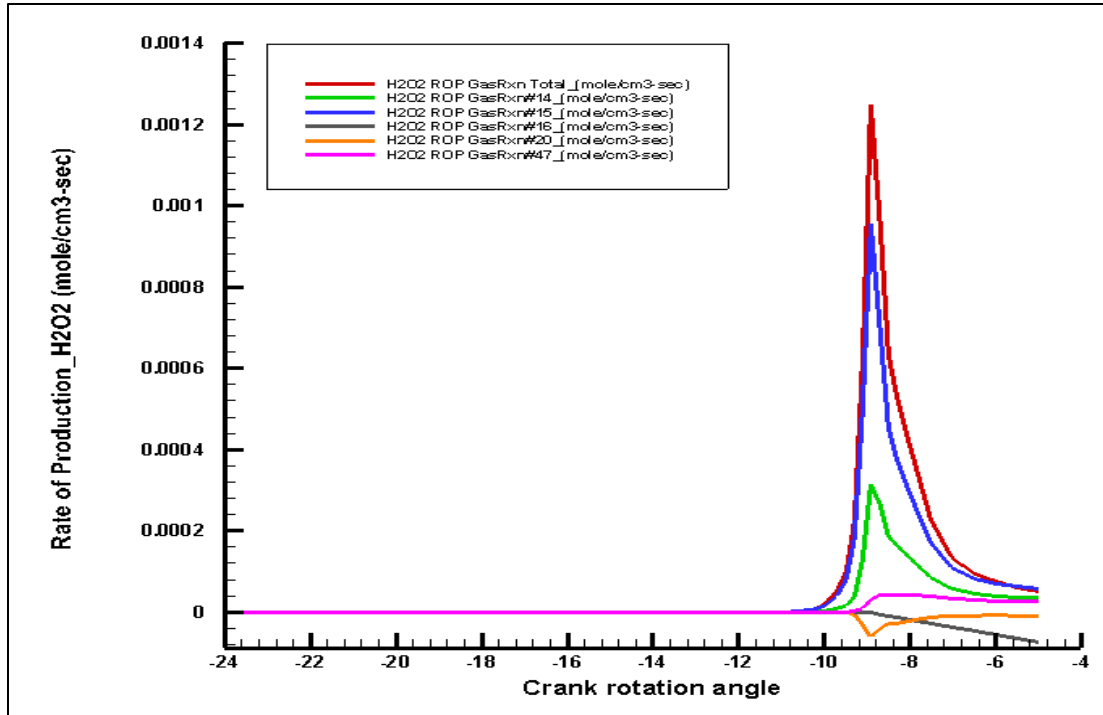


Figure 21a: Rate of Production of H<sub>2</sub>O<sub>2</sub> in Reactor 3 [IC Engine2]

Figure 21b: Rate of Production of H<sub>2</sub>O<sub>2</sub> in Reactor 5 [IC Engine3]

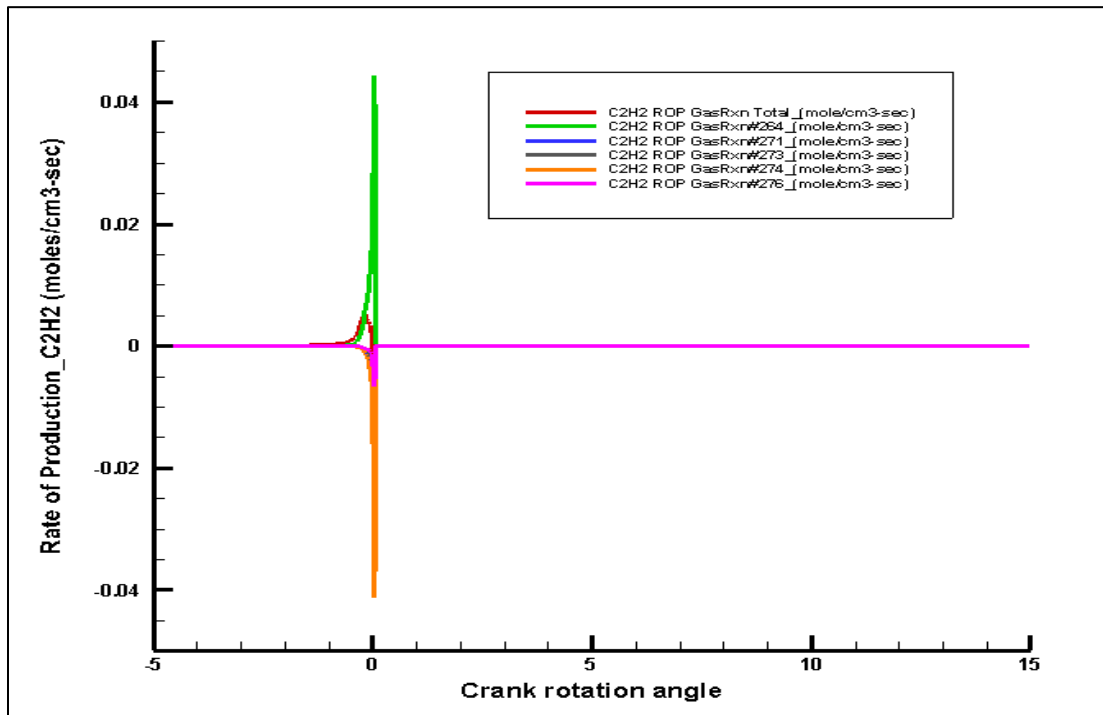
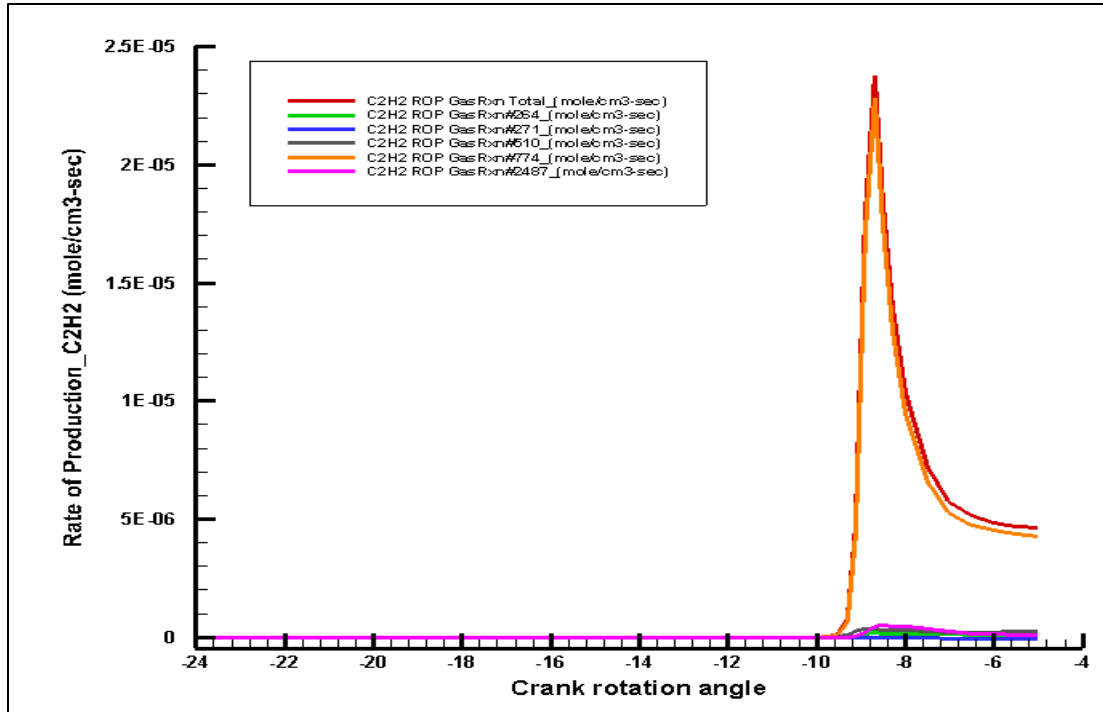


Figure 21c: Rate of Production of C<sub>2</sub>H<sub>2</sub> in Reactor 3 [IC Engine2]

Figure 21d: Rate of Production of C<sub>2</sub>H<sub>2</sub> in Reactor 5 [IC Engine3]

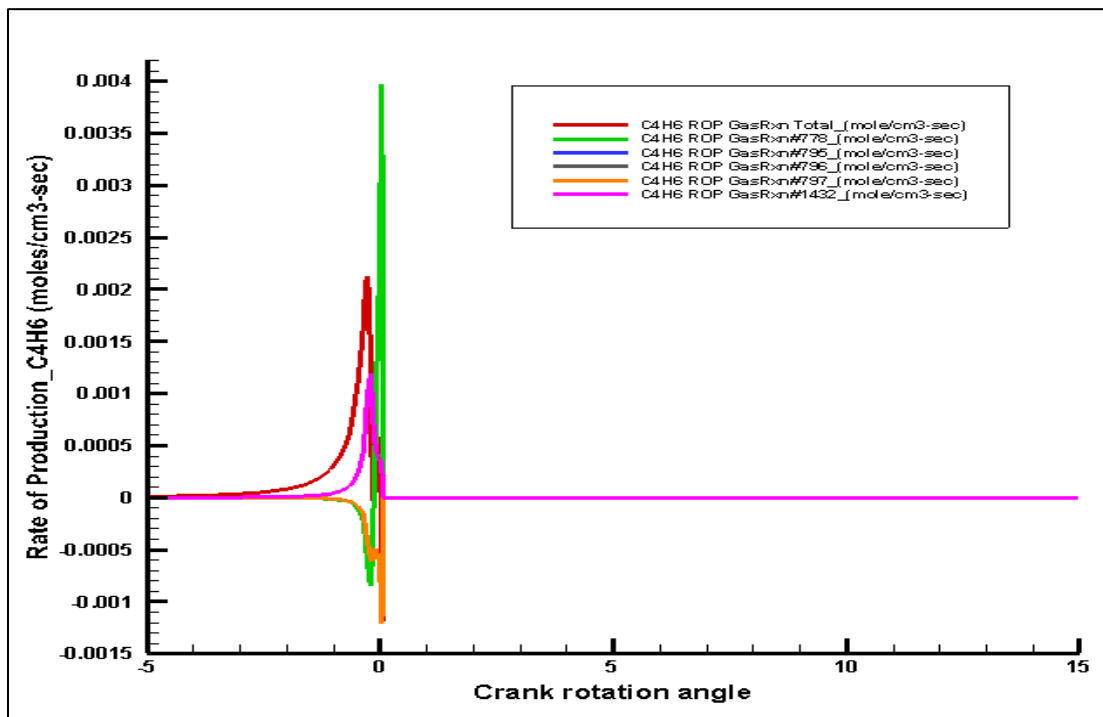
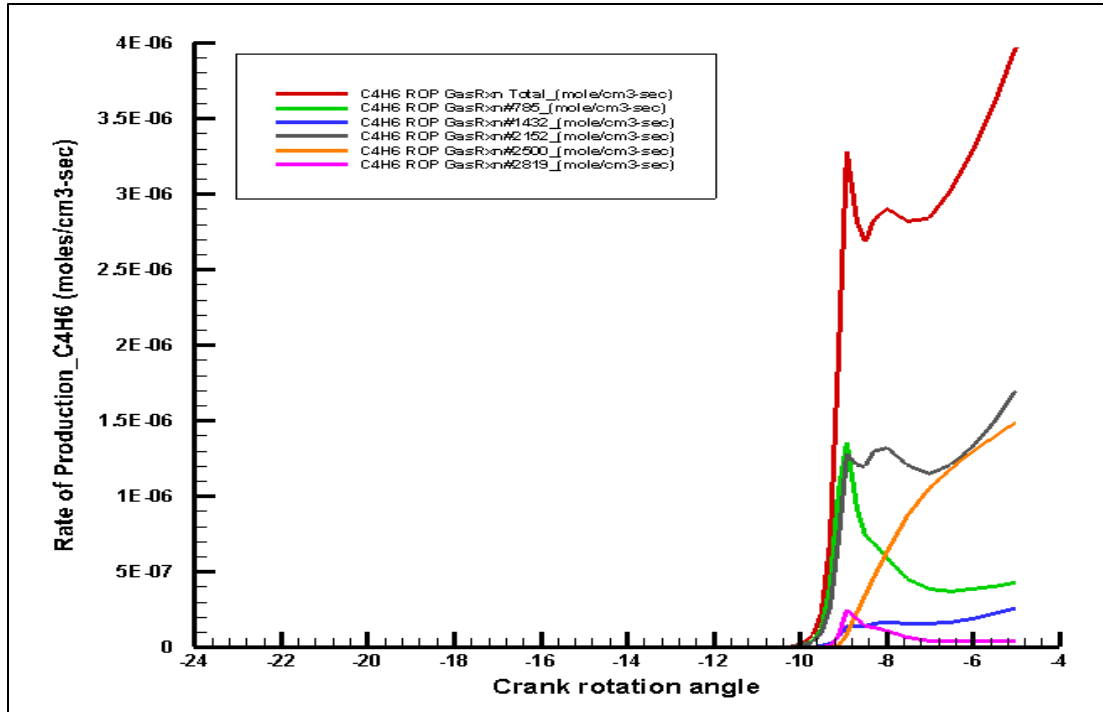


Figure 21e: Rate of Production of C<sub>4</sub>H<sub>6</sub> in Reactor 3 [IC Engine2]

Figure 21f: Rate of Production of C<sub>4</sub>H<sub>6</sub> in Reactor 5 [IC Engine3]

Figures from 21a to 21f show the top five reactions leading to rate of production of H<sub>2</sub>O<sub>2</sub>, C<sub>2</sub>H<sub>2</sub> and C<sub>4</sub>H<sub>6</sub> species in each of reactor 3 and reactor 5, having pilot injection timing at -25 CAD. The major reaction contributing to H<sub>2</sub>O<sub>2</sub> production is Rxn# 15 compared to the other three reactions. Rxn# 16 starts to consume the H<sub>2</sub>O<sub>2</sub> radicals with the start of LTHR of pilot ignition. The reaction rate of Rxn# 16 is slow initially but gains momentum during the main combustion in the last reactor; thus, the rate of production of H<sub>2</sub>O<sub>2</sub> goes negative due to the formation of OH radicals by Rxn# 16 which is associated with the HTHR. In case of C<sub>2</sub>H<sub>2</sub> formation in reactor 2, Rxn# 774 is the main contributor compared to other reactions. The C<sub>4</sub>H<sub>6</sub> is being formed during LTHR of pilot fuel ignition by all the reactions given in table 4.4 for reactor 3. The C<sub>4</sub>H<sub>6</sub> is produced in the last reactor by Rxn# 778 and 1432 only. The forward and reverse reactions with their respective Arrhenius constants controlling H<sub>2</sub>O<sub>2</sub>, C<sub>2</sub>H<sub>2</sub> and C<sub>4</sub>H<sub>6</sub> species fractions are given in Table 4.2, 4.3 and 4.4 respectively. Thus, the intermediate species formed during pilot combustion play an important role in heat release of the main fuel ignition and its combustion phasing in this range of pilot injection timings.

Reaction #	Reactions	Arrhenius Coefficients					
		Forward Reaction			Reverse Reaction		
		A	n	Ea	A	n	Ea
14	H <sub>2</sub> O <sub>2</sub> +O <sub>2</sub> =2HO <sub>2</sub>	1.14E+16	-0.347	4.97E+04	1.03E+14	0.00E+00	1.10E+04
15	H <sub>2</sub> O <sub>2</sub> +O <sub>2</sub> =2HO <sub>2</sub>	2.14E+13	-0.347	3.73E+04	1.94E+11	0.00E+00	-1.41E+03
16	H <sub>2</sub> O <sub>2</sub> (+M)=2OH(+M)	2.95E+14	0	4.84E+04			
20	H <sub>2</sub> O <sub>2</sub> +OH=H <sub>2</sub> O+HO <sub>2</sub>	2.00E+12	0	4.27E+02	3.66E+10	5.89E-01	3.13E+04
47	CH <sub>2</sub> O+HO <sub>2</sub> =HCO+H <sub>2</sub> O <sub>2</sub>	7.10E-03	4.517	6.58E+03	2.43E-02	4.11E+00	5.77E+03
Reactor 5 [IC Engine 3]							
14, 15, 16, 47	Same as above						
21	H <sub>2</sub> O <sub>2</sub> +OH=H <sub>2</sub> O+HO <sub>2</sub>	1.70E+18	0	2.94E+04	3.12E+16	5.89E-01	6.03E+04

**Table 4.2: Reactions for rate of production of H<sub>2</sub>O<sub>2</sub>**

Reaction #	Reactions	Arrhenius Coefficients					
		Forward Reaction			Reverse Reaction		
		A	n	Ea	A	n	Ea
Reactor 3 [IC Engine 2]							
264	$C_2H_3+O_2=C_2H_2+HO_2$	2.12E-06	6	9.48E+03	1.09E-05	5.91E+00	2.40E+04
271	$C_2H_2+O_2=HCCO+OH$	2.00E+08	1.5	3.01E+04	2.04E+06	1.50E+00	3.22E+04
510	$C_3H_5-A+O_2=C_2H_2+CH_2O+OH$	9.72E+29	-5.71	2.14E+04			
774	$C_4H_7-1=C_2H_2+C_2H_5$	1.07E+15	-0.56	3.03E+04	2.00E+11	0.00E+00	7.80E+03
2487	$C_5H_9-1=C_2H_2+NC_3H_7$	2.76E+15	-0.67	3.08E+04	2.00E+11	0.00E+00	7.80E+03
Reactor 5 [IC Engine 3]							
264, 271	Same as above						
273	$C_2H_2+O=CH_2+CO$	6.94E+06	2	1.90E+03	4.05E+01	3.20E+00	4.84E+04
274	$C_2H_2+O=HCCO+H$	1.35E+07	2	1.90E+03	4.76E+07	1.65E+00	2.08E+04
276	$C_2H_2+OH=CH_2CO+H$	3.24E+13	0	1.20E+04	3.06E+17	-8.02E-01	3.60E+04

**Table 4.3: Reactions for rate of production of C<sub>2</sub>H<sub>2</sub>**

Reaction #	Reactions	Arrhenius Coefficients					
		Forward Reaction			Reverse Reaction		
		A	n	Ea	A	n	Ea
Reactor 3 [IC Engine 2]							
785	$C_4H_7-3+O_2=C_4H_6+HO_2$	1.00E+09	0	0.00E+00	1.00E+11	0	1.70E+04
1432	$C_5H_9-3=C_4H_6+CH_3$	7.55E+14	-0.52	3.85E+04	1.00E+11	0	7.80E+03
2152	$C_7I_3-3=C_4H_6+NC_3H_7$	1.11E+19	-1.53	4.07E+04	8.50E+10	0	8.30E+03
2500	$C_4H_6CHO-1-13=C_4H_6+HCO$	8.95E+17	-1.28	4.62E+04	8.00E+10	0	1.14E+04
2819	$C_6H_{10}-3+OH=C_2H_3+C_4H_6+H_2O$	2.76E+04	2.64	-1.92E+03			
Reactor 5 [IC Engine 3]							
778	$C_4H_7-3=C_4H_6+H$	1.20E+14	0	4.93E+04	4.00E+13	0	1.30E+03
795	$C_4H_6+OH=C_2H_5+CH_2CO$	1.00E+12	0	0.00E+00	3.73E+12	0	3.00E+04
796	$C_4H_6+OH=CH_2O+C_3H_5-A$	1.00E+12	0	0.00E+00	3.50E+06	0	7.11E+04
797	$C_4H_6+OH=C_2H_3+CH_3CHO$	1.00E+12	0	0.00E+00	5.44E+11	0	1.86E+04
1432	Same as above						

**Table 4.4: Reactions for rate of production of C<sub>4</sub>H<sub>6</sub>**

### 4.3.2 Part C: Pilot injection timings between 12 CAD BTDC to 7 CAD BTDC & Main Injection only at 5 CAD BTDC

Part C shows the effect of very retarded pilot injection timings (between -12 CAD to -7 CAD) on the succeeding main ignition. As a benchmark, for reference, it also shows the kinetic behavior of single main injection case. Figure 22 shows only the important parameters and species for pilot timings of Part C. As the pilot injection is retarded to occur near the main injection, the HTHR of pilot timings advances from -12 CAD to -10 CAD, but for pilot injection after -9 CAD to -7 CAD as well as single injection case, the crank angle location of the HTHR of the main fuel is retarded. The combustion taking place here seems to be behaving like the combustion in constant volume combustion chamber (CVC) showing its dependence on the temperature of the mixture.

Therefore, to explain the behavior of the pilot injection timings in this part on main ignition, a constant volume combustion chamber (CVC) was employed in Chemkin with n-heptane/air mixture. A temperature parameter study was set up to investigate the effect of initial temperature on the ignition delay of the mixture. The initial temperature from 800 K to 1000 K was tested with an initial pressure as 40 Atm and considering an adiabatic process. The data obtained using this simulation gave very interesting result as shown in figure 23.



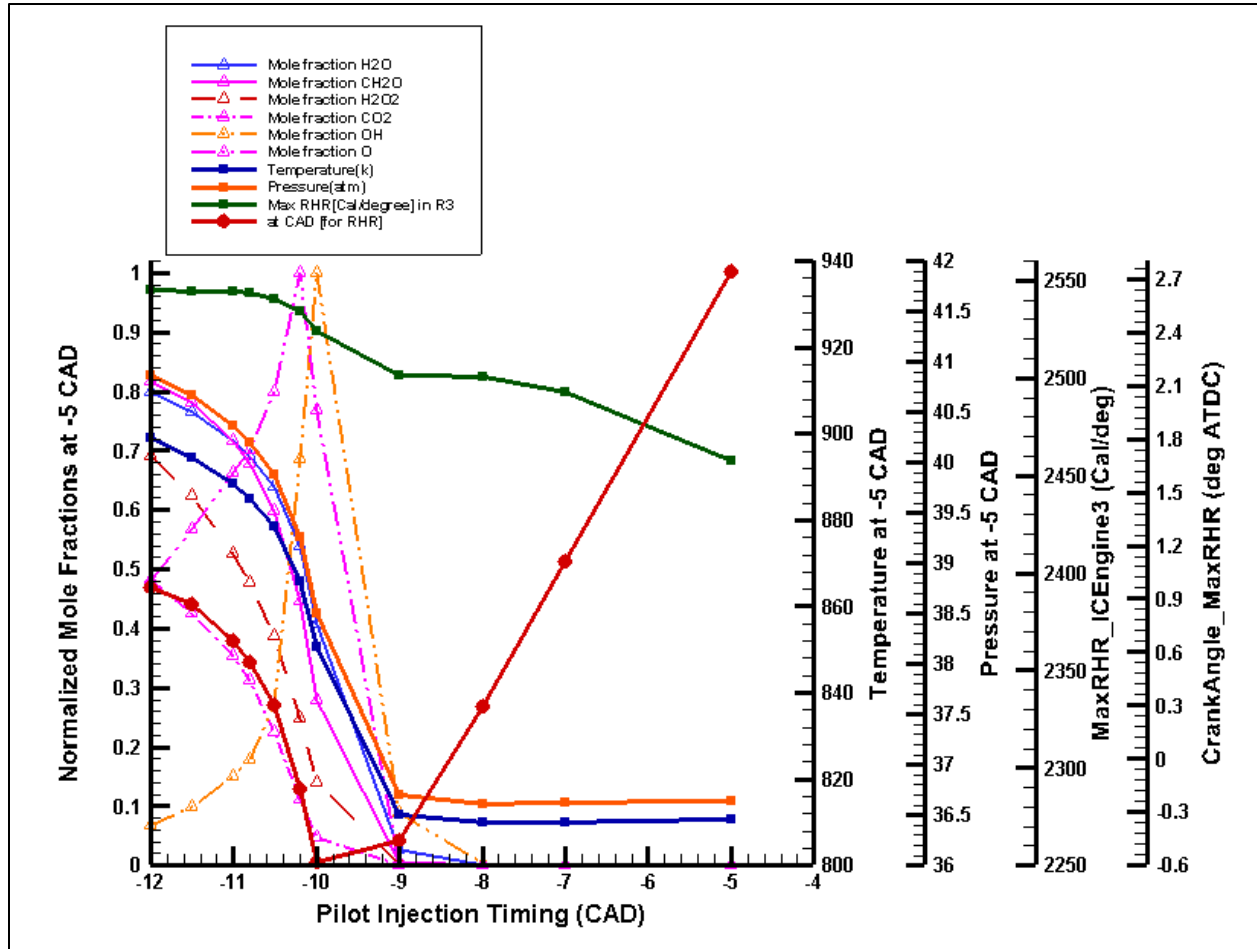


**Figure 22: Part C- Effect of Pilot injection timings between -12 CAD to -7 CAD and single fuel injection case at -5 CAD on Main Ignition**

As can be seen in figure 23, the ignition delay (ID) is advanced as the temperature is increased from 800 K to 840 K. When the temperature is increased further till 940 K, the ID is delayed. Any further increase in initial temperature again advances the ID. In the simulation result of split injection model for Part C (figure 22), the occurrence of max HTHR of main ignition for pilot injection timing of -10 CAD is more advanced than other pilot timings in this part. The initial temperature at the start of main fuel addition for pilot timing of -10 CAD is ~850 K. As the pilot injection timing is advanced compared to -10 CAD, the temperature is increasing (>850 K) and the combustion phasing of the HTHR of main ignition is also getting delayed

which is similar to the results obtained from CVC simulation. Moreover, when the pilot injection timing is retarded (after -10 CAD), the initial temperature is reduced ( $< 840$  K) which results in increase in combustion phasing of main. The single fuel injection case also shows the retarded combustion phasing due to the initial temperature being  $< 840$  K. Thus, the main fuel ignition for the pilot injection timings from -12 CAD to -5 CAD proceed as constant volume combustion with the dependence of combustion phasing on initial temperature of the mixture.

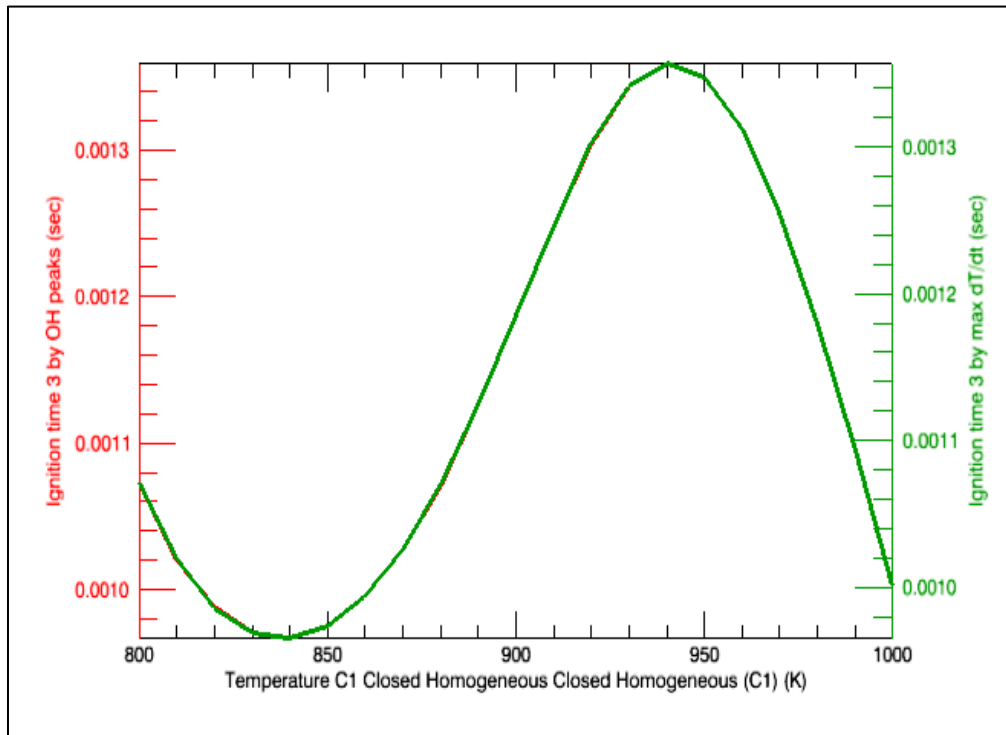


**Figure 23: Temperature parameter study in CVC**

Figure 22 also shows the changes in the mole fraction of few selected species. The normalized mole fraction of OH and O is increasing for pilot timings between -12 CAD to -10 CAD which implies that the exothermic reactions leading to combustion of main fuel are very active in this region of pilot timings. Thus, there is rapid combustion of the main fuel with reduced ignition delay. As the OH level drops (figure 22) for pilot timings later than -10 CAD, the combustion phasing is also delayed.

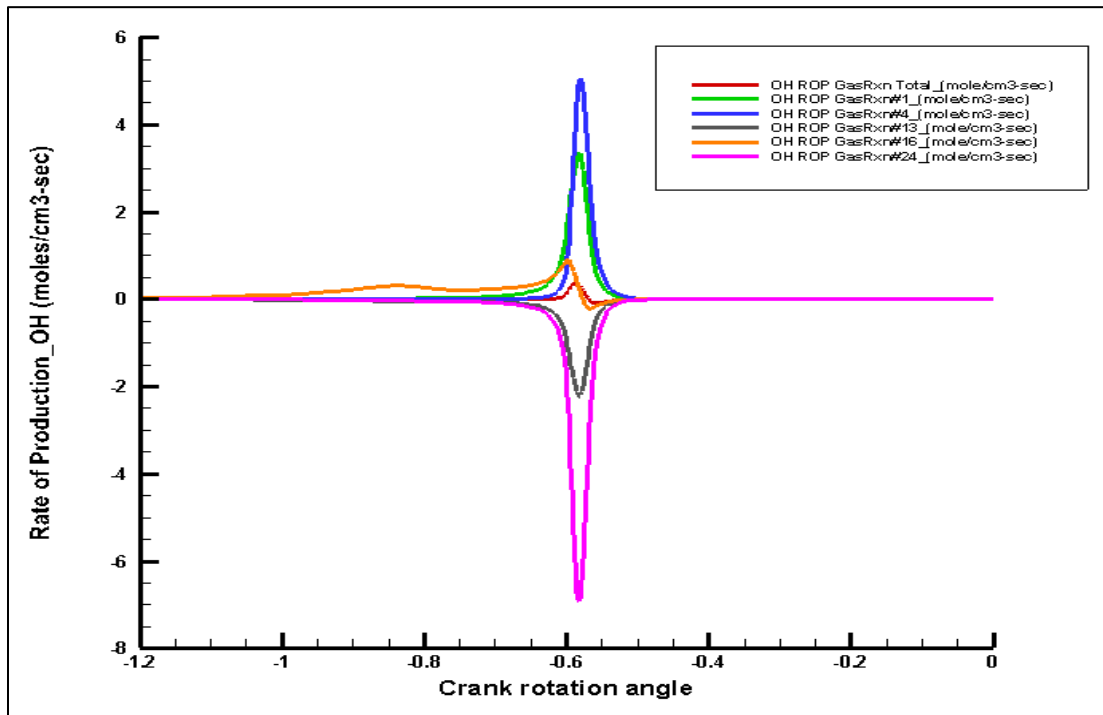
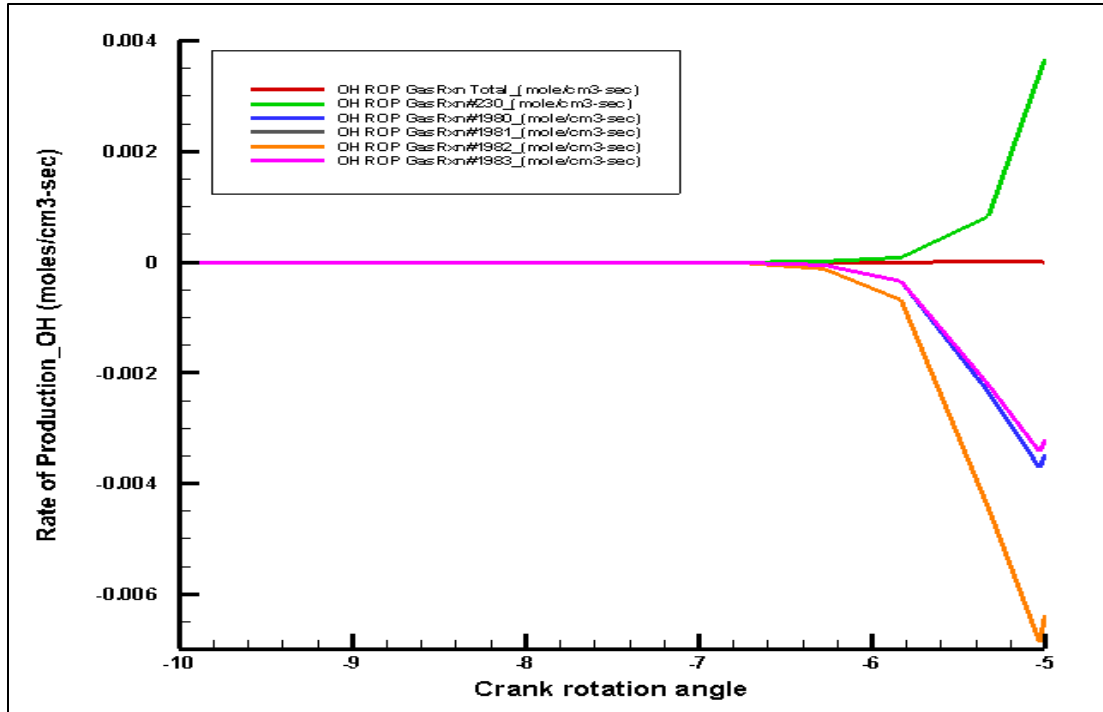


Figure 24a: Rate of Production of OH in Reactor 3 [IC Engine2]

Figure 24b: Rate of Production of OH in Reactor 5 [IC Engine3]

Figures 24a and 24b show the top five reactions leading to rate of production of the OH specie in each of reactor 3 and reactor 5 for the pilot timing of -10 CAD. The reactions with Arrhenius constants for forward and reverse reactions for OH species are given in Table 4.5. The OH is getting consumed by n-heptane in the Rxn# 1980, 1981, 1982 and 1983 as soon as it is getting produced by Rxn# 230 in reactor 3, i.e. I C Engine2. In the last reactor, Rxn# 1, 4 and 16 are producing OH radicals and Rxn# 13 and 24 are consuming it.

Reaction #	Reactions	Arrhenius Coefficients					
		Forward Reaction			Reverse Reaction		
		A	n	Ea	A	n	Ea
Reactor 3 [IC Engine 2]							
230	CH <sub>2</sub> CHO+O <sub>2</sub> =CH <sub>2</sub> O+CO+OH	8.95E+13	-0.6	1.01E+04			
1980	NC <sub>7</sub> H <sub>16</sub> +OH=C <sub>7</sub> H <sub>15</sub> -1+H <sub>2</sub> O	2.57E+07	1.80	9.54E+02	2.95E+04	2.33	1.82E+04
1981	NC <sub>7</sub> H <sub>16</sub> +OH=C <sub>7</sub> H <sub>15</sub> -2+H <sub>2</sub> O	4.90E+06	2	-5.96E+02	3.62E+02	2.87	1.91E+04
1982	NC <sub>7</sub> H <sub>16</sub> +OH=C <sub>7</sub> H <sub>15</sub> -3+H <sub>2</sub> O	4.90E+06	2	-5.96E+02	3.62E+02	2.87	1.91E+04
1983	NC <sub>7</sub> H <sub>16</sub> +OH=C <sub>7</sub> H <sub>15</sub> -4+H <sub>2</sub> O	4.90E+06	2	-5.96E+02	3.62E+02	2.87	1.91E+04
Reactor 5 [IC Engine 3]							
1	H+O <sub>2</sub> =O+OH	3.55E+15	-0.406	1.66E+04	1.03E+13	-1.50E2	-1.33E+02
4	O+H <sub>2</sub> O=2OH	2.97E+06	2.02	1.34E+04	1.45E+05	2.11	-2.90E+03
13	HO <sub>2</sub> +OH=H <sub>2</sub> O+O <sub>2</sub>	1.97E+10	0.962	-3.28E+02	3.99E+10	1.20	6.93E+04
16	H <sub>2</sub> O <sub>2</sub> (+M)=2OH(+M)	2.95E+14	0	4.84E+04			
24	CO+OH=CO <sub>2</sub> +H	2.23E+05	1.89	-1.16E+03	5.90E+11	6.99E01	2.43E+04

**Table 4.5: Reactions for rate of production of OH**

## CHAPTER 5

### CONCLUSIONS AND RECOMMENDATIONS

#### 5.1 Conclusions:

The kinetics of a split injection model was simulated in Chemkin-Pro to study the effects of ignition of pilot injection on the combustion phasing of the following main injection. The HCCI model was studied for the pilot injections timing sweep from 165 deg BTDC to 7 deg BTDC with constant main injection timing of 5 deg BTDC. Also, the single fuel injection case was used as reference to study the split injection results. The following are the conclusions for the split injection simulation:

1. The split injection showed four stages of heat release- first stage is low temperature heat release due to ignition of the pilot fuel; followed by second stage as LTHR of ignition of main fuel, third stage as ITHR of main fuel ignition and finally, fourth stage as HTHR of main ignition. These four stages were exhibited by the pilot injection timings from -165 CAD to -90 CAD and for pilot timing of -11 CAD but the pilot timings from -70 CAD to -12 CAD showed only first stage, third stage and fourth stage. The pilot timing of -10 CAD had combined first stage heat release with second stage heat release followed by last two stages of heat release- ITHR and HTHR; whereas pilot injection timings from -9 CAD onwards up to -7 behaved like the single injection case exhibiting all the stages of main fuel ignition only with LTHR being higher than that for other pilot timings.
2. It was observed that the phasing of the main fuel combustion is retarded when the pilot fuel is introduced at crank angle location from 165 deg BTDC to 90 deg BTDC. The reason for this behavior of main ignition was the increasing level of formaldehyde ( $\text{CH}_2\text{O}$ ) mole

fraction at the start of main fuel addition. Thus,  $\text{CH}_2\text{O}$  acted as auto ignition inhibitor of the main fuel for pilot injection timings: 165 deg BTDC to 90 deg BTDC.

3. For the pilot injection events between 90 deg BTDC to 12 deg BTDC, it was detected that the intermediate species- hydrogen peroxide ( $\text{H}_2\text{O}_2$ ), acetylene ( $\text{C}_2\text{H}_2$ ) and 1,3-butadiene ( $\text{C}_4\text{H}_6$ ) have a noteworthy impact on the heat release and combustion phasing of main injection. All three were shown to promote the autoignition of the main fuel and thus advance the combustion phasing. The most significant of all three was  $\text{H}_2\text{O}_2$  followed by  $\text{C}_2\text{H}_2$  and then  $\text{C}_4\text{H}_6$ . These three species reached a peak value at 25 deg BTDC. Therefore, the pilot injection timing 25 deg BTDC showed advanced phasing of main combustion. When the levels of these species started to drop after -25 CAD, the combustion phasing also started to retard.
4. The main fuel ignition for pilot injection cases between 12 deg BTDC to 7 deg BTDC as well as single main injection case was noted to be dependent on the initial temperature of the mixture at the start of main fuel injection. This effect was also seen in constant volume combustion chamber study of initial temperature variation. The combustion phasing was advanced for pilot timing 10 deg BTDC which had initial temperature  $\sim 850$  K. As the temperature was increased ( $850 \text{ K} < T < 940 \text{ K}$ ), the combustion phasing was retarded as seen for pilot timings earlier than 10 deg BTDC up to 12 deg BTDC. This was also observed when the temperature was  $< 850$  K for pilot events from 10 deg BTDC onwards and the single fuel injection case.
5. The oxidation reactions were very fast for the main combustion for the pilot injection cases between 12 deg BTDC to 10 deg BTDC which showed the presence of increasing levels of OH and O.

## 5.2 Recommendations:

1. The above results are based on simulation of pilot injection sweep in HCCI model in Chemkin-Pro; it would be interesting to validate these results by carrying out the experiment on a real time engine.
2. The simulation was run for pilot injection sweep by keeping the speed, compression ratio, main injection timing constant. The future work could be to run this split injection model by varying these parameters.
3. Moreover, the simulation was run with equal quantities of split injection, it would give some interesting results if carried out with varying amount of pilot injection and main injection fuel quantities.

## REFERENCES

1. Singh, J., “An investigation of low temperature combustion concept in a small bore high speed direct injection diesel engine”, Master’s thesis report, Wayne State University, 2006
2. Jaaskelainen, H., “Low temperature combustion”, DieselNet Technology Guide on ([http://www.dieselnet.com/tech/engine\\_ltc.php](http://www.dieselnet.com/tech/engine_ltc.php))
3. “Subsystems required to control low temperature combustion engines”, an article published in 2013 on National Instruments website, (<http://www.ni.com/white-paper/13516/en/>)
4. Sandia, 2005. “CFR Newsletter: Imaging of advanced low-temperature diesel combustion”, Combustion Research Facility News, Sandia National Laboratories, Livermore, CA, USA, 25(5), 2
5. Musculus, M., "Multiple Simultaneous Optical Diagnostic Imaging of Early-Injection Low-Temperature Combustion in a Heavy-Duty Diesel Engine," SAE Technical Paper 2006-01-0079, 2006, doi:10.4271/2006-01-0079
6. Koci, C. P., Ra, Y., Krieger, R., Andrie, M., Foster, D. E., Siewert, R. M., Durett, R. P., “Multiple event fuel injection investigations in a highly dilute diesel low temperature combustion regime”, SAE paper 2009-01-0925
7. Thirouard, B., Mendez, S., “Using multiple injection strategies in diesel combustion: potential to improve emissions, noise, and fuel economy trade-off in low CR engines”, SAE paper 2008-01-1329



8. Anselmi, P., Kashdan, J., Bression, G., Ferrero-Lesur, E., Thirouard, B., Walter, B., "Improving emissions, noise and fuel economy trade-off by using multiple injection strategies in diesel low temperature combustion (LTC) mode", SAE paper 2010-01-2162
9. Fang, T., Coverdill, R. E., Lee, C. F., White, R. A., "Combustion and soot visualization of low temperature combustion within an HSDI diesel engine using multiple injection strategy", SAE paper 2006-01-0078
10. Zuehl, J. R., Gandhi, J., Hagen, C., Cannella, W., "Fuel effects on HCCI combustion using negative valve overlap", SAE International 2010-01-0161
11. Tanaka, S., Ayala, F., Keck, J. C., Heywood, J. B., "Two-stage ignition in HCCI combustion and HCCI control by fuels and additives", *Combustion and Flame*, 132: 219-239, 2003
12. Lu, X., Ji, L., Zu, L., Hou, Y., Huang, C., Huang, Z., "Experimental study and chemical analysis of n-heptane homogeneous charge compression ignition combustion with port injection of reaction inhibitors", *Combustion and Flame*, 149: 261-270, 2007
13. Takada, K., Yoshimura, F., Ohga, Y., Kusaka, J. et al., "Experimental study on unregulated emission characteristics of turbocharged DI diesel engine with common rail fuel injection system," SAE Technical Paper 2003-01-3158
14. Heywood, J. B., *Internal Combustion Engine Fundamentals*, McGraw-Hill New York, ISBN 0-13-978-0070286375, 1988
15. Jansons, M., Brar, A., Estefanous, F., Florea, R. et al., "Experimental investigation of single and two-stage ignition in a diesel engine," SAE Technical Paper 2008-01-1071
16. Fieweger, F., et al., 1997. "Self-ignition of S.I. engine model fuels: a shock tube investigation at high pressure", *Combust. Flame*, 109, 599-619

17. Barckholtz, T. A., "Modelling the negative temperature coefficient in the low temperature oxidation of light alkanes", American Chemical Society, Division Fuel, 2003
18. Jayakumar, C., Zheng, Z., Joshi, U. M., Bryzik, W., Henein, N. A., Sattler, E., "Effect of inlet air temperature on auto ignition of fuels with different cetane number and volatility", ASME, ICEF 2011-60141
19. Juttu, S., Thipse, S. S., Marathe, N. V., Gajendra Babu, M. K., "Diesel HCCI combustion control parameters study using n-heptane reduced chemical kinetic mechanism", SAE paper 2008-28- 0036
20. Barckholtz, T. A., "Modelling the negative temperature coefficient in the low temperature oxidation of light alkanes", 2003
21. Kook, S., Bae, C., Miles, P., Choi, D. et al., "The influence of charge dilution and injection timing on low-temperature diesel combustion and emissions," SAE Technical Paper 2005-01-3837
22. Suh, H. K., "Investigation of multiple injection strategies for the improvement of combustion and exhaust emission characteristics in a low compression ratio (CR) engine", Applied Energy, 88: 5013-5019, 2011
23. Machrafi, H., Cavadiasa, S., "An experimental and numerical analysis of the influence of the inlet temperature, equivalence ratio and compression ratio on HCCI autoignition process of primary reference fuels in an engine", Fuel Processing Technology, 89: 1218-1226, 2008
24. Ju. Y., Sun, W., Burke, M. P., Gou, X., Chen, Z., "Multi-timescale modeling of ignition and flame regimes of n-heptane-air mixtures near spark assisted homogeneous charge compression ignition conditions", Proceedings of Combustion Institute, 33: 1245-1251, 2011

25. Ishiyama, T., Shioji, M., Ihara, T., Katsuura, A., "Modelling and experiments on ignition of fuel sprays considering the interaction between fuel-air mixing and chemical reactions", SAE paper 2003-01-1071
26. Fitzgerald, R. and Steeper, R., "Thermal and chemical effects of NVO fuel injection on HCCI combustion," SAE Int. J. Engines 3(1):46-64, 2010, doi:10.4271/2010-01-0164
27. Choi, S., Min, K., "Analysis of the combustion and emissions of a diesel engine in early-injection, partially premixed charge compression ignition regimes", Proceeding of IMechE, Part D: Journal of Automobile Engineering, 227:939, 2013
28. Miles, P. C., Sahoo, D., Busch, S., Trost, J., Leipertz, A., "Pilot injection ignition properties under low-temperature dilute in-cylinder conditions", SAE Int. J. Engines, 2013-01-2531
29. Mueller, C. J., Martin, G. C., Briggs, T. E., Duffy, K. P., "An experimental investigation of in-cylinder processes under dual-injection conditions in a DI diesel engine", SAE paper 2004-01-1843
30. Xingcai, L., Yuchun, H., Linlin, Z., Zhen, H., "Experimental study on the auto ignition and combustion in the homogeneous charge compression ignition (HCCI) combustion operation with ethanol/n-heptane blend fuels by port injection", Fuel, 85: 2622-2631, 2006
31. Jansons, M., Florea, R., Zha, K., and Florea, E., "The combined effect of HCHO and C<sub>2</sub>H<sub>4</sub> addition on combustion in an optically accessible diesel engine fueled with JP-8," SAE Int. J. Engines 4(1):2048-2064, 2011, doi:10.4271/2011-01-1392
32. Walker, R. W., "Reactions of HO<sub>2</sub> radicals in combustion chemistry", Twenty Second Symposium (International) On Combustion, The Combustion Institute, p. 883-892, 1988

33. Goto, K., Iijima, A., Yoshida, K., and Shoji, H., "Analysis of the characteristics of HCCI combustion and ATAC combustion using the same test engine," SAE Technical Paper 2004-32-0097
34. Wong, Y. K., Karim, G. A., "A kinetic examination of the effects of recycled exhaust gases on the autoignition of homogeneous n-heptane-air mixtures in engines", SAE paper 2000-01-2037
35. Puranam, S., Steeper, R., "The Effect of Acetylene on iso-octane Combustion in an HCCI Engine with NVO", SAE Int. J. Engines 5(4):1551-1560, 2012, doi:10.4271/2012-01-1574
36. Mehl, M., Pitz, W., Sarathy, M., Yang, Y., Dec, J., "Detailed Kinetic Modeling of Conventional Gasoline at Highly Boosted Conditions and the Associated Intermediate Temperature Heat Release", SAE paper 2012-01-1109
37. Vuilleumier, D., Selim, H., Dibble, R., and Sarathy, M., "Exploration of Heat Release in a Homogeneous Charge Compression Ignition Engine with Primary Reference Fuels," SAE Technical Paper 2013-01-2622, 2013
38. Ando, H., Sakai, Y., and Kuwahara, K., "Universal Rule of Hydrocarbon Oxidation," SAE Technical Paper 2009-01-0948, 2009

**ABSTRACT****AN INVESTIGATION OF KINETIC EFFECTS OF SPLIT INJECTION TIMING ON LOW TEMPERATURE COMBUSTION**

by

**TEJASWINI A. KAMBLE****May 2014****Advisor:** Dr. Marcis Jansons**Major:** Mechanical Engineering**Degree:** Master of Science

Low temperature combustion (LTC) modes of operating internal combustion engines are of great interest for their potential to achieve high thermal efficiencies while maintaining low nitrogen oxide ( $\text{NO}_x$ ) and particulate matter emissions below levels requiring costly after-treatment systems. While various strategies for realizing LTC have been developed, including homogeneous charge compression ignition (HCCI), reactivity controlled compression ignition (RCCI) and premixed charge compression ignition (PCCI), a common challenge is the control of the kinetically-driven auto-ignition processes over appreciable load ranges.

This study examines the chemical kinetics of split-injection timing and the kinetic effect of this parameter on combustion phasing and pressure rise rate. Detailed reaction mechanisms are applied in CHEMKIN-based kinetic simulations to model the production and composition of combustion intermediates produced by a pilot injection through different pressure-temperature histories. The influence of these intermediates on the combustion phasing of the following main fuel ignition is examined. Different pilot injection timings were tried keeping the main fuel addition timing constant. The temperature, pressure and rate of heat

release profiles during the combustion cycle for varied pilot fuel injection timings were compared along with the species composition at the start of main fuel addition. The results will provide insight to the role of pilot injection timing on LTC control.

**AUTOBIOGRAPHICAL STATEMENT****Tejaswini A. Kamble**

- 1987** Born in Kolhapur, Maharashtra, India
- 2006-2010** Studied Mechanical Engineering in University of Mumbai, India
- June, 2010** Bachelor of Engineering (Mechanical Engineering), University of Mumbai, India
- 2011-2014** Graduate Student, Mechanical Engineering Department, Wayne State University, Detroit, MI, U.S.A
- 2011-2012** Student Assistant, Mechanical Engineering Department, Wayne State University, Detroit, MI, U.S.A
- 2012-2013** Graduate Teaching Assistant & Research Assistant, Mechanical Engineering Department, Wayne State University, Detroit, MI, U.S.A
- 2013- Present** Engineering Assistant, Commercial Engines, FEV North America, Inc., Auburn Hills, MI, U.S.A